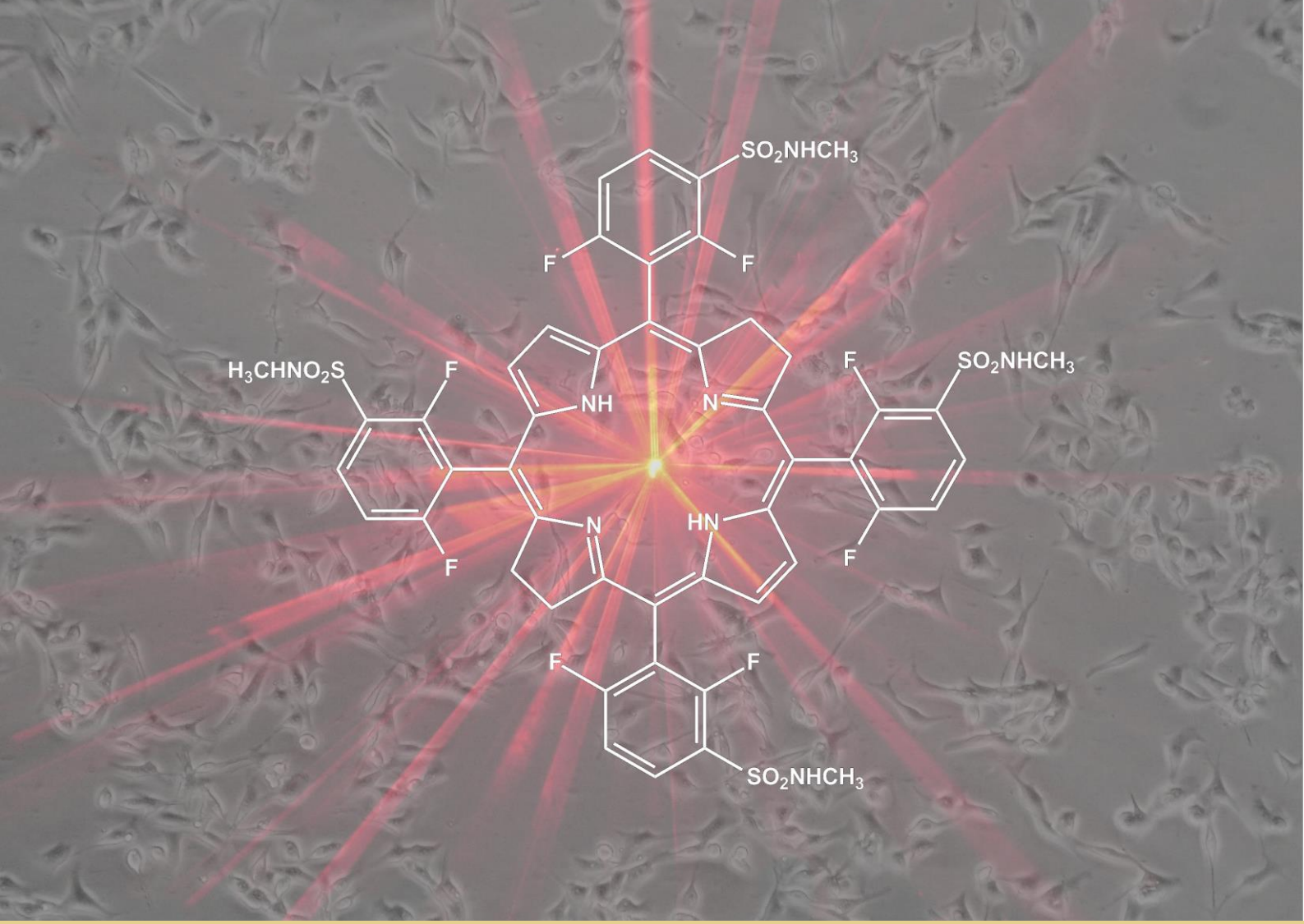

Luís Gabriel Borges Rocha

Development of a novel photosensitizer for Photodynamic Therapy of cancer

Tese de doutoramento em Ciências Farmacêuticas, especialidade em Biotecnologia Farmacêutica, orientada pelo Professor Doutor Sérgio Simões e pelo Professor Doutor Luís G. Arnaut e apresentada à Faculdade de Farmácia da Universidade de Coimbra

Outubro de 2015

· U C ·

Universidade de Coimbra

Luís Gabriel Borges Rocha

Development of a novel photosensitizer for Photodynamic Therapy of cancer

2015

FACULDADE DE FARMÁCIA

DA

UNIVERSIDADE DE COIMBRA

Tese de doutoramento em Ciências Farmacêuticas, especialidade em Biotecnologia Farmacêutica, apresentada à Faculdade de Farmácia da Universidade de Coimbra

Doctoral thesis in Pharmaceutical Sciences, specialty in Pharmaceutical Biotechnology, presented to the Faculty of Pharmacy of the University of Coimbra.

Orientadores Científicos / Scientific Supervisors:

Professor Doutor Sérgio Simões

Faculdade de Farmácia da Universidade de Coimbra

Professor Doutor Luís G. Arnaut

Faculdade de Ciências e Tecnologia da Universidade de Coimbra

The studies presented in this thesis were performed at Bluepharma – Indústria Farmacêutica, SA, Chemistry Department of the Faculty of Sciences and Technology of the University of Coimbra, Centre for Neuroscience and Cell Biology of the University of Coimbra and Instituto Nacional de Investigação Agrária e Veterinária in Santarém, Portugal. The work was funded by Bluepharma – Indústria Farmacêutica, SA and Luzitin, SA, which received additional financial support from the National Strategic Reference Framework's Programme (QREN) nº 5356, from November 2010 until October 2013.

Para a Sónia, Beatriz e Rodrigo,

as estrelas mais brilhantes no meu Universo!

Science is the only light in the dark paths of the unknown.

Let there be light

Genesis 1:3

Table of Contents

Agradecimentos

Pessoalmente, este trabalho representa o ponto mais alto de uma fascinante viagem que teve início no já longínquo ano de 2006. A todos os que durante este trajeto contribuíram de forma construtiva para o resultado final, quero manifestar o meu profundo reconhecimento e imensa gratidão. Manifesto um agradecimento particular:

Ao Professor Sérgio pela visão estratégica com que abraçou este projecto, pela oportunidade que me deu de fazer parte da família Bluepharma, abrindo-me a porta do desafiante mundo da Terapia Fotodinâmica, pela confiança, incentivo e amizade que sempre me transmitiu, pela partilha da sua experiência e conhecimento verdadeiramente enriquecedora e motivante.

Ao Professor Arnaut por me ter guiado através das prodigiosas subtilezas da Terapia Fotodinâmica, partilhando o seu vasto conhecimento e paixão pela ciência, pelas produtivas discussões científicas que permitiram dar resposta aos problemas mais complexos, para logo conduzirem a novos desafios, pela capacidade de fomentar o espírito crítico, pelo constante apoio, confiança e amizade.

À administração da Bluepharma, em especial ao Dr. Paulo, à Dra. Isolina e ao Dr. Miguel, pela aposta estratégica na investigação e na inovação como bases para o crescimento sustentado da empresa, fundamental para a concretização deste projecto, e pela simpatia de todos os dias.

Ao Doutor Luís Almeida por ter embarcado com a Luzitin nesta aventura, partilhando a sua vasta experiência em desenvolvimento de novos medicamentos, e por contribuir de forma decisiva para manter a equipa motivada e no rumo certo.

À equipa do Laboratório de Química da Luzitin, nomeadamente à Doutora Mariette, por todo o conhecimento e experiência que trouxe ao projecto, e também ao Carlos, Artur, Nuno, Gonçalo e Vanessa, por todo o trabalho e dedicação que empregaram na criação, caracterização e produção da molécula objecto de estudo desta tese, para além das inúmeras contribuições no sentido de ultrapassar os obstáculos que foram surgindo e pelos agradáveis convívios de final de dia.

To Janusz, Fábio, Lígia and Raquel for all the precious help in the several tasks and studies that compose this project, for all the insightful scientific and non-scientific discussions, and the friendship of every day.

À “família” Bluepharma, especialmente aos colegas e amigos dos departamentos de Investigação e DAG, pelo interesse que sempre demonstraram, pelas palavras de incentivo e, acima de tudo, pelo convívio e amizade constantes.

Aos colaboradores do Biotério do Centro de Neurociências e Biologia Celular da Universidade de Coimbra, em especial à Cristina, Carmen e Mónica, por toda o apoio prestado com a logística, manutenção e cuidado dos animais em experimentação.

Ao Doutor Ramiro Mascarenhas e restante equipa do Instituto Nacional de Investigação Agraria em Santarém, por toda a assistência prestada no estudo com os minipigs.

Aos amigos de sempre, aos da academia e aos que chegaram depois, que dão cor ao “caminho”, ajudando a suavizar as curvas e os obstáculos, por estarem sempre presentes, ainda que por vezes apenas por via digital, por todos os momentos únicos de convívio que nos aproximam e nos fazem lembrar do que é verdadeiramente importante.

Aos meus pais, Tinita e Manuel Maria, por terem lançado as bases do que hoje sou, pessoal e profissionalmente, pela confiança e apoio incondicionais que sempre demonstram… e por tudo o resto.

À minha irmã Raquel, pela partilha de uma vida cheia de bons momentos, pela amizade, companheirismo e presença constantes, ajudando a tornar este “trilho” menos sinuoso.

À minha restante família, pela amizade e interesse que sempre demonstraram.

Finalmente, à Sónia, Beatriz e Rodrigo, por encherem a minha vida de amor e alegria, por serem a minha inspiração e por fazerem tudo valer a pena.

Thesis Abstract

Photodynamic Therapy (PDT) for cancer treatment is a safe and clinically-approved procedure that experienced great progresses over the last two decades. It is based on the interaction between a photosensitizer (PS) molecule, light and oxygen that react to generate reactive oxygen species (ROS). These ROS trigger a cascade of reactions that lead to the destruction of tumour cells and tumour vasculature. In comparison with the traditional oncological therapies, PDT has the advantages of a good tolerability profile, the absence of specific resistance mechanisms, a good cosmetic outcome and the ability to stimulate the immune system. This later aspect is regarded as a major therapy-differentiating factor. However, the widespread use of PDT is yet to be reached since the systemic photosensitizers currently on the market have been overshadowed by their limited efficacy and prolonged skin photosensitivity. Thus, there is a significant room for improvement, especially in the area of new PS molecules. Better PS molecules should be rationally designed to match, as close as possible, the properties that define the profile of the ideal PS.

This work describes the nonclinical development of a new fluorinated sulfonamide bacteriochlorin, redaporfin, with very promising properties for anticancer PDT: simple and affordable synthesis, high purity and stability, molar absorptivity of 140000 $M^{-1}cm^{-1}$ at 743 nm, high quantum yields of ROS formation, photostability, solubility in biocompatible formulations, low toxicity in the dark and high phototoxicity.

Direct comparison between PS based on literature data is often hindered because different experimental conditions are employed. To overcome this gap the *in vitro* performance of redaporfin was assessed against the two systemic PS for PDT of cancer on the market, Photofrin® and Foscan®, using the same experimental conditions. The comparison focused on the photosensitizing efficiency of the PS, the ratio between the dark toxicity and the phototoxicity, in two cancer cell lines. The results demonstrate that the *in vitro* performance of redaporfin is clearly superior to both competitors.

Prior to the *in vivo* evaluation of redaporfin, three intravenous (iv) formulations were designed and optimized in mice with subcutaneous tumour, to determine its correspondent biodistribution and pharmacokinetic profiles. The most promising formulation was able to optimize the balance between a selective accumulation of redaporfin in the tumour, between 24 and 72 hours after administration, and a high bioavailability immediately after the injection. This versatility was exploited either in protocols that aim for a selective action, with longer drug-light-interval (DLI), and in protocols that aim for the vascular effect, with shorter DLI. *In vivo* studies confirmed the efficacy of redaporfin-PDT in the treatment of mice

bearing subcutaneous tumours. We were able to cure mice using protocols with DLI of 72 h and 15 min. In addition, this redaporfin formulation was not associated with significant skin photosensitivity reactions in rats exposed to a solar simulator 7 days after the administration, which represent substantial reduction in skin photosensitivity in comparison to the systemic PS commercially available.

The preliminary nonclinical safety evaluation of the redaporfin formulation revealed no signs of significant or long-term toxic reactions. The formulation was very well tolerated in mice and rats up to 100 and 20 mg/kg, respectively. The toxicity was assessed in rats and the results showed that, only after PDT, significant increases were observed on some serum biochemistry markers and on the circulating neutrophils population. Nevertheless, all significant changes were transient and returned to baseline levels within 1 week after PDT.

The following development stage was dedicated to the exhaustive optimization of the treatment parameters in a mouse tumour model, leading to a vascular-PDT protocol 100% safe and with an overall long-term cure rate of 86%. This protocol was applied to treat the same tumours in immunosuppressed mice and completely fail to produce long-term cures, which suggests that the high antitumour efficacy of the treatment depends on the existence of a functional immune system. To further understand the role of the immune system on the treatment outcome, the ability of redaporfin vascular-PDT to induce antitumor immune memory was evaluated. The results showed that 67% of the mice, cured with the optimized PDT protocol for more than three months, completely rejected a second inoculation of the same tumour cells. In the control group the development of all reinoculated tumours was observed. This is a strong indication that this PDT protocol is able to induce an effective long-term antitumor immune memory. In addition, the systemic effect of redaporfin vascular-PDT was tested in a pseudo-metastatic mouse model. The results showed a significant decrease in the number of lung metastasis after PDT, in comparison with the non-treated control, demonstrating that this protocol is capable of producing a systemic effect against non-treated tumours. Globally, these studies produced strong evidences of the decisive contribution of the host immune system to the outcome of redaporfin vascular-PDT.

In summary, redaporfin proved to be an extremely safe and highly effective PS for vascular-PDT. We hope that the promising results here presented can be successfully translated to the clinic, representing a significant contribution to improve the well-being of cancer patients.

Keywords: cancer, photodynamic therapy, photosensitizer, bacteriochlorin, redaporfin, anticancer drug, drug development, pharmaceutical formulation, safety toxicology, antitumour efficacy, metastasis, immunotherapy.

Resumo da Tese

A Terapia Fotodinâmica (PDT) para o tratamento do cancro é um procedimento seguro e aprovado clinicamente que foi alvo de grandes progressos nas últimas duas décadas. Baseia-se na interacção entre um fotossensibilizador (PS), luz e oxigénio, que reagem gerando espécies reactivas de oxigénio (ROS). Estas desencadeiam uma cascata de reacções que conduzem à destruição das células e vasculatura tumoral. Em comparação com as terapias oncológicas tradicionais, a PDT tem como vantagens o bom perfil de tolerabilidade, a ausência de mecanismos de resistência específicos, o bom efeito cosmético e a capacidade de estimular o sistema imunitário. Este último aspecto é visto como um grande factor de diferenciação. No entanto, a aplicação generalizada da PDT ainda está por alcançar, uma vez que os fotossensibilizadores para administração sistémica actualmente no mercado têm sido ensombrados pela sua eficácia limitada e fotossensibilidade cutânea prolongada. Assim, existe uma margem significativa para melhoria da PDT, nomeadamente na área das novas moléculas fotossensibilizadoras. Melhores PS devem ser idealizados de forma a corresponder, tão bem como possível, às propriedades que definem o perfil do PS ideal.

Este trabalho descreve o desenvolvimento não-clínico de uma nova bacterioclorina sulfonamida fluorada, redaporfin, com propriedades muito promissoras para PDT do cancro: síntese simples e de baixo custo, elevada pureza e estabilidade, absortividade molar de 140000 $M^{-1}cm^{-1}$ a 743 nm, elevados rendimentos quânticos de formação de ROS, fotoestabilidade, solubilidade em formulações biocompatíveis, baixa toxicidade no escuro e elevada fototoxicidade.

A comparação directa entre PS com base em dados da literatura é frequentemente dificultada pela utilização de diferentes condições experimentais. Para ultrapassar esta lacuna a performance *in vitro* da redaporfin foi comparada com a dos PS sistémicos no mercado para PDT do cancro, Photofrin® e Foscan®, nas mesmas condições experimentais. A comparação focou-se na eficiência fotossensibilizadora dos PS, razão entre a toxicidade no escuro e a fototoxicidade, em duas linhas celulares tumorais. Os resultados demonstraram que a performance *in vitro* da redaporfin é claramente superior à dos dois competidores.

Antes da avaliação *in vivo* da redaporfin, três formulações intravenosas (iv) foram idealizadas e optimizadas em murganhos com tumor subcutâneo, para determinar os correspondentes perfis de biodistribuição e de farmacocinética. A formulação mais promissora foi capaz de optimizar o equilíbrio entre a acumulação selectiva de redaporfin no tumor, 24 a 72 horas após a administração, e uma elevada biodisponibilidade logo após

a injecção. Esta versatilidade foi explorada em protocolos que visam uma acção selectiva, com intervalo fármaco-luz (DLI) longos, e em protocolos que pretendem um efeito vascular, com DLI curtos. Estudos *in vivo* confirmaram a eficácia da PDT com redaporfin no tratamento de murganhos com tumor subcutâneo. Foi possível curar animais usando protocolos com DLI de 72 h e 15 min. Adicionalmente, esta formulação de redaporfin não originou reacções de fotossensibilidade cutânea significativas em ratos, expostos a um simulador solar 7 dias após a administração, o que representa uma redução substancial da fotossensibilidade cutânea em comparação com os PS sistémicos disponíveis comercialmente.

A avaliação não-clínica preliminar da segurança da formulação de redaporfin não revelou sinais de toxicidade significativa ou de longo prazo. Esta foi muito bem tolerada em murganhos e ratos para doses de redaporfin até 100 e 20 mg/kg, respectivamente. A toxicidade foi avaliada em ratos e os resultados mostraram que apenas após a PDT se observaram aumentos significativos em alguns marcadores bioquímicos séricos e na população de neutrófilos circulantes. Apesar disso, todas as alterações foram transitórias, tendo regressado aos valores basais uma semana após a PDT.

A fase seguinte de desenvolvimento foi dedicada à optimização exaustiva dos parâmetros de tratamento num modelo tumoral de murganho, tendo conduzido a um protocolo de PDT vascular 100% seguro e com uma taxa de cura a longo prazo de 86%. Este protocolo foi aplicado para tratar os mesmos tumores em murganhos imunodeprimidos, sem conseguir obter nenhuma cura a longo prazo, o que sugere que a elevada eficácia anti-tumoral do tratamento está dependente da existência de um sistema imunitário funcional. Para aprofundar o papel do sistema imunitário no resultado final da terapia foi avaliada a capacidade da PDT vascular com redaporfin induzir memória imunitária. Os resultados mostraram que 67% dos murganhos, curados há mais de três meses com o protocolo de PDT optimizado, rejeitaram totalmente uma segunda inoculação das mesmas células tumorais. No grupo controlo verificou-se o desenvolvimento de todos os tumores reinoculados. Isto constitui um forte indício de que este protocolo de PDT é capaz de induzir memória imunitária anti-tumoral efectiva e de longo prazo. Adicionalmente, o efeito sistémico da PDT vascular com redaporfin foi testado num modelo pseudo-metastático de murganho. Os resultados traduziram-se numa diminuição significativa do número de metástases pulmonares após a PDT, comparativamente ao grupo controlo não tratado, o que demonstra que este protocolo é capaz de produzir um efeito sistémico em tumores não tratados. Globalmente, estes estudos geraram evidências sólidas da contribuição decisiva do sistema imunitário para o resultado final da PDT vascular com redaporfin.

Em suma, a redaporfin provou ser um PS para PDT vascular extremamente seguro e altamente eficaz. Esperamos que os resultados promissores aqui apresentados possam ser aplicados com sucesso na clínica, contribuindo de forma significativa para melhorar o bem-estar dos doentes com cancro.

Palavras-chave: cancro, terapia fotodinâmica, fotossensibilizador, bacterioclorina, redaporfin, fármaco anticancerígeno, desenvolvimento de fármacos, formulação farmacêutica, toxicologia de segurança, eficácia anti-tumoral, metástases, imunoterapia.

Nota: Os textos anteriores foram escritos de acordo com a grafia anterior ao Acordo Ortográfico de 1990.

List of Abbreviations

AAPM – American Association of Physicists in Medicine
ABC – ATP-binding cassette
EtOAc – Ethyl acetate
AK – Actinic keratosis
ALA – Aminolevulinic acid
ALP – Alkaline phosphatase
ALT – Alanine aminotransferase
AMD – Age-related macular degeneration
apoE – Apolipoprotein E
AST – Aspartate aminotransferase
ATP – Adenosine triphosphate
AUC – Area under the curve
BA – Basophil
BCC – Basal cell carcinoma
Bcl-2 – B-cell lymphoma 2
BD – Biodistribution
BIL – Total bilirubin
BPD – Benzoporphyrin derivative monoacid ring A
BUN – Blood urea nitrogen
BW – Body weight
CD – Cluster of differentiation
CHOL – Total cholesterol
CHS – Contact hypersensitivity syndrome
CK – Creatine kinase
ClBEt – 5,10,15,20-*tetrakis*(2-chloro-5-*N*-ethylsulfamoylphenyl) bacteriochlorin
cm – Centimetre
CNS – Central nervous system
CPI – Critical Path Initiative
CRD – Chemistry Research Department
CRE – Creatinine
CrEL – Cremophor EL
CRO – Contract research organization
CRT – Calreticulin
CY – Cyclophosphamide
DAB – 3,3'-diaminobenzidine
DAMP – Damage-associated molecular pattern
DC – Dendritic cell
DCS – Diffuse correlation spectroscopy
DFS – Diffuse fluorescence spectroscopy
DGAV – Direção-Geral de Alimentação e Veterinária
DLI – Drug-light interval
DMEM – Dulbecco's Modified Eagle Medium
DMSO – Dimethyl sulfoxide
DNA – Deoxyribonucleic acid
DOS – Diffuse optical spectroscopy

DRS – Diffuse reflectance spectroscopy
EDTA – Ethylenediamine tetraacetic acid
e.g. – For example (from the Latin *exemplī grātiā*)
EMA – European Medicines Agency
EO – Eosinophil
EPR – Enhanced permeability and retention
ER – Endoplasmic reticulum
EtOH – Ethanol
F_2BMet – 5,10,15,20-*tetrakis*(2,6-difluoro-3-*N*-methylsulfamoylphenyl) bacteriochlorin
F_2P – *5,10,15,20-Tetrakis(2,6-difluorophenyl) porphyrin*
F_2PMet – 5,10,15,20-*tetrakis*(2,6-difluoro-3-*N*-methylsulfamoylphenyl) porphyrin
FBS – Foetal bovine serum
FDA – Food and Drug Administration
GLP – Good laboratory practices
GLU – Glucose
GPx – glutathione peroxidase
GR – Glutathione reductase
GSH – Glutathione
GSSG – Glutathione dissulfide
ɣ-GT – *gamma*-glutamyl transferase
h – Hour
HAL – Hexaminolevulinate
Hb – Haemoglobin
HBO – Hyperbaric oxygen
HCT – Haematocrit
HDL – High density lipoprotein
HEPES – 4-(2-hydroxyethyl)-1-piperazineethanesulfonic acid
HPD – Hematoporphyrin derivative
HPPH – 2-(1-hexyloxyethyl)-2-devinyl pyropheophorbide-α
HO-1 – Haeme oxygenase-1
HRMS - High-Resolution Mass Spectrometry
HSP – Heat shock protein
Hz – Hertz
IC50 – Concentration that inhibits cell viability in 50%
ICD – Immunogenic cell death
ICH – International Conference on Harmonization of Technical Requirements for Registration of Pharmaceuticals for Human Use
IL-1β – Interleukin-1β
IL-6 – Interleukin-6
ip – Intraperitoneal
iPDT – Interstitial photodynamic therapy
IR – Infrared
ITF – Innovation task force
IU – International units
iv – Intravenous
J – Joule
LDH – Lactate dehydrogenase
LDL – Low density lipoprotein

LED – Light-emitting diode
Log P_{ow} – Logarithm to base 10 of the *n*-octanol:water partition coefficient
LUZ11 – 5,10,15,20-*tetrakis*(2,6-difluoro-3-*N*-methylsulfamoylphenyl) bacteriochlorin
LY – Lymphocyte
mAb – Monoclonal antibody
MAL – Methyl aminolevulinate
MCH – Mean corpuscular haemoglobin
MCHC – Mean corpuscular haemoglobin concentration
MCV – Mean corpuscular volume
MDR – Multi-drug resistance
MeOH – Methanol
min – Minute
MIP-1 and MIP-2 – Macrophage inflammatory proteins 1 and 2
mm – Millimetre
MO – Monocyte
MPV – Mean platelet volume
MTD – Maximum tolerated dose
mTHPC – 5,10,15,20-Tetrakis(3-hydroxylphenyl) chlorin
NADPH – Reduced form of nicotinamide adenine dinucleotide phosphate
NBO – Normobaric oxygen
NE – Neutrophil
NIR – Near-infrared
nm – Nanometre
NM – Not measurable
NMR – Nuclear magnetic resonance
NP – Not performed
PBS – Phosphate-buffered saline
PCT – Plateletcrit
PDW – Platelet distribution width
PE – Photosensitizing efficiency
PEG – Polyethylene glycol
PDR – Photodynamic reaction
PDT – Photodynamic Therapy
PG – Propylene glycol
PK – Pharmacokinetic
PLT – Platelets
PP IX – Protoporphyrin IX
ppm – Parts per million
PS – Photossensitizer
RBC – Red blood cells
R&D – Research and development
RDW – Red blood cell distribution width
RES – Reticuloendothelial system
Retic – Reticulocytes
ROS – Reactive oxygen species
rpm – Revolutions per minute
RPMI – Roswell Park Memorial Institute medium
SD – Standard deviation

SC – Subcutaneous
SCC – Squamous cell carcinoma
sec – Second
SEM – Standard error of the mean
SOD – Superoxide dismutase
TG – Triglycerides
THF – Tetrahydrofuran
TI – Therapeutic index
TLC – Thin-layer chromatography
T/M – Tumour-to-muscle
TNF-α – Tumour necrosis factor α
TP – Total protein
Treg – Regulatory T cell
T/S – Tumour-to-skin
UK – United Kingdom
USA – United States of America
UV – Ultraviolet
W – Watt
WBC – White blood cell

List of Figures

List of Tables

Chapter 1

General Introduction

Chapter 1 – General Introduction

Part of this review on the state-of-the-art of Photodynamic Therapy was published as a book chapter in:

Biomateriales aplicados al diseño de sistemas terapéuticos avanzados. H.C. De Sousa, M.E.M. Braga, A. Sosnik, Editors. Coimbra University Press, 2015. p. 637-674.

Terapia Fotodinâmica para tratamento do cancro

Luís B. Rocha[1,2], Luís G. Arnaut[1,3], Mariette M. Pereira[1,3], Luís Almeida[1] and Sérgio Simões[1,2]

[1] Luzitin SA, Rua da Bayer 16, 3045-016 Coimbra, Portugal

[2] Bluepharma – Indústria Farmacêutica, SA, Rua da Bayer 16, 3045-016 Coimbra, Portugal

[3] Department of Chemistry, University of Coimbra, Rua Larga, 3004-535 Coimbra, Portugal

1.1. Preamble

Photodynamic Therapy (PDT) is a clinical strategy that was first approved for oncology applications more than twenty years ago. It was a significant achievement and for some time the expectations around the newly approved treatment remained elevated. However, the first photosensitizer approved for clinical use and the few that some years later reached the same regulatory status, soon evidenced shortcomings in cancer treatment, namely in their clinical efficacy. In addition, systemic photosensitizers met with a bad negative perception among clinicians and their patients, mainly due to the long periods of skin photosensitivity after the treatment. Thus, PDT of cancer, other than non-melanoma skin cancer, has not yet achieved a satisfactory clinical acceptance. This motivated intense research efforts that led to the discovery of several new promising molecules and to significant progress in light delivery technology. Nevertheless, no new photosensitizer with significant reach was approved in recent years for PDT of cancer. This represents an important translational gap that needed to be addressed.

The challenge of overcoming the limitations of the clinically approved photosensitizers was embraced by an academic research team at the University of Coimbra. After a long process of discovery they succeeded in rationally designing a new family of photosensitizers. Among this family one molecule stood out because of its near ideal properties for application in PDT of cancer, and was selected as the lead compound. To further develop this new molecule, the university research team formed a partnership with Bluepharma, a privately-owned pharmaceutical company based in Coimbra. Bluepharma was convinced by the extraordinary features of the new photosensitizer and decided to contribute to its development. This led to the creation of Luzitin, a start-up biotech company that became responsible for the development of this new drug candidate. The primary objective established for Luzitin was to successfully translate this new drug candidate from the bench to the clinic and thus to demonstrate its therapeutic value in oncology.

In this context, my own challenge was to contribute to the development programme of the lead compound, by demonstrating its nonclinical safety and efficacy in relevant animal models, and optimizing a treatment protocol that would be translated to the clinical trial. This had to be timely accomplished and without deviating from the primary objective of Luzitin. Accordingly, a series of studies, covering distinct scientific areas, from the *in vitro* screening and pharmaceutical development, to the *in vivo* pharmacology, toxicology and immunology, were performed and the main results reported in this thesis. The presentation of such results is preceded by a thorough review of the literature on PDT.

1.2. Challenges in cancer therapy – Photodynamic Therapy as an alternative for cancer treatment

The steady scientific progress in life sciences fields have allowed scientists to improve our understanding on the complexity of the human organism and its pathologies. However, regardless of the immense global research efforts, cancer remains a major causes of death worldwide with 8.2 million deaths in 2012, representing an extremely high socioeconomic burden [1, 2].

Traditional therapeutic strategies for cancer like surgery, chemotherapy and radiotherapy, have provided significant advances in the management of cancer, offering high cure rates for some types of cancer. Nevertheless, for many common cancers they are responsible for the occurrence of serious adverse effects, while their efficacy is sometimes disappointing. This can be explained by the heterogeneity and genetic complexity of tumours within the population, which demands to the continuous search for new, safer and more effective therapies [3]. The growing knowledge about cancer genesis, progression, and dissemination mechanisms allowed the design and development of several alternative therapeutic strategies like angiogenesis inhibitors, active targeting of cytotoxic drugs, gene therapy, immunotherapy, or photodynamic therapy (PDT). Some of these strategies can be more effective and safe for some types of cancer or for subpopulations of patients (e.g. with tumour cells that express a particular phenotype) [4].

Among these newer cancer therapies, one the most promising is PDT. Its concept is based on the dynamic interaction between a photosensitizer molecule (PS), light with specific wavelength and molecular oxygen, which promotes the selective destruction of the target tissue. Clinical applications of PDT have shown high cure rates for some types of early-stage tumours, most frequently in dermatology, such as in the treatment of precancerous lesions and non-melanoma skin cancers [5]. In addition, PDT was able to prolong the survival time and to improve the quality of life in patients with advanced head and neck cancers, presenting for this indication a superior cost-benefit than surgery [6]. The concept of PDT is known for more than 100 years, nevertheless the first PS drug for PDT of cancer, porfimer sodium (Photofrin®), was only approved for clinical practice for the first time in 1993. The advances over the last twenty years that led to new, safer and more effective PS, and to better, cheaper and user-friendly light sources, transformed PDT from a curiosity to a highly promising therapeutic strategy with applications in fields such as oncology, dermatology, ophthalmology, cardiology, rheumatology or infectious diseases, and also in medical imaging [7-9].

1.3. History of Photodynamic Therapy

Since ancient times light has been used to treat diseases. Heliotherapy, the therapeutically use of sunlight, was used since 5000 years ago. In India and ancient Greece different forms of phototherapy were also used to treat psoriasis and vitiligo, with a combination of psoralens with sunlight [10]. Nevertheless, the current concept and clinical application of PDT were only described in the early years of the twentieth century by Raab, von Tappeiner and Jesionek, which after a decade of work used the topical application of eosin followed by exposure to sunlight to treat skin cancer [11, 12]. However, their results did not have the desired impact and PDT remained dormant for many years. The interest in PDT only resurfaced in 1960 with the discovery of hematoporphyrin derivative (HPD) by Lipson and Baldes, which demonstrated some therapeutic efficacy after PDT in a patient with bladder cancer [13]. The true potential of PDT was only perceived after the extensive work by Dougherty and co-workers who, between 1975 and 1978, reported the complete cure of malignant tumours by combined application of HPD and red light, initially in a model of mice breast cancer and later in patients with skin, prostate, breast and colon tumours [14, 15]. These promising results were confirmed in clinical trials with improved versions of HPD in patients with skin and bladder cancer. Finally, in 1993 a milestone for PDT was achieved with the regulatory approval in Canada of porfimer sodium (Photofrin®), a semi-purified version of HPD, for bladder cancer treatment [8].

Later, porfimer sodium was approved in other countries, including the USA, for the treatment of oesophageal and bronchial cancer and Barrett's oesophagus. However, it was soon realized that the improvement of PDT required new and more effective molecules with fewer side effects. A major inconvenience of PDT with HPD is the severe and prolonged skin photosensitivity after the treatment. With this objective, the attention was focused on the discovery and development of new and safer PS molecules, leading to the regulatory approval in 2000 of verteporfin (Visudyne®), a benzoporphyrin derivative, for the treatment of age-related macular degeneration (AMD), and temoporfin (Foscan®) in 2001, a chlorin, for the treatment of head and neck cancer [16, 17]. The approval of porfimer sodium and temoporfin represented significant advances in PDT for cancer treatment, however their wide clinical acceptance was hampered by their limited efficacy and adverse effects. These were attributed to the reduced absorption of red and infrared light, where tissues are more transparent, to inadequate pharmacokinetics, with slow clearance rates leading to prolonged skin photosensitivity of patients, and to ineffective treatment of metastatic disease and, thus with only palliative value in the treatment of advanced cancer [18].

Figure 1.1 presents examples of marketed PS and their structures, together with newer PS that are currently in clinical development for oncology indications.

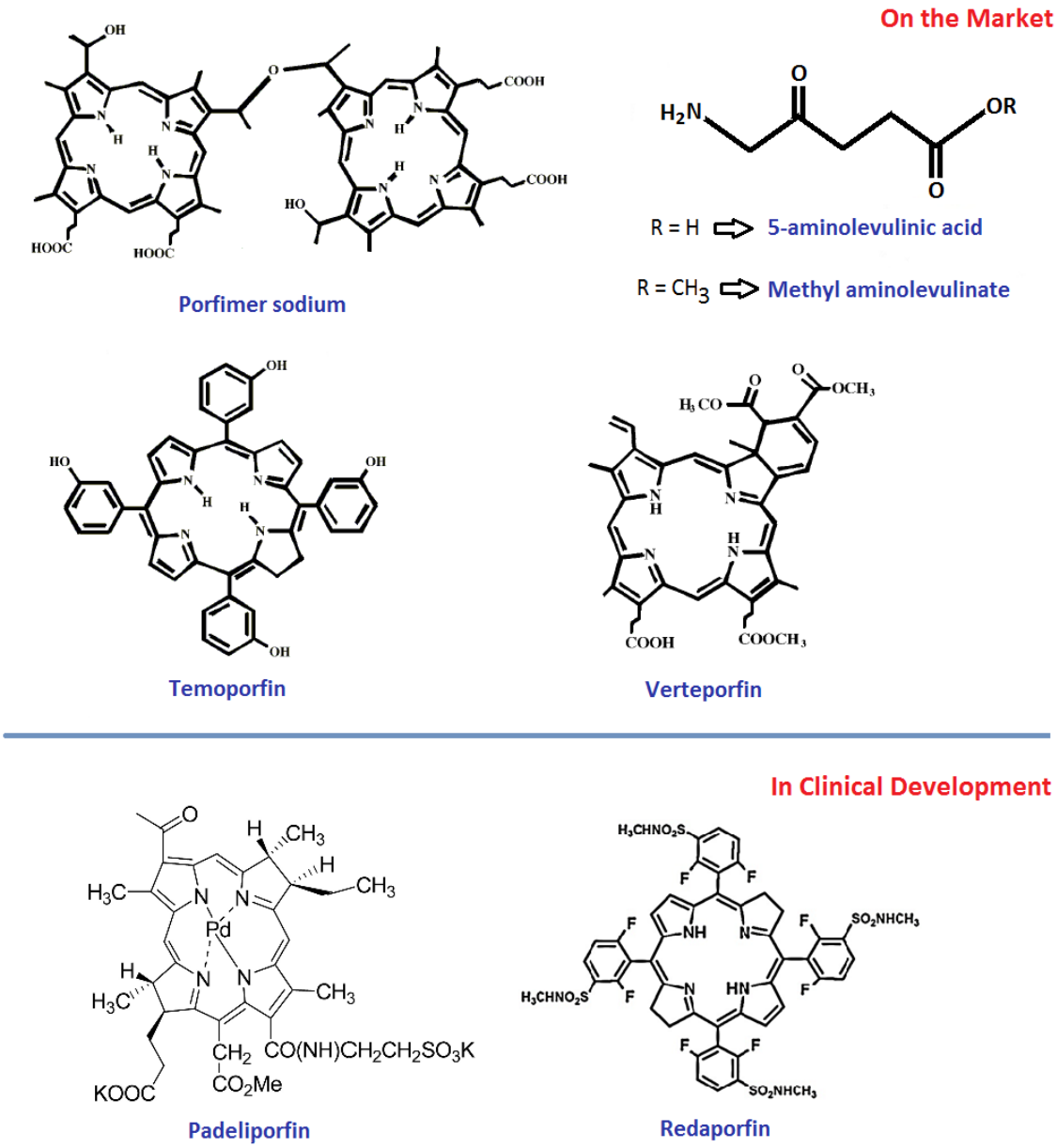

Figure 1.1 – Chemical structure of some photosensitizers approved or in clinical development for PDT.

1.4. Mechanism of action

The ultimate goal of PDT is the selective destruction of a target tissue. For this to occur the simultaneous combination of three components must take place in the target tissue: the photosensitiser, visible light and molecular oxygen. The photodynamic reaction (PDR)

begins with light absorption by the PS in the target tissue, which triggers a series of photochemical reactions that lead to the generation of reactive oxygen species (ROS). A ROS typically implicated in PDT is the electronically excited oxygen molecule in its lowest energy singlet state – singlet oxygen ($^1O_2$) – that can cause extensive oxidative damage to biomolecules and cellular structures, thus leading to cell death [19]. Other ROS that may be generated in PDT are the superoxide ion ($O_2^{-\bullet}$), hydrogen peroxide (H_2O_2) and the hydroxyl radical ($OH^\bullet$) [20].

Figure 1.2 illustrates the basic principles of PDT where the PS in the ground state (a singlet state) absorbs light and goes to an electronically excited state (also a singlet state) with a very short life time (a few nanoseconds or less). From here, it can decay back to the ground state with emission of fluorescence, or it can undergo intersystem crossing to a more stable excited state (a triplet state), through spin conversion of the electron in the higher energy orbital. The triplet state has a higher life time (up to tens of microseconds), which allows for sufficient time for its interaction with molecular oxygen or other substrates present in the tissues [20, 21].

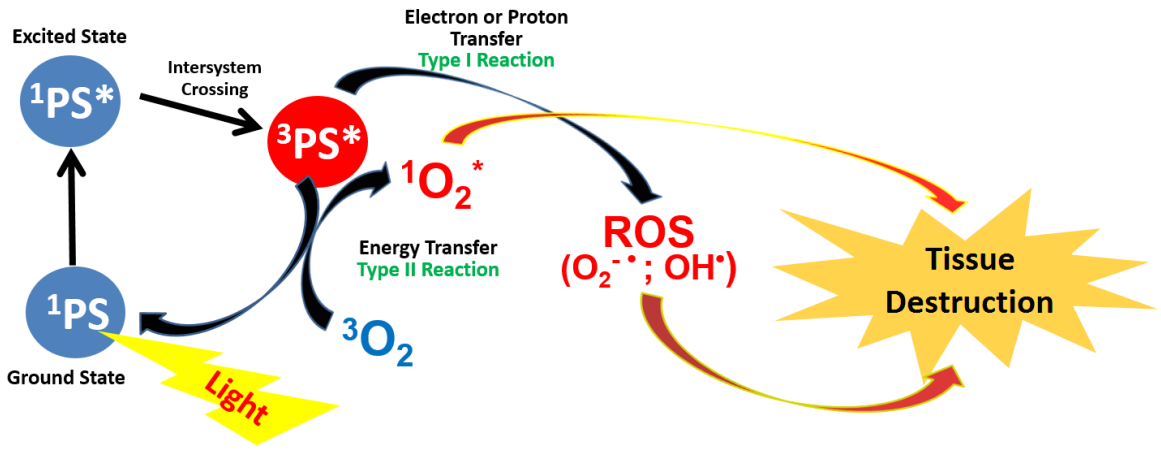

Figure 1.2 – Schematic depiction of the photophysical and photochemical events of the PDT mechanism.

The PS excited triplet state has two alternative pathways leading to ROS generation:

i) Direct energy transfer to ground state O_2 (a triplet state) to form singlet oxygen ($^1O_2$) – type II reaction. This pathway is allowed only when the PS triplet energy is higher than the $^1O_2$ excitation energy, which is 94.5 kJ/mol;

ii) Electron transfer to O_2, with super oxide anion ($O_2^{-\bullet}$) formation (photooxidation), or electron or proton transfer from an organic substrate, originating a radical cation and $O_2^{-\bullet}$ (photoreduction) – type I reaction. The radical cations can further react with molecular oxygen to form a peroxyl radical, another cytotoxic species [22, 23].

The type II reaction, because it has a simpler mechanism and it is in general thermodynamically favoured for red-absorbing PS, tends to occur preferentially than the type I reaction. This explains, why $^1O_2$ is regarded as the main mediator of PDT phototoxicity. The quantum yield of $^1O_2$ formation ($\Phi\Delta$) is one of the most important features of a PS, and is determined by the quantum yield (Φ_T) and lifetime (τ_T) of its triplet excited state [21].

For a few PS both mechanisms can occur competitively, leading to an amplified PDT response. The relative extension of type I and type II mechanisms is dictated by the PS characteristics, the PDT protocol and, possibly, by the local oxygen concentration [20, 24]. The tumour microenvironment is often described as hypoxic, especially near its centre due to insufficient blood flow [25]. This in combination with oxygen consumption by the PDT, can reduce drastically the local oxygen concentration, and favour the occurrence of type I reaction [26, 27] .

The superoxide anion by itself is not capable of major oxidative tissue damage, but it can undergo dismutation, catalysed by the enzyme superoxide dismutase (SOD), originating hydrogen peroxide (H_2O_2). The $O_2^{-\bullet}$ can also reduce metal ions, like ferric ion (Fe^{3+}) to its ferrous form (Fe^{2+}), which catalyse the conversion of H_2O_2 in hydroxide ion (OH^-) and hydroxyl radical ($OH^\bullet$), an extremely reactive oxidizing agent that initiates a chain of oxidative reactions responsible for tissue damage. This mechanism is known as Fenton reaction [28]. In addition, superoxide anion can react with the hydroxyl radical to produce singlet oxygen, or with nitric oxide to form another highly reactive species, peroxynitrite ($OONO^-$) [20].

The ROS produced during PDT are responsible for a complex cascade of oxidative reactions that target many biomolecules like DNA, lipids or proteins, which take part in several cellular structures. Protein amino acid residues tyrosine, tryptophan, methionine, histidine and cysteine are some of the major targets of ROS due to their reactivity [20]. The oxidation of tyrosine residues is specially critic because of their involvement in intracellular signal transduction pathways, and may result in radicals that can form dityrosine dimers [29]. Unsaturated lipids from cell membranes and other intracellular membranous organelles, like the endoplasmic reticulum, can undergo ene-type reactions to form lipid hydroperoxides, leading to increased membrane permeability, cell-cycle arrest or membrane disruption [21]. Also DNA nucleotides, especially guanine, can suffer oxidation by ROS. This can lead to DNA strand rupture or DNA-protein cross-link and, consequently, to cell death [20].

1.5. Photodynamic Therapy in clinical practice

The mechanism of PDT has the ultimate aim of selective destruction of a target tissue. This concept has been applied in different therapeutic areas, including oncology, where the therapeutic targets include non-metastasized solid tumours that can be accessed by light. One of the most successful applications of PDT has been the treatment of non-melanoma skin cancers, such as basal cell carcinoma (BCC) or squamous cell carcinoma (SCC), and precancerous lesions such as actinic keratosis (AK) [5]. PDT has also been used in "off-label" regime in the treatment of acne [30]. This success is explained both by the ease of topical application of the drug formulation and of light delivery to the target tissue, and by the cosmetic advantages, in comparison with other therapeutic strategies such as surgery or cryotherapy. Furthermore, in cutaneous applications, PDT has the advantage of allowing the treatment of multiple lesions simultaneously [31]. Currently, PDT with topically administered PS is approved for the treatment of actinic keratosis, basal cell carcinoma and squamous cell carcinoma *in situ*, and PDT with systemically administered PS is approved for the treatment of Barrett's esophagus, esophageal cancer, endobronchial carcinoma and head and neck cancer [32, 33] (Table 1.1).

In addition, several PS are currently in clinical development for several oncologic indications, including head and neck, dermal neurofibroma, colon, lung, mesothelioma, kidney, prostate, bladder, liver, bile duct, skin, cervix and brain cancers [34, 35].

Table 1.2 presents a more comprehensive list of PS in clinical trials with their respective cancer indications.

The PDT protocol is applied in two sequential steps: first, it is necessary to deliver the PS to the target tissue and then perform its irradiation with light of a suitable wavelength. The combination of PS and light initiates the photochemical reaction that generate the ROS responsible for the oxidative cellular damages that eventually will lead to the destruction of the target tissue (Figure 1.3). After the administration, it is necessary to wait a certain period of time so that the PS reaches and preferably accumulates in the target tissue. This period is designated drug-light interval (DLI) and depends on the route of administration, the type of PS and its pharmacokinetics and biodistribution properties. After the DLI period, when the amount of PS in the target tissue reaches its optimal value, the irradiation is performed with light of specific wavelength (often corresponding to the PS absorption band with longer wavelength) in order to deliver a predetermined light dose [36].

During the irradiation the ROS produced will cause oxidative damage to biomolecules and cells structures, thus promoting cell death and eventually tumour destruction [24].

The efficacy of PDT depends on the precise conjugation of the three PDT components and their variables, which represents a major challenge in the optimization of therapeutic protocols in clinical practice. The attainment of the desired therapeutic effect depends on

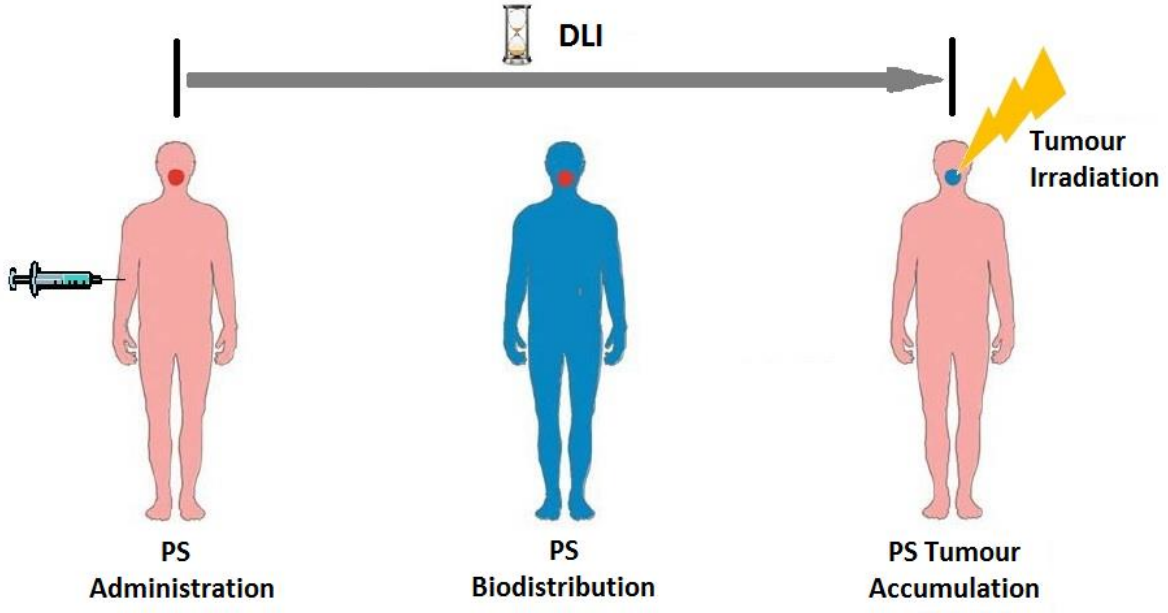

Figure 1.3 – Representation of the clinical application of a PDT protocol for the treatment of a solid and localized tumour.

the type of PS and dose administrated, its intracellular location, the DLI, the total light dose applied, its wavelength and fluence rate, the tumour characteristics, and the local oxygen availability [37, 38].

1.6. Advantages and limitations

The two most critical factors that contribute to the selectivity of PDT are the intrinsic ability of some PS to preferentially accumulate in tumour tissue, and the delivery of light exclusively to the target tissue [39]. The selective accumulation of PS in the tumour is facilitated in the case of topical applications, since the PS is applied directly and only to the lesions to be treated. When PS administration is intravenous (iv), it needs to remain in circulation long enough to reach and accumulate in the tumour. This is often favoured by the fenestrated vasculature and reduced lymphatic drainage, which are characteristics of most solid tumours, allowing the extravasation of PS molecules through tumour vasculature and their passive accumulation in the tumour tissue. This phenomenon is known as the enhanced permeability and retention (EPR) effect [40, 41].

The selectivity of PDT is reinforced by the fact that both singlet oxygen and hydroxyl radical have half-lives of less than one microsecond, which limits its destruction range to not more than 20 nm from where they were formed, avoiding oxidative reactions to spread to the surrounding healthy tissues [29, 42].

The high selective nature of PDT, the ability to destroy tumours while preserving the surrounding healthy tissue, is one of its main features, and is recognized as one of PDT major advantages over traditional therapeutic strategies. The reduced side effects, as a consequence of the high selectivity, and the absence of specific mechanisms of resistance, allow PDT treatments to be repeated if necessary, as in cases of recurrence or presence of multiple lesions. PDT can also be used in combination with surgery, chemotherapy or radiation therapy, since it does not interfere with these treatment modalities, nor presents their typical side effects. Many combinations of PDT with conventional anticancer drugs are also being studied in order to find synergistic effects [43].

The absence of significant sequels after PDT treatments constitutes also a remarkable advantage. During the treatment there should be no thermal effects, although in dermatological treatments patients often report a painful burning sensation, and there is no destruction of connective tissue, allowing tissues to maintain their anatomical and functional integrity [44]. An example is the good cosmetic effect obtained after dermatological treatments, as opposed to the scars that often remain after surgery [39].

PDT can be extremely effective with just one treatment for localized and early stage solid tumours [45]. However, in advanced cases, where tumours are usually larger, PDT has been applied only as palliative treatment, because of the limited ability of light to penetrate through tissues. In such cases, PDT can delay cancer progression and improve the patient quality of life [13, 46].

The difficulties arising from the low penetration of light in tissues demanded for the development of new strategies for efficient light delivery to internal or bulky tumours. The irradiation of internal tumours facing the lumen of body cavities has been successfully accomplished through endoscopy using laser-coupled optic fibres. In larger tumours, the homogeneous distribution of the light dose in the target tissue can be achieved by interstitial irradiation, with the introduction of several optic fibres inside the tumour mass, to ensure that all tumour cell receive the appropriate amount of light [19].

PDT has been mostly recognized as a local therapy that could not treat metastatic disease, and this has been pointed as one of its main limitations [39]. Although, over the years there were clinical reports describing the effects of PDT on patients immune system that affect the development of lesions outside the irradiated area [47]. Today this has become one of the hottest topics in the PDT field, with many research groups committed in understanding and modulating the immune system response induced by PDT. The aim is to favour the

generation of a systemic antitumor immune response with the ability to recognise and eliminate tumour cells outside the irradiated area (e.g. metastasis). If successful, this will bring to PDT a systemic action capability, to complement its local action on the primary tumour [48, 49].

Prolonged skin photosensitivity reactions have been identified as the most significant adverse effect of PDT. This is due to the tendency of some PS to accumulate in the patient skin after the treatment. If activated by sunlight or strong artificial light, the molecules of PS in the skin may start photodynamic reactions, which can cause skin lesions [50, 51]. Thus, patients must avoid direct sunlight exposure, remaining at home under subdued light several weeks after treatment, until the levels of PS in the skin decrease to safe values. Although at first glance this limitation can be considered a small price to pay for the benefits of the therapy, the risk of photosensitivity was responsible for a bad perception of PDT by patients and by doctors, and might have contributed to the slow penetration of PDT in the clinical practice. In the PDT treatments using porfimer sodium (Photofrin®) the skin photosensitivity period can last between 4 and 12 weeks, as with temoporfin (Foscan®) this period is 2 to 4 weeks [51]. Some 3rd generation PS currently in development have pharmacokinetic profiles characterized by a rapid elimination of the compound from the body, which reduces the extension of skin accumulation, and as consequence decreases significantly the risk of photosensitivity reactions [52-54].

1.7. Light, photosensitizers and oxygen

1.7.1. LIGHT

Following the progresses achieved in the development of new PS, the technologies related to light sources and light delivery devices for PDT also experienced significant advances. The selection of the irradiation system depends on the PS absorption spectrum, on the characteristics, size and location of the tumour, and on the size and cost of the system [55]. For dermatological treatments, where the access to the target area is facilitated, the use of lamps associated with optical filters was the standard. Lamps are affordable, require low maintenance and provide a wide spectral output. This fact requires the use of a narrowband filter in front of the lamp allow the selection a wavelength range to match the absorption maximum of the PS. This filter was combined with a longpass filter and a shortpass filter, to cut the lamp UV and the IR emissions, respectively, thus avoiding UV damage and IR-induced heating of the target area [55]. Lamps have been gradually replaced by light-emitting diodes (LED) systems, which are good alternatives due to the low cost and reduced

size. Additionally, LEDs are characterized by fixed narrowband emission, eliminating the need of optical filters, and can be assembled to cover large irradiation areas or complex anatomic shapes [56].

The PDT treatment of internal and/or larger tumours, not readily accessible to light, requires the use of laser systems, which can be coupled to with optic fibres to allow the delivery of light accurately, endoscopically or interstitially, and in appropriate doses to most parts of the organism [24]. The complex, bulky and expensive laser systems used in the past have been replaced by user friendly, reliable and cost-effective diode lasers, The diode laser emits light with fixed wavelength, which requires the existence of PS-specific irradiation devices to match the absorption band of the PS [13, 39].

Being light an essential component of PDT, the clinical efficacy is highly dependent from its accurate delivery to the target tissue and from its precise dosimetry, which is defined by the total light dose (J), fluence (J/cm^2) and fluence rate (W/cm^2) for the PDT protocols with frontal irradiation [24]. For protocols with interstitial irradiation, where cylindrical diffusers are the standard, the irradiation parameters should reflect the length of the diffuser that is introduced in the tumour tissue, with fluence in J/cm and the fluence rate in W/cm [57]. For the purposes of this work only frontal irradiation will be addressed.

The propagation of light in tissues is determined mainly by scattering and absorption, but also by reflection and transmission phenomena, depending on the composition of the tissue and on the wavelength of light. The tissues structure is not uniform due to the presence of macromolecules, cellular organelles and other structures, which have a strong contribution to light scattering, especially at shorter wavelengths [56]. Light absorption by endogenous chromophores, such as haemoglobin or melanin, occurs below 600 nm, while above 1300 nm light absorption by tissue water increases substantially. In addition, light with wavelength longer than 800 nm does not provide enough energy to generate triplet states of PS that can efficiently transfer their energy to molecular oxygen. In PDT, the combination of these factors constraint the useful range of wavelengths in a “phototherapeutic window” that lies between 600 and 800 nm [24, 48].

Light penetration through the tissues is highly dependent on its wavelength, which determines the effective treatment depth of PDT. At wavelengths where endogenous chromophores have weak absorption, light scattering is the most relevant contributor to light attenuation. It is determine by tissue properties and is inversely related to light wavelength. For instance, in human skin the optical penetration depth of light can vary from 1.7 mm at 630 nm, to 2.2 mm at 750 nm [58]. Nevertheless, the effective depth of the treatment may be pushed to around 10 mm at 750 nm depending on the other parameters required by PDT, such as the PS absorptivity coefficient, its local concentration and efficiency of ROS generation, the oxygen local concentration and the tissue sensitivity to oxidative damage

[59]. Great efforts that are been made in the development of new photosensitizers with high absorption at longer wavelengths, with the objective to increase PDT efficacy in larger or deep-seated tumours [20].

1.7.2. PHOTOSENSITIZERS

Many PS used in PDT are porphyrins or their reduced derivatives, such as chlorins or bacteriochlorins, which have in common the tetrapyrrole macrocycle, found also in the haem group of haemoglobin, and in chlorophylls. These molecules present a strong absorption band around 400 nm (Soret band – $\varepsilon \approx 5\times10^5\ M^{-1}.cm^{-1}$) and weaker absorption bands (Q bands) between 500 and 800 nm. The wavelength of the Soret band is not suitable for PDT application because it sits outside of the phototherapeutic window. The Q band with the longest wavelength (Q1) is preferable for PDT, despite its much lower intensity in porphyrins, because it is in the phototherapeutic window, favouring light penetration in the tissues. Within this big family of PS, the typical wavelength of the Q1 band can go approximately from 630 nm in porphyrins up to 750nm in bacteriochlorins [23]. Other suitable properties for PDT applications are their low toxicity in the absence of light and long lifetime of the triplet state [60]. This is of the utmost importance because the higher the triplet lifetime the higher the probability of the triplet state of the PS to encounter and oxygen molecule and generate ROS, which are the key component for the treatment efficacy [61].
As mentioned above, the first compounds to demonstrate therapeutic potential for PDT of cancer were hematoporphyrin derivatives (HPD), of which the purified version and commercially approved porfimer sodium (Photofrin®) represents the 1st generation of PS for PDT. Porfimer sodium is a mixture of photo-active molecules and has a spectrum with several absorption bands which decrease in intensity for longer wavelengths up to 630 nm. To maximize light penetration in the tissue, the excitation of porfimer sodium is carried out at 630 nm (Q1 band), which require the application of high light doses (100-200 J/cm^2) to compensate for its low light absorption. Although it still continues to be used in the clinic, it quickly became apparent that porfimer sodium showed several limitations, e.g. low efficiency due to reduced light absorption and limited light penetration at 630 nm, and a long period of skin photosensitivity as the main side effect [13].
The approval of 5-aminolevulinic acid (Levulan®), followed by its less polar methyl ester aminolevulinate (Metvix®), for actinic keratosis and superficial non-melanoma skin cancers, were important milestones in the history of PDT. Both molecules are prodrugs that, once inside the cell, are metabolized to form the true PS, protoporphyrin IX, an endogenous PS.

Topical application of these prodrugs leads to the accumulation of protoporphyrin IX in cancer cells within 3-4 h of the application [12].

As a result of the continuous efforts to develop more effective PS, in 2001 temoporfin (Foscan®) was approved in Europe. Temoporfin, from the chlorin family, is a pure compound with higher light absorption at a longer wavelength (652 nm) in comparison with porphyrins. Thus, it requires light doses ten times lower and allows an effective treatment depth slightly higher than porfimer sodium. Furthermore, the period of skin photosensitivity after treatment was significantly reduced from 4 to 12 weeks with porfimer sodium to 2 to 4 weeks with temoporfin [13]. Although the approval of temoporfin represented a significant progress when compared with porfimer sodium, there was still a wide margin for improvement regarding the development of betters PS, with improved pharmacokinetic profiles and higher phototherapeutic indexes. In this context, the phototherapeutic index of a PS can be defined as the ratio between its phototoxicity and its toxicity in the dark. This index is an indicator of the advantage of PS with no toxicity in the dark that is well tolerated by the organism, but becomes locally very cytotoxic when illuminated with light of the appropriate wavelength [62].

The characteristics of the ideal photosensitizer for PDT of cancer are consensual among scientists and were described and discussed in several review papers [12, 24, 39]. The ideal PS should be a pure compound with adequate shelf-life and low production cost. It should be capable of strong light absorption ($\varepsilon > 10^5\ M^{-1}.cm^{-1}$) at the longest wavelengths of the phototherapeutic window (700 nm< λ_{max}<800 nm) and high quantum yields of ROS formation (Φ_{ROS}>0.5), to maximize tissue penetration depth and the treatment efficacy, respectively. It should be non-toxic in the absence of light and its physicochemical characteristics should allow the administration in biocompatible formulations and the pharmacokinetic profile should favour its selective accumulation in the target tissue and fast clearance from healthy tissues, in order to minimize the occurrence of side effects. Furthermore, it should demonstrate an adequate resistance to photodecomposition ($\Phi_{pd}< 10^{-5}$) to be able to perform its role before being destroyed by the ROS it produced.

Over the last decade researchers have been working on the development of 3rd generation PS for PDT, which should by activated by light of longer wavelengths, minimize or eliminate the occurrence of skin photosensitivity reactions and demonstrate greater selectivity for tumour tissue [13]. Bacteriochlorins have been regarded as good PS candidates because they typically present intense Q1 bands, with ε around $1\times10^5\ M^{-1}.cm^{-1}$ or higher, in the near-infrared region (720 – 850 nm) where the tissues are more transparent to light and porphyrins and chlorins don't absorb. In addition, they have high quantum yields of triplet state formation, with long half-lives and energies above 115 kJ/mol, which translates in a high potential for ROS production, including $^1O_2$ [63]. Naturally occurring and non-

substituted bacteriochlorins are known for their intrinsic chemical instability, thus the enhancement of their potential as PS candidates requires structural modifications like the introduction of functional groups around the macrocycle or metals in the central cavity. These modifications can be tuned to improve molecular stability, water solubility, quantum yields of ROS formation, and PK/BD profiles [63].

Padoporfin (WST09 – Tookad®), from the bacteriopheophorbide family, and its water soluble derivative padeliporfin (WST11– Tookad® Soluble) have been in clinical development for prostate and kidney cancer, and are examples of 3rd generation PS [57, 64].

Also, a novel family of bacteriochlorins for PDT was recently synthesized and characterized, demonstrating near-ideal photophysical and photochemical properties [65, 66]. The results from non-clinical development are very promising, in terms of *in vivo* safety profile and antitumour efficacy [67, 68], and the lead compound redaporfin (or LUZ11), the subject of the present thesis, is already in clinical trial for patients with advanced head and neck cancer [69]. Redaporfin is an amphiphilic bacteriochlorin rationally designed to closely fulfil the characteristics of the ideal PS. Its design strategy, chemical structure and properties will be addressed in section 1.15.1.

Table 1.1 lists the approved PS for PDT of cancer in Europe and United States of America (USA). Table 1.2 shows the PS currently in clinical development for oncologic indications.

1.7.3. OXYGEN

The third key component in the PDT mechanism is molecular oxygen. Its importance to the effectiveness of PDT may be neglected, if one assumes that its presence in the tissues is constant. In fact, the O_2 concentration can vary significantly between different tumours and even between different regions of the same tumour, depending on the vasculature density [70]. Especially in deeper solid tumours, often characterized by its anoxic micro-environment, the lack of oxygen can be a limiting factor [71]. In a PDT treatment, the irradiation of the tumour with a high fluence rate may lead to local temporary depletion of O_2. This will stop the production of ROS, and reduce the treatment efficacy [72]. Oxygen depletion occurs when the rate of O_2 consumption by the photodynamic reaction exceeds the diffusion rate of O_2 into the irradiated area [73]. In addition, PDT can cause the occlusion of peritumoral vasculature, reducing the blood flow to tumour tissue and causing more hypoxia [72]. There are strategies to control the O2 levels in the tumour that should be considered during the PDT protocol optimization phase. Through techniques for monitoring

Table 1.1 – Approved photosensitizers for PDT of cancer or precancerous skin lesions in Europe and USA [32, 33].

Photosensitizer	Excitation λ (nm)	Brand Name	Approved Indication
Porfimer sodium	630	Photofrin (USA)	• Oesophageal cancer • Endobronchial cancer • High-grade dysplasia in Barrett's oesophagus
5-aminolevulinic acid (5-ALA)	635	Levulan (USA)	• Actinic keratosis
		Ameluz (Europe)	• Actinic keratosis
		Gliolan (Europe)	• Glioma (contrast agent in surgery)
Methyl aminolevulinate (MAL)	635	Metvixia (USA)	• Actinic keratosis
		Metvix (Europe)	• Actinic keratosis • Basal cell carcinoma • *in situ* squamous cell carcinoma
Hexaminolevulinate (HAL)	635	Hexvix (USA)	• Bladder cancer (contrast agent in diagnostic)
Temoporfin	652	Foscan (Europe)	• Head & neck cancer

the amount of O_2 in the tissues it is possible to adjust the light fluence rate (compensated with the increase of irradiation time to maintain the total light dose) until the rate of O_2 consumption matches its rate of diffusion into the target tissue [70]. This balance can also be achieved by the use of light dose fractioning, i.e. through intermittent irradiation of the tumour [74, 75]. These strategies to increase oxygen reperfusion in tumour showed a limited improvement in tumour response, because they cannot affect pre-treatment hypoxic cells. In addition, they increase treatment duration since more time is needed to deliver the required light dose [71].

Other methods to increase oxygen availability in the tumour have been tested. The combination of PDT with hyperbaric oxygen (HBO) was evaluated in clinical trials that involved the application of PDT inside a hyperbaric chamber. Although the results were not conclusive, there were some cases where the survival time of patients with oesophageal cancer was extended [76]. Other strategy to increase tissue oxygen is the combination of PDT with 100 % normobaric oxygen (NBO) breathing. This was tested *in vivo* with better results than HBO, in terms of long term tumour cures [77].

Table 1.2 – Photosensitizers in clinical development for PDT of cancer [35, 78]

Photosensitizer	Excitation λ (nm)	Indication under study	Clinical Phase
Porfimer sodium	630	• Breast cancer skin metastasis • Hepatocellular carcinoma • Pancreatic cancer • Bladder cancer • Head & neck cancer • Mesothelioma • CNS tumours • Cholangiocarcinoma	I I I II II II II II/III
5-ALA	635	• Head & neck cancer • Benign dermal neurofibroma • Basal cell carcinoma • Colon cancer • Cervix cancer	I I II II II
HAL	635	• Cervix cancer • Basal cell carcinoma	II I/II
Temoporfin	652	• Non-small cell lung cancer	I
Chlorin e6	654	• Non-small cell lung cancer	II
Talaporfin sodium	664	• Glioma • Hepatocellular carcinoma	II III
HPPH	665	• Head & neck cancer • Mesothelioma • Lung cancer	II I II
Silicon phthalocyanine 4 (Pc 4)	675	• Non-melanoma skin cancer • Cutaneous T-cell Non-Hodgkin Lymphoma	I I
Verteporfin	689	• Vertebral metastasis • Pancreatic Cancer • Soft tissue sarcoma	I I/II II
Padeliporfin	753	• Kidney cancer • Prostate cancer	II III
LUZ11	749	• Advanced head & neck cancer	I/II

HPPH – 2-(1-hexyloxyethyl)-2-devinyl pyropheophorbide-α; CNS – Central nervous system; LUZ11 - 5,10,15,20-tetrakis(2,6-difluoro-3-*N*-methylsulfamoylphenyl) bacteriochlorin.

1.8. Photosensitizer biodistribution and intracellular localization

1.8.1. TOPICAL APPLICATION

The easy access to skin lesions contributed decisively for the selection of topical administration as the preferred route for cutaneous PDT treatments. However, the high molecular weight of porphyrin-based PS is an obstacle to skin permeation, which led to the development of prodrugs with lower molecular weights. The 5-aminolevulinic acid (5-ALA) and its ester methyl aminolevulinate (MAL) are much smaller molecules and, therefore, in appropriate formulations for topical application, have a higher ability to permeate the physical barrier of the skin, especially the less polar MAL. Both molecules are metabolic precursors of protoporphyrin IX (PP IX), a photosensitizer molecule produced in the haem biosynthetic pathway (Figure 1.4), present in all types of nucleated cells in the body [12].
The treatment protocol begins with the application of a topical formulation with the precursor molecule directly to the lesions. After the application it is necessary to wait several hours (4-6 h for %-ALA or 3-4 h for MAL) for the compound to penetrate the target cells and be converted into PP IX, which is synthesized in the mitochondria and then accumulates in other intracellular membrane systems [39]. This accumulation is favoured by the saturation of the ferrochelatase enzyme, which converts PP IX in the haem group, and that in some tumour types shows less activity than in normal tissues. This PP IX accumulation in the target cell contributes significantly to the treatment selectivity [79].

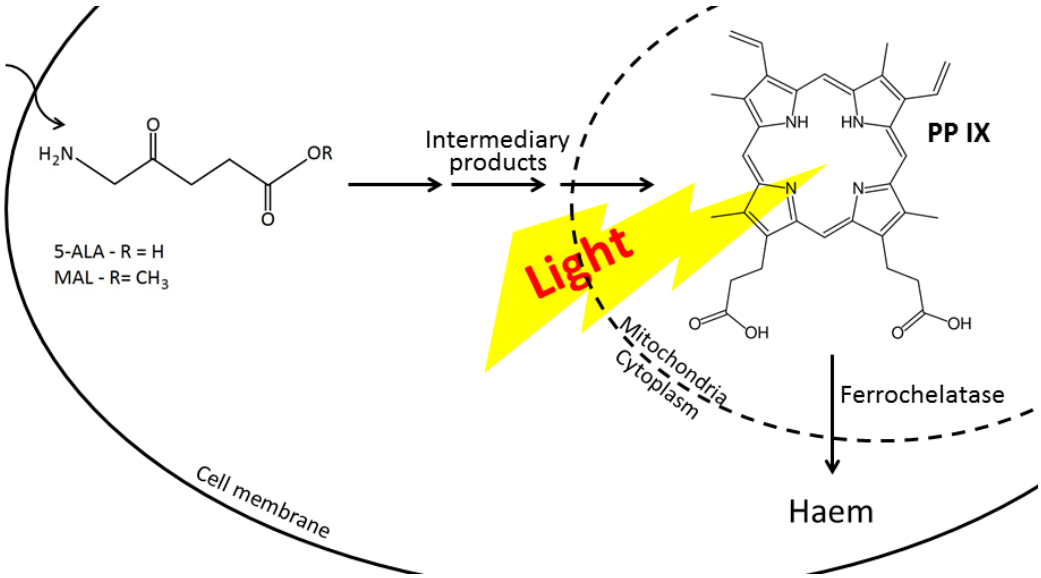

Figure 1.4 – Schematic representation of the production of PP IX through the haem biosynthetic pathway. The exogenous 5-ALA or MAL favours the intracellular synthesis and accumulation of PP IX. After the defined DLI the target tissue is irradiated with 635 nm light.

1.8.2. SYSTEMIC ADMINISTRATION

For the treatment of larger or internally located tumours, the PS must be administered intravenously, so that it can distribute throughout the body and reach the tumour cells. To accomplish this, the PS must be formulated in a suitable vehicle, capable of preventing its aggregation, precipitation and degradation, and prolong its circulation time [80]. The polarity of the PS and the composition of the iv formulation are major factors that determine its pharmacokinetic and biodistribution profiles, and consequently the ability of the PS to accumulate in the tumour [40]. On the one hand, hydrophilic PS are easier to formulate and can be administered in isotonic aqueous media without precipitation and, once in circulation, they preferentially bind to albumin or globulins. However, their polar character can hinder the passage through the cellular membrane (with hydrophobic characteristics), which results in low levels of accumulation in tumour cells, and may favour their clearance from the organism [81]. On the other hand, hydrophobic PS have very low aqueous solubility and a high tendency for aggregation, which strongly decreases its bioavailability and photodynamic activity, so their intravenous administration is not straightforward, often requiring complex formulations such as micelles, liposomes, polymeric nanoparticles or conjugation with hydrophilic polymers [82]. Once in circulation many hydrophobic PS tend to bind to the lipid core of lipoproteins, mainly low density lipoproteins (LDL), taking advantage of the over-expression of LDL receptors in many tumour cells to achieve a selective accumulation. This higher expression of LDL receptors allows tumour cells to capture the extra cholesterol necessary for the biosynthesis of cell membranes required for their rapid proliferation [40].

Some formulations aim to favour PS passive accumulation in the tumour tissue via EPR effect, while other approaches have been developed to further improve PS tumour-specificity, cellular uptake and bioavailability through the use of active targeting strategies, like the PS conjugation with LDL, peptides, monoclonal antibodies (mAb) or other molecules with high affinity for tumours [83].

The optimal formulation should be biodegradable, non-immunogenic and allow the accumulation of PS in the target tissue in therapeutic amounts while minimizing or eliminating its interaction with healthy tissue. It must also allow the delivery of PS in its monomeric and therapeutically active form [84].

Redaporfin is an amphiphilic PS in development for iv administration, with very low solubility in aqueous media. Thus, the development of a suitable formulation must be rationally planned. The vehicle should be composed by approved and well tolerated excipients, to facilitate its translation to the clinic and avoid unnecessary safety risks. It should be capable

of deliver a large dose of PS, and an adequate clearance rate to allow to evaluate the effect of a broad range of DLI on the treatment efficacy. In addition, it should be simple to produce in large scale, affordable and with long shelf-life.

1.8.3. INTRACELLULAR LOCALIZATION

As mentioned above, one of the factors that contributes to the selectivity of PDT is the very short life of ROS at the site of irradiation, which limits their range of destructive action to less than 20 nm [42]. Thus, the localization of the PS in the tumour determines, to a large extent, where the oxidative stress induced by PDT will produce the first cellular damage. The cellular uptake and intracellular localization depend mostly of the charge, polarity, size and degree of asymmetry of the PS molecule. Hydrophobic PS with up to two negative charges can enter cells by diffusion through the cellular membrane and subsequently localize in the non-polar environment provided by the intracellular membrane structures such as the endoplasmic reticulum (ER) or Golgi apparatus. This type of PS tend to accumulate in tumour cells even when its concentration in the extracellular medium is low. The ER is a very important target of oxidative stress because of its role on the immunogenic cell death (ICD) that will be further discussed in section 1.13.3. On the other hand, hydrophilic PS or compounds with more than two negative charges, because they are too polar to cross the cellular membrane by diffusion, they can only be internalised by endocytosis, and be located in lumen of the lysosomes formed by the endocytic pathway [20, 80].

Positively charged but hydrophobic PS tend to be located in inner membrane of mitochondria, attracted by the negative membrane potential and nonpolar environment. Mitochondria are considered a very important intracellular target in PDT because their destruction by photodynamic reaction can trigger apoptosis, a mechanism of programmed cell death [20].

The PS don't have the tendency to localize in the cell nucleus and, therefore ROS generated by PDT have no direct effect on its DNA, which greatly reduces the risk of occurrence of mutagenic effects, often associated with chemotherapy or radiotherapy treatments [37, 85].

In PDT, the study of PS intracellular localization is of great importance, because it allows to relate the preferred intracellular localization with the photodynamic effect obtained, and thus can guide the selection of the most suitable PS for the intended application [86].

1.9. Mechanisms of cell death

Studies carried out so far show that cell death caused by PDT can be mediated by three mechanisms of cell death (apoptosis, necrosis or autophagy) mentioned in a previous section. The contribution of each one to the final outcome of PDT depends on the tumour type, the PS characteristics and the multiple factors related to the treatment protocol. The results suggest that in more aggressive PDT protocols (high PS and light doses, and short DLI) tend to cause extensive cell death by necrosis, unlike less intense protocols that appear to favour apoptotic cell death [87]. It should be remembered that light distribution in tumour tissue is not homogeneous, because of the strong attenuation of light by tissues. Also the oxygen concentration is not constant through the tumour tissue. The combination of both factors will result in a heterogeneous intra-tumour ROS production, with different areas of the tumour subjected to different levels of oxidative damage. This will certainly have a negative impact on the overall efficacy of the treatment and on the predictability of the outcome. Thus, it is pivotal to understand the influence of the factors that define the PDT protocol on the cell death mechanisms elicited by PDT, and to correlate them with tumour response and treatment outcome.

1.9.1. AUTOPHAGY

Autophagy is a catabolic cellular mechanism that enables eukaryotic cells to recycle their components. In a normal situation this mechanism allows cells to digest proteins and damaged organelles or pathogens, but in stress situations it may allow the redistribution of nutrients to processes essential to their survival. However, in more extreme conditions it can also lead to cell death due to excessive digestion of essential components [37, 87].
Autophagy can also present this functional dichotomy in response to PDT. Under certain conditions it may allow cells to recover from the damage inflicted by PDT and survive and, in other, may lead to cell death in response to the treatment [88]. The available data seem to indicate that with PDT protocols where apoptosis is the major cell death pathway, autophagy functions as a cell repair mechanism, protecting the cells affected by oxidative destruction and reducing treatment efficacy. In other situations, when the cell apoptotic mechanisms are destroyed by PDT, there can be a sharp increase in autophagic activity that promotes cell death, leading to tumour destruction [89, 90]. However, the mechanism responsible for switching between the protective and the destructive autophagic pathways is still unknown [24, 91].

1.9.2. APOPTOSIS

Apoptosis is described as a mechanism of programmed cell death that is genetically encoded and energy dependent (in the form of ATP). In morphological terms, it is characterized by chromatin condensation, cleavage of chromosomal DNA, cell shrinkage, wrinkling of the cell membrane with formation of apoptotic bodies, and exposure of phosphatidylserine on the cell membrane outer leaflet [87, 91].

PS that tend to localize in mitochondria, the ER or lysosomes are often very effective in promoting tumour cell death via apoptosis after irradiation. In response to PDT, the apoptotic mechanism can be triggered by the release of cytochrome C from photodamaged mitochondria, or by the destruction anti-apoptotic protein Bcl-2, present both in mitochondria and the ER. This triggers a complex signalling pathway, involving ATP-dependent activation of caspases, that lead to the cell morphological alterations described above, and finally to cell death [92, 93]. In addition, apoptotic cells secrete into the extracellular environment signalling molecules that attract phagocytic cells, which are responsible for the removal of the resulting apoptotic bodies, avoiding the inflammation process and the subsequent activation of the immune system [85].

The fact that less intense PDT protocols favours cell death via apoptosis, can be explained by the necessity that the required complex cellular machinery remain functional, which may not be the case after more aggressive PDT protocols [87].

1.9.3. NECROSIS

Necrosis is a cell death mechanism described as a form of rapid degeneration of relatively large cell populations, which is characterized by expansion of the cytoplasm, organelle destruction and cell membrane disintegration, leading to the release of the cytoplasmic contents and pro-inflammatory mediators into the extracellular medium, which trigger the development of a local inflammatory reaction [37, 94]. This mechanism tends to be favoured by more aggressive PDT protocols, with high doses of PS and/or light, and also by PS that tend to accumulate in the cell membrane [87].

Necrosis since long has been described as a passive and uncontrolled mechanism of cell death. However, there are evidences suggesting that necrosis can be triggered by mitochondria-related signal transduction pathways, with definable molecular effectors, that can be common with apoptotic pathways. The degree of mitochondria damage seems to

determine the cell death mechanism, with necrosis being favoured by damaged mitochondria, incapable of ATP production [95, 96]. This led to a new concept of cell death termed regulated necrosis [93, 97].

The cell death mechanisms elicited by PDT depend mainly on the cellular structures directly affected by the oxidative stress. It seems that the autophagic pathway can be activated as a cell defence mechanism in attempt to control the oxidative damages though the recycling the affected proteins and structures. Above a certain threshold of destruction, when cellular repair is no longer viable, occurs the activation of the apoptotic pathway. When the PDT protocol is extremely aggressive, causing the destruction of the cellular machinery necessary for autophagy and apoptosis and the loss of cell integrity, necrosis becomes the only possible route for cell death [87].

1.10. Mechanisms of resistance

The development of drug resistance is a major barrier to efficacy in cancer therapy. This is often attributed to the appearance of populations of tumour cells that are insensitive to cytotoxic drugs, due to reduced drug uptake or increased drug efflux, modifications on the drug target, or activation of alternative cell survival pathways [92]. PDT efficacy can also be affected by alterations in PS uptake, intracellular localization, or efflux from tumour cells. In addition, decreased activation of PS, by insufficient delivery of light, oxygen, or both, or increase inactivation, due to PS photodegradation or ROS quenching by intracellular antioxidants, are factors that have been recognized as responsible for reducing PDT efficacy [98]. As stated before, autophagy can also play a role as a repairing mechanism that allows tumour cells to recycle oxidative-damaged organelles and other structures and recover from the PDT-inflicted damages [92].

The active transport of a large class of hydrophobic anticancer drugs from the cytoplasm to the extracellular medium, mediated by a family of membrane transporters known as ATP-binding cassette (ABC), is one of the mechanisms generally associated with multi-drug resistance (MDR) in chemotherapy, and has also been implicated in some cases of decreased susceptibility of some types of cells to PDT [99, 100].

Cellular antioxidants like glutathione (GSH), haeme oxygenase-1 (HO-1) play an important roles in the defence system against oxidative stress. The GSH system represents the first line of defence against intracellular free radicals. GSH acts by reducing free radicals through the action of glutathione peroxidase (GPx), being oxidized to glutathione dissulfide (GSSG), which is then reduced back do GSH by glutathione reductase (GR), using NADPH as

electron donor. HO-1 is an enzyme that catalyses the degradation of haem. Its expression is induced in response to several stress conditions, such as oxidative stress, and has been described as a response to ROS generated by PDT [100, 101]. The superoxide dismutase (SOD), catalase and lipoamide dehydrogenase are other examples of enzymes that can scavenge ROS, thus contributing to reduce cell sensitivity to PDT [100].
Although, these type of mechanisms are part of an intrinsic resistance to oxidative stress that is present on most cells, their levels are not the same in all types of cells, which explain for their distinct antioxidant capabilities and, as consequence, their ability to manage and survive an external oxidative challenge [92].

1.11. PDT dosimetry

In clinical practice, the routine use of PDT requires the application of standard protocols, where all parameters have been previously optimized and defined in order to maximize treatment safety and efficacy. The critical protocol parameters comprising the drug dose, DLI, light dose and fluence rate, and area of irradiation (tumour plus safety margin of healthy tissue), are extensively optimized during the clinical development stage, however in the clinical routine, treatment outcomes can often fall short of the expectations [102]. There are several causes for the low efficacy of PDT protocols, the most common being reduced bioavailability of PS, due to inter-patient PK or metabolic variations, differences in tumour tissue structure that may affect light penetration or distribution, or distinct vasculature densities that can influence PS or oxygen concentration/homogeneity [103]. The unique conjugation of all these factors in each patient is difficult to predict, and is highly prone to negatively interfere with local ROS production, compromising treatment efficacy. To overcome the difficulties in the management of such a complex array of variables, there was the need to create tools for PDT dosimetry, which are still being developed and improved. The objective is to control in real time the availability of the critical parameters during PDT treatment, namely PS, light and oxygen concentration, in order to assure the generation of the amount of ROS needed to obtain the expected clinical outcome [104]. The tools for PDT dosimetry are mainly based on quantitative optical imaging and spectroscopic techniques. The cumulative generation of $^1O_2$ can be monitored directly (direct dosimetry) by following its phosphorescence at 1270 nm, but the complex instrumentation required and the low signal-to-noise ratio are obstacles to its clinical application [105]. Diffuse optical spectroscopy (DOS) technics are being applied in clinical PDT dosimetry, and include diffuse reflectance spectroscopy (DRS), diffuse fluorescence spectroscopy (DFS) and diffuse correlation spectroscopy (DCS). With these methods it's

possible quantify in real time several PDT-dose related parameters, such as the effective local light dose, the PS concentration (and photobleaching) in the target tissue, as well as tissue blood flow and oxygenation (explicit dosimetry). These tools can provide precious information to the design of individually-adjusted PDT protocols that can help to overcome the problems arising from individual tumour environment variations [106].
The constraints associated with inter-patient bioavailability, PK or metabolic variations can be minimized with the optimization of vascular-PDT protocols, e.g. DLI=15 min, when C_{max} is attained and is practically independent of all those factors. The issues related to light penetration can be improved through the modulation of the PS molecular structure, in order to maximise the amount of light, and wavelength, absorbed by the PS. Those were the principles adopted during the design and development of redaporfin.

1.12. Photodynamic threshold dose and effective treatment depth

The level of ROS produced during a PDT treatment must be able to cause a sufficient amount of oxidizing events to promote tumour cell death, otherwise the affected cells will be able to recover from the inflicted damages and continue to proliferate. This borderline level of toxic photoproducts has been termed “PDT threshold dose”, and is determined by the local light fluence, the local concentration of PS and availability of molecular oxygen, and tissue sensitivity to oxidative damage [59].
As stated before, light suffers strong attenuation in the tissues. The light fluence for frontal irradiation of the target tissue (E, in J/cm^2) that effectively reaches at tumour cells located at a certain depth (*z*) beneath the surface can be estimated using the equation [107]:

$$E = E_0 \cdot e^{-\frac{z}{\delta}} \qquad (1.1)$$

where E_0 is the light fluence at the surface and δ is optical penetration depth in cm, which is the distance that causes the light intensity to be reduced to 1/*e* or 37% of its initial value. The optical penetration depth for a given wavelength is determined by the composition and structure of the tissue. For human skin, δ can vary from 1.7 mm at 633 nm, 1.8 at 660 nm, to 2.2 mm at 750 nm, whereas in human mucous tissue, δ is approximately 3 mm at 633 nm [58]. The local concentration of PS at the time of irradiation can be quantified through biodistribution/PK studies or by direct measurement of tissue fluorescence, and the O_2 concentration in the target tissue can be assessed *in vivo* by EPR [108]. The ability of tumour cells to withstand oxidative stress is variable and dependent on the antioxidant defences that characterize the cells of a specific tissue. The reports on the threshold level

of ROS that needs to be generated for cell death to occur can vary between 0.9 and 12.1 mM, which probably covers a wide range of tumour types [109, 110]. Without considering PS photodecomposition, the local concentration of ROS (M) produced by PDT can be estimated using the following equation [107]:

$$[ROS]_{local} = \phi_{ROS} \cdot \left(\frac{\lambda \cdot 1000}{h \cdot c \cdot N_A}\right) \cdot E \cdot \varepsilon \cdot [PS]_{local} \qquad (1.2)$$

where ϕ_{ROS} is the PS quantum yield of ROS production, λ is the light wavelength (cm), h is the Planck's constant (6.6×10^{-34} J.s), c is the speed of light (3.0×10^{10} cm/s), N_A is the Avogadro's number (6.0×10^{23}), E is the light fluence that reaches the target tissue, determined with equation (1), ε is the PS extinction coefficient ($M^{-1}.cm^{-1}$), and $[PS]_{local}$ is the local concentration of PS (M). The influence of the PS photophysical properties on the effective depth of PDT can be better understood though the comparison between distinct PS, with similar photodecomposition constants, using the data reported in the literature. With equations (1) and (2) and assuming an hypothetical PDT protocol with a light fluence of 50 J/cm^2 that needs to generate 10 mM of ROS to promote cell death, applied to a tumour when the local PS concentration is 10 μM, it's possible to estimate the maximum depth of necrosis that a given PS would reach. In this conditions temoporfin (Foscan®) [111], a chlorin, should be capable to cause cell death up to z = 3 mm, while Porfimer sodium (Photofrin®) [112], from the porphyrin family, would need a local concentration around 140 μM just to reach a depth of necrosis of z = 1 mm in this conditions. In the same conditions a bacteriochlorin named ClBEt [65], in development for PDT of cancer, should be able to double the depth of necrosis obtained with temoporfin, to reach a z of at least 6 mm.

1.13. Modes of action of Photodynamic Therapy

In oncology, the objective of a PDT treatment is the complete and definitive elimination of a solid tumour. This outcome depends on three distinct effects, depicted in Figure 1.5, that appear to be interconnected [40].

1.13.1. EFFECTS ON TUMOUR CELLS

The oxidative damages directly inflicted by PDT-generated ROS on tumour cells have been the primary goal of PDT in cancer treatment. As described in a previous section, the three

main cell death mechanisms - necrosis, apoptosis and autophagy - can be observed in result of the irreversible oxidative destruction of key biomolecules and cell structures by ROS generated in the photodynamic reaction [113]. The extension of each cell death mechanism depends on the cellular organelles damaged, which in turn are determined by the intracellular localization of the PS at the time of irradiation [37].

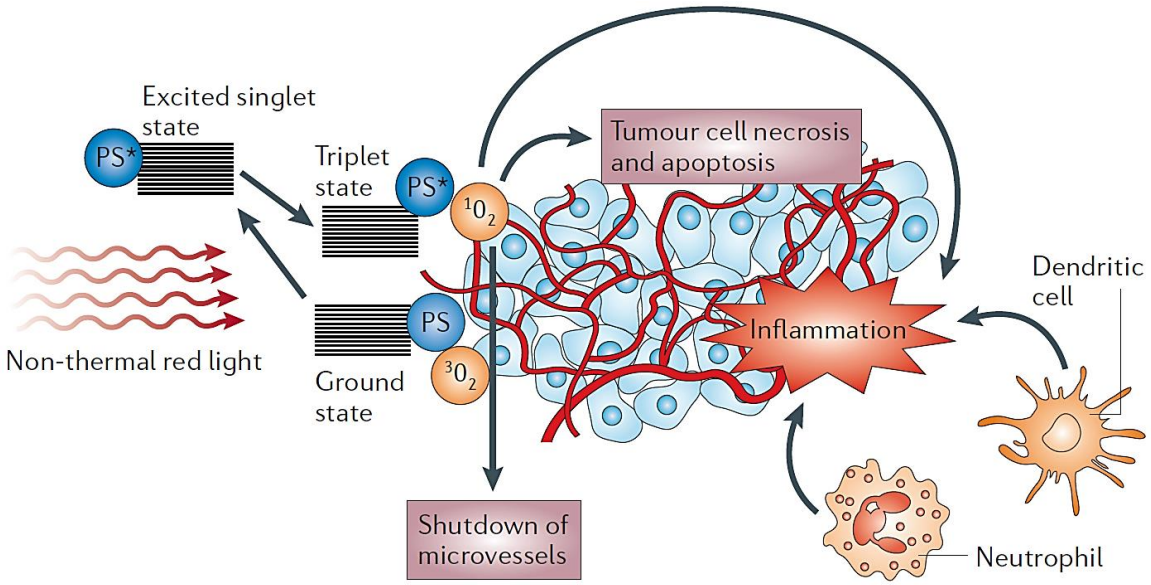

Figure 1.5 – Representation of the photodynamic reaction mechanism and the consequent effects leading to tumour destruction after PDT (Reprinted by permission from Macmillan Publishers Ltd: Nature Reviews Cancer [48], copyright 2006).

The direct cytotoxic effect on tumour cells can be favoured by protocols with long DLI (e.g. > 24 hours), to allow the selective accumulation of PS in tumour cells relative to surrounding healthy tissues and vascular compartment, contributing to increase the treatment selectivity. This type of PTD action is known by cellular-PDT [40].

1.13.2. EFFECTS ON BLOOD VESSELS

In addition to the oxidative damage caused directly on tumour cells, the application of PDT often leads to the destruction of tumour microvasculature, leading to the interruption of oxygen and nutrients supply and, consequently, to tumour cell death [114]. The effects of PDT in tumour microvasculature are mainly related to endothelial cell damage. Depending on the PS used, these effects may be related to decrease in nitric oxide levels, platelet activation and thromboxane release, which cause vasoconstriction, leukocyte adhesion, platelet aggregation and thrombus formation [57, 108, 115]. Several studies showed that

this vascular effect is very important for the long-term efficacy of PDT, and therefore the development of protocols for vascular-PDT is a strategy currently under great attention. In practical terms, the PDT protocols that favour the photodamage of tumour vasculature require the iv administration of the PS and a short DLI (e.g. <30 minutes), so that tumour irradiation is performed when most of the PS is still in the vascular compartment [53]. Thus, it sacrifices the potential gain in selectivity that could be obtained with the selective accumulation of the PS in the tumour (which requires longer DLI) to obtain a gain in efficiency through the destruction of the tumour vasculature. In vascular-PDT protocols selectivity is achieved by the precise application of light on the tumour plus a safety margin of the surrounding healthy tissue [115].

There are several advantages of vascular-PDT, in comparison to PDT protocols that require PS accumulation in the tumour cells (cellular-PDT), namely the higher long-term efficacy, the use of PS with PK/BD profiles that favour their rapid clearance from the body, decreasing the risk of skin photosensibility reactions, and the possibility to be performed in one short clinical session in an out-patient basis [116].

1.13.3. EFFECTS ON THE IMMUNE SYSTEM

Traditional antitumour therapies are known by their undesirable side effects. Among others, the therapeutic doses of chemotherapy or radiation therapy usually cause immunosuppression due to their bone marrow toxicity, which decreases the production of cells essential for the immune system's activity [48].

For many years PDT was considered a localized treatment, affecting only tumour cells and tumour microvasculature. More recently, it has been demonstrated that PDT can have a significant impact on the patient's immune system, either through stimulation or by suppression of the immune response. The PDT-induced immune response can contribute significantly to the effectiveness of the therapy, and may even affect the development of disseminated tumours, in regions outside the irradiation field [117-120]. These important breakthroughs were mostly from studies with animal models, but there are also clinical PDT reports that confirm the existence of a systemic antitumour response induced by PDT [47, 121].

In certain conditions PDT can also induce immunosuppression, which have mostly been associated with reactions to topical treatments with high fluence rates and in large irradiation areas. They can be local [48, 122] or systemic [123], and may contribute to reduce treatment efficacy. Most studies available have been focused on contact hypersensitivity (CHS) reactions to evaluate local immunosuppression induced by topical

PDT. Some clinical studies suggest that immunosuppression may be related with the decreasing of Langerhans cells or with DNA damage, and that it can be significantly reduced by using low fluence rate protocols or with concomitant oral or topical administration of nicotinamide (to replenish cellular ATP levels and favour DNA repair) [124-126].

In contrast, non-topical PDT treatments are often described as immunostimulatory. The oxidative damage inflicted by PDT on tumour stroma (mainly tumour cells, endothelial cells, fibroblasts, pericytes and macrophages) will eventually result in cell death. This change in tissue integrity and homeostasis elicits an acute inflammatory response initiated by the release, secretion or surface exposure by the damaged or dying cells of pro-inflammatory mediators known as damage-associated molecular patterns (DAMPs). The type of DAMPs released/exposed are dependent on the intracellular structures that were oxidatively damaged and, consequently on the induced cell death mechanisms, and can include heat shock proteins (HSP), calreticulin (CRT), ATP or other molecules such as tumour necrosis factor α (TNF-α), interleukin-1β (IL-1β) or interleukin-6 (IL-6), macrophage inflammatory proteins 1 and 2 (MIP-1 and MIP-2), adhesion molecule E-selectin and intercellular adhesion molecule [87, 127, 128]. These mediators attract the host innate immune cells like neutrophils, mast cells, macrophages and dendritic cells (DC), which infiltrate in damaged tissue to restore homeostasis in the affected region. They promote the phagocytosis of damaged cells and cell debris, resulting from cell death, in the target tissue and are fundamental to the subsequent activation of the adaptive arm of the immune system [48].

The local acute inflammatory response following PDT has been considered the trigger for the activation of specific antitumor immunity, which can play an important role in long-term tumour control [87, 127].

DC play a relevant role in the bridge between the innate and the adaptive arms of the immune system. When infiltrating in the region affected by PDT, DC are activated by pro-inflammation mediators, capture tumour antigens present in the extracellular environment and then return to nearby lymph nodes. Once there they expose tumour antigens, making them accessible to CD4+ T cells that become activated. These in turn stimulate CD8+ cytotoxic T lymphocytes, which acquire the ability to recognize and specifically destroy tumour cells and can circulate throughout the body for long periods of time, ensuring a systemic antitumour immune response [24, 40, 48]. The scheme in

Figure *1.6* represents the mechanism of immune system activation induced by the PDT.

The balance between the occurrence of apoptosis and necrosis depends on the PS characteristics and on the PDT protocol parameters and has direct influence on the extent of the immune response induced by PDT [91]. This is a very complex and controversial issue is dividing opinions among researchers and there are conflicting theories about which pathway is more effective in the activation of the immune system. On the one hand, there

are those who stand by the traditional theory that apoptosis is a highly regulated cell death mechanism, meant to avoid inflammatory processes and immune system activation [129, 130] . They argue that the PDT protocols favouring necrotic cell death are much more effective in stimulating the immune response because, unlike apoptosis, where the cell

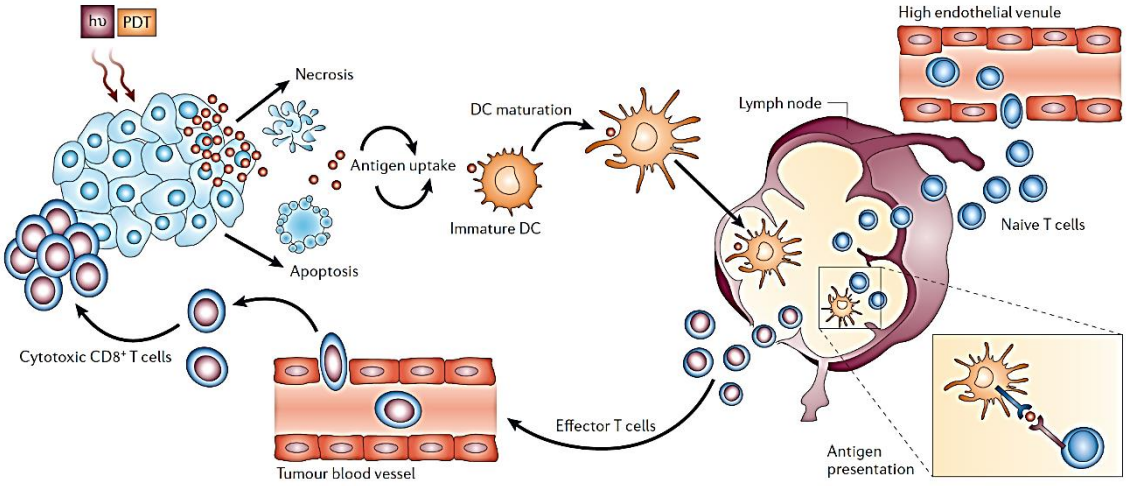

Figure 1.6 – Representation of the activation of the host immune system following PDT (Reprinted by permission from Macmillan Publishers Ltd: Nature Reviews Cancer [48], copyright 2006).

cytoplasmic contents remain in isolated membrane vesicles, necrosis is characterised by disintegration of cellular membrane with release of cytoplasmic contents into the extracellular medium. This results in the exposure of tumour antigens that are usually confined to the intracellular environment, and originates a strong local inflammatory response that favours the systemic mobilization of the innate and adaptive immunity [24, 48, 87]. On the other hand, there has been a growing number of voices defending that, under certain stress conditions, like oxidative stress, apoptotic cell death can also promote local inflammation and immune response [91]. They distinguish the physiological apoptosis, a cell death mechanism meant to avoid inflammation and favour immune tolerance, from stress-induced apoptosis, which is associated with the release/exposures of DAMPs that are able to induce an immune response against the dying cells. This apoptotic mechanism has been associated with the cellular oxidative stress elicited by PDT protocols that target the ER [131]. Because it's now clear that the immunogenicity of the dying tumour cells can have a high impact on PDT clinical outcome, and that both PDT-induced apoptosis and necrosis are capable of triggering immune system activation, a new concept has been defined and pursued as the Holy Grail of cancer treatment, the Immunogenic Cell Death (ICD) [130, 132, 133].

The in-depth study of the mechanisms involved in the immune response induced by PDT is thus a major priority for many research groups. There are many studies with animal models, mostly rodents, with important contributions towards the understanding of the phenomenon, and that have also tried various combination strategies of PDT with adjuvants in order to enhance the response of the immune system and its contribution for PDT efficacy [134-137].

One of those studies by Mroz and co-workers, was able to demonstrate that, in BALB/c mice with subcutaneous colon tumour of CT26.CL25 cells, the application of a vascular-PDT protocol resulted in a high rate of long term cures. The high efficacy was attributed to the activation of the immune system by PDT, confirmed by the analysis of specific molecular markers. It was also demonstrated that the systemic antitumor immune response was strong enough to allow the cure of a tumour located outside the irradiation field, and sustained over time, allowing animals previously cured by PDT to reject a second inoculation of the same tumour cells, three months after the PDT treatment. The need for a functional adaptive immune system was confirmed when, under the same conditions, the protocol was used for treating tumours in immunocompromised animals. In this case there was no definitive cure of the primary tumour and there was no influence on the growth of a second tumour outside the irradiation field [120].

In other *in vivo* studies, it was reported that the combination of vascular-PDT with an approved chemotherapy drug cyclophosphamide (CY) was able to enhance the immune system activation, with a significant contribution towards long-term tumour cures and the induction of sustained and systemic antitumour immune memory. The role of CY was to deplete the regulatory T cell population (Treg) that are involved in the maintenance of immune homeostasis and tolerance to self-antigens [135, 138].

This systemic antitumor immunity induced by PDT is currently being described as the key to the improvement of long-term PDT efficacy, complementing the effect of ROS in the destruction of tumour cells. Ideally, PDT treatments would act as antitumour vaccines with sustained systemic action capable to destroy metastases that may exist elsewhere in the body [139].

1.14. Recent developments

Although the concept of PDT for cancer treatment had appeared more than one century ago, the penetration of PDT in oncological clinical practice has been quite slow. The lack of PS with the ideal attributes, the complexity in treatment protocol optimization and the technological resources required may discourage its clinical application, leaving PDT as a

last resort option or as palliative treatment. Also contributing for the low clinical acceptance are the relatively long periods of skin photosensitivity associated with the marketed photosensitizers, which demand that patients have to stay indoors, in environments with reduced light, during several weeks [24].

For a long period of time the main limitations of PDT were the localization of tumours in areas not accessible by light and tumours with sizes beyond the capacity of light penetration in the tissues. However, the efforts to circumvent these difficulties have succeeded and with the use of light sources coupled to optical fibres that through endoscopy or vascular catheterization it is possible to deliver light to virtually all regions of the body [24]. Moreover, the effective irradiation of larger tumours, has been accomplished by the combination of advanced PDT dosimetry techniques with interstitial application of light (iPDT), which consists in the image-guided introduction of one or more optical fibres into the tumour mass, so that the appropriate amount of light can be homogeneously delivered to all target cells [140].

Despite all difficulties, PDT continues to be a valued therapeutic strategy with great potential for cancer treatment. PDT is progressively gaining acceptance in the clinical setting due to the continuous efforts towards the better knowledge of the mechanisms and physiological responses involved, together with the technical improvements on dosimetry technics, light sources and the ability to deliver light to the tumour, which will allow the better exploitation of the existing PS and also the new PS with properties closer to the ideal [12].

Many efforts are currently focused in the improvement of PS specificity to the tumour tissue. Various strategies have been tested, namely the encapsulation of PS molecules in nanoparticles, such as liposomes, with or without active targeting, or its coupling with specific ligands for receptors on the target tissue [141, 142]. However, the potential benefits of this strategy have been questioned, since the vascular-PDT protocols have shown greater efficacy than those that aim at the selective accumulation of PS in the tumour [12, 24].

Two-photon PDT is a strategy to increase the effective depth of treatment in PDT and is being studied for some time. This technique uses high-peak-power laser pulses (approximately $100x10^{-15}$ seconds), which allows each PS molecule to absorb two photons simultaneously. Since the energy of the two photons absorbed is combined, it is possible to use light with a wavelength above 800 nm and still overcome the energy threshold that trigger the PDR, unlike of what occurs with traditional PDT. The use of longer wavelength light significantly increase its tissue penetration depth, allowing the treatment of larger or deeper tumours. Using the pulsed laser it is also possible to substantially increase the selectivity of light application, by focusing the beam only in one particular point in depth, it allows the treatment of small areas with reduced damage to adjacent tissues. The technical

challenges that need to be overcome are still significant and are mainly related to the development of new PS with high two-photon cross sections and that simultaneously exhibit adequate pharmacological properties [143]. In addition, the high cost and complexity of pulsed laser systems, the onset of thermal effects with femtosecond lasers, or the difficulties with optical fibres coupling, may discourage the clinical application of this strategy [102].

Metronomic PDT is another approach that is being explored for use in situations where the inflammatory response caused by cell necrosis is discouraged. In this strategy the PDT treatment is performed with low doses of PS and light to favor the occurrence of apoptosis and minimize the occurrence of necrosis. This technique has been applied in the treatment of glioma, for the elimination of tumor cells in the margins left after surgery, preventing the occurrence of acute inflammatory response, which in that cases can be harmful for the surrounding healthy tissue [144].

Other promising strategies are exploring the ability of PDT to stimulate the patient's immune system, especially in the areas related to immunogenic cell death and antitumour vaccines, which are currently among the most desirable topics of modern medicine. Several strategies are being studied in order to amplify the intrinsic immune activation effect of PDT, either by combination with nonspecific immuno-stimulants, like microbial-derived agents or drugs [43, 49], or through the creation of a PDT antitumour vaccine with systemic and antitumor-specific action. The strategy of conventional vaccines is based on the introduction into the body of the inactivated infectious agent, which leads to the production of specific antibodies that in a future contact with the same agent will initiate the immune response for its elimination [119, 145]. To generate an antitumour vaccine with PDT, tumour cells would be removed from the patient through biopsy or surgery and cultured *in vitro*. These cells would then be destroyed using PDT, to create a highly immunogenic tumour cell lysate that would be reintroduced into the patient circulation to stimulate the immune system response against tumour cells. In clinical terms, this approach would target the primary tumour and its potential metastasis. These strategies are still in early stages of development, but there are high expectations regarding their future application in oncology [146].

1.15. Development of redaporfin for PDT of cancer

Cancer represents a growing worldwide socioeconomic concern that can be attributed to the increase in the overall incidence rates and in the types of cancer that do not respond to current therapies [147]. In addition, the costs of development of innovative drugs has been increasing dramatically, while the approval rates of new drugs are going in the opposite direction, affecting also the oncologic segment [148, 149]. The process of development of

new drug candidates is very long and increasingly complex, thus bearing a high risk of failure. Typically, it begins at the process of drug discovery, with target identification and validation and lead compound screening, followed by further nonclinical studies, focused on the evaluation of safety and efficacy. Here the main goals are the identification of the pharmacologic properties of the drug candidate, and the evaluation of its toxicological profile *in vitro* and *in vivo*, highly relevant for the first clinical trial application. The clinical development stage is, by far, the longest, most complex, and expensive part in the development programme of a new drug. At that stage, the main objective is to gather evidence that demonstrate the safety and efficacy in the intended patient population, which will largely support the final regulatory approval [150, 151].

This state of affairs since long forced the regulatory authorities to take action in order to soften the attrition rates in the drug development pathway and to attract R&D investment for unmet medical needs, like high risk drug candidates or rare diseases, and to increase the number of candidates entering the clinical development stage and to reach the market [152]. As examples, the Innovation Task Force (ITF) created by EMA in 2001, and the Critical Path Initiative (CPI) implemented by FDA since 2004, both contributing for the introduction of a new drug development paradigm, based on powerful scientific and technological methods to identify and eliminate sooner the bad candidates, thus saving millions on developments costs [153]. Such methods include *in silico* predictive models, validated biomarkers for safety and efficacy, together with new clinical evaluation techniques [148].

These strategies were followed by the implementation of specify drug development programmes, created to facilitate and reduce the costs of the development, and accelerate de review of new drug candidates for indications categorized as rare diseases, serious or life-threatening conditions and unmet medical needs [154, 155]. These global efforts to expedite the translation of new medicines into the clinic, through the optimization of resources and regulations for the development and approval of new drug candidates were accompanied by significant changes in the guidelines related to nonclinical and clinical drug development [150].

This was the main motivation behind the implementation of the ICH S9 guideline in 2010, which applies specifically to the “Non-clinical evaluation for anticancer pharmaceuticals”, either small molecules or biologics [156]. This guideline provides recommendations for the non-clinical studies necessary to support the design and approval of the first clinical trials in cancer patients with advanced disease and limited treatment options, contributing to expedite de development of new and effective anticancer drugs. The main focus is to improve development efficiency and reduce the time to the clinic, by increasing the acceptable health risks in the treatment of advanced cancer patients [157]. In practice, it

allows the reduction of the non-clinical toxicology package necessary to support the first clinical trial in advanced cancer patients, which aim to assess the safety of the drug through dose escalation and dose-limiting toxicity studies. Several standard toxicology studies like the repeated dose toxicity in a non-rodent species, genotoxicity or reproductive toxicity can then be reduced or deferred to later stages of the development [150, 157].

This strategy was adopted for the development of redaporfin in order to expedite the approval of the first-in-man clinical trial, in patients with advanced head-and-neck cancer. Following the non-GLP studies to assess the safety and efficacy *in vivo*, presented in this thesis, the non-clinical GLP toxicology package was outsourced to a CRO. This package included the evaluation of metabolic profile of redaporfin *in vitro* and the single-dose toxicity in two animal species. Based on the metabolic profile results, the rat (rodent) and the dog (non-rodent) were selected as the relevant species for the single-dose toxicity studies. These included the evaluation of the pharmacokinetic profile of redaporfin and its effects on the respiratory function and on the central nervous system, and constituted a fundamental part of the clinical trial application for redaporfin.

1.15.1. PROJECT CONTEXT

The origin of this adventure can be traced back to 1994 and to the Chemistry Department of the University of Coimbra. It started with a research project “Molecular modulation of heterocycles and structure-activity relationships” that intended to design and synthesis of a new generation of PS, using physical and mathematical models. This was followed in 2002 by another project “Synthesis of novel PS for PDT modulated by Franck-Condon factors”. At that point, the expected attributes of the ideal photosensitizer and the promising reports on the photodynamic activity of some naturally occurring bacteriochlorins that shared some of those attributes [158, 159], inspired the idea to rationally design bacteriochlorins with potential for PDT application. Back then synthetic bacteriochlorins were characterized by their very low stability, and because of that, the focus of most research groups was on chlorins [160]. However, the team successfully created a new family of *ortho*-halogenated tetra phenyl porphyrin derivatives, including stable bacteriochlorins that showed an impressive set of near-ideal photophysical and photochemical properties, which could take advantage of the higher light absorption at longer wavelengths to potentially increase the effective treatment depth in PDT. The synthetic route to prepare this new family of PS was developed following the principles of simplicity, economy and feasibility of scale-up, and is thoroughly described in the literature [161-164]. The next project was focused on the optimization of the PS properties to improve their potential for application in PDT of cancer. The synthesis, characterization and *in vitro* screening activities progressed closely together,

with constant feedback on the structure-activity relationships, allowing the gradual tuning of the PS properties, through the modification of functional groups and substituents, to create a PS candidate with near-ideal attributes [165]. The substitution of an hydrogen by an halogen atom in the positions 2 or 2,6 of the phenyl groups increased the intersystem crossing rate by promoting the spin–orbit coupling in the electronically excited orbital, a phenomenon known as the "heavy atom" effect. This contribute to a significant enhancement in the PS triplet state quantum yield and lifetime, and consequently can lead to an increase in the singlet oxygen quantum yield. Moreover, the substitution with fluorine atoms also increased the oxidation potential of the molecule, resulting in a higher stability against oxidation [61]. In addition, the modulation of the amphiphilic properties of the porphyrins was done through the functionalization in the phenyl *meta* positions by chlorosulfonation, followed by reaction with water or amines with different chain lengths to give molecules with partition coefficients (Log $P_{n\text{-octanol/water}}$) between -3 and 4 [166, 167], similar to those measured for the correspondent bacteriochlorins [65]. This family of bacteriochlorins is also characterized by an absorption maximum at approximately 745 nm with a molar absorptivity above 100000 $M^{-1}.cm^{-1}$ [168]. During the course of the project two patents were registered to protect the intellectual property [169, 170].

Table 1.3 – Properties of 5,10,15,20-*tetrakis*(2,6-difluoro-3-*N*-methylsulfamoylphenyl) bacteriochlorin [171]

Alternative Names		**F_2BMet, LUZ11**
INN		Redaporfin
CAS Number		1224104-08-8
Molecular formula		$C_{48}H_{38}F_8N_8O_8S_4$
Molecular weight (g/mol)		1135.11
Log P $_{n\text{-octanol/water}}$		1.90
Absorption [a]	λ_{max} (nm)	743
	ε_{max} ($M^{-1}.cm^{-1}$)	140000
Fluorescence [a]	λ_{max} (nm)	746
	Φ_F	0.138
	τ_F (ns)	3.0
Triplet [b]	Φ_T	0.65
	τ_T (ns)	216
	k_q ($M^{-1}.s^{-1}$)	2.2
$^1O_2$ formation quantum yield (Φ_Δ) [a]		0.43
Redox potentials [c] **(vs SCE)**	E^o_{red1} (V)	-0.74
	E^o_{ox1} (V)	0.80
	E^o_{ox} (V)	0.80
Photodecomposition quantum yield (Φ_{pd}) [d]		1.0×10^{-5}

[a] in ethanol, [b] in air saturated ethanol, [c] in dichloroethane with 0.1M tetra-*n*-butylammonium perchlorate, SCE - saturated calomel electrode, E_{red1} and E_{ox1} refer to the macrocycle and E_{ox} to the sulfonamide groups, [d] in PBS/methanol.

The possibility to control the physicochemical properties of these molecules is a great advantage because they can be specifically tailored to suit different routes of administration and a broad range of PDT applications.

The biological activity of the new bacteriochlorins was evaluated *in vitro* and *in vivo* in an interactive process that allow to fine tune the molecules that were being tested to maximize their photodynamic activity. All these efforts converged in the selection of 5,10,15,20-*tetrakis*(2,6-difluoro-3-*N*-methylsulfamoylphenyl) bacteriochlorin, code name LUZ11 (INN – redaporfin), as the lead compound to advance further in the nonclinical development, which is the central subject of the work henceforth presented. The most important characteristics of the redaporfin molecule are listed in Table 1.3 and its chemical structure is presented in Figure 1.7.

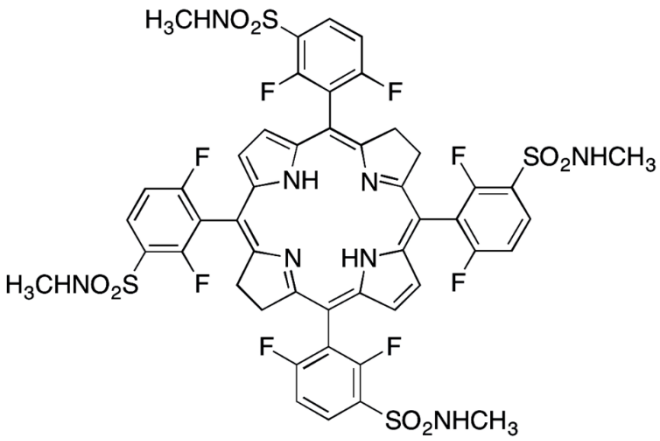

Figure 1.7 – Chemical structure of the lead compound, redaporfin.

This project can be regarded as a good example of translational science. It was born from fundamental research in academic environment, which evolved for a new product/technology that was further develop for clinical application, and has already reached the first clinical trial. The work described in this thesis represents an important contribution for the long and challenging development programme of a new PS for PDT of cancer.

1.16. Objectives

The main goal of the project was to successfully complete the initial stages of the nonclinical development of redaporfin, focusing on the exploratory evaluation of its safety and on the demonstration of its efficacy *in vivo*.

The first tasks aimed at the characterization of biological activity of redaporfin against cancer cells in culture, through the evaluation of the toxicity in the absence of light and the phototoxicity after laser irradiation, and the establishment of a rigorous comparison with the two systemically administered PS already on the market.

This was followed by the development of a suitable formulation for the iv administration of the PS. The target product profile defined for the formulation stated that it should be simple to prepare and to scale-up, well tolerated, capable to deliver a therapeutically relevant dose of photodynamicaly active redaporfin to the target tissue. Its PK/BD profiles should allow a flexible exploration of the different PDT modes of action, for the development of either vascular or selective protocols, in combination with fast elimination after treatment and minimal accumulation in the skin, to avoid the occurrence of adverse reactions.

The next stage was the exploratory evaluation of possible signs of toxicity, related to the PDT treatment with the redaporfin formulation. This *in vivo* preliminary toxicology package included a dose escalation study to determine the Maximum Tolerate Dose (MTD) in mice, the evaluation of haematology and serum biochemistry markers after iv administration and irradiation in rats and the study of skin photosensitivity reactions after the iv administration of redaporfin formulation in rats. These studies served as a guidance for the formal toxicity and safety studies that were subsequently conducted under GLP conditions.

The following task consisted in the development and optimization of a safe and effective PDT protocol in a mouse tumour model. This covered a broad range of DLI, drug and light doses, fluence rates and healthy tissue safety margins. The last, but highly important part of the project focused on the effects of PDT on the host immune system. To understand and to harness the power of the immune system against tumour cells is what separates PDT from being a limited therapy with localized action from its full potential as an anticancer therapy with broad systemic reach. This was accomplished by studding the immune system response after PDT with redaporfin *in vivo*, focusing on the formation of antitumour immune memory, and the development of a systemic immune response capable of targeting tumour metastasis far away from the irradiation field.

Chapter 2

In vitro biological activity

Chapter 2 – *In vitro* Biological Activity

Part of the work presented in this chapter was published in:

Chemistry - A European Journal (2014) 20(18), 5346 – 5357.

Photodynamic Therapy Efficacy Enhanced by Dynamics: The Role of Charge Transfer and Photostability in the Selection of Photosensitizers

Luis G. Arnaut [1, 2], Mariette M. Pereira [1], Janusz M. Dąbrowski [3], Elsa F. F. Silva [1], Fábio A. Schaberle [2], Artur R. Abreu [2], Luis B. Rocha [4], Madalina M. Barsan [1], Krystyna Urbanska [5], Grazyna Stochel [3] and Christopher M. A. Brett [1]

[1] Chemistry Department, University of Coimbra, 3004-535 Coimbra, Portugal

[2] Luzitin SA, Ed. Bluepharma, S. Martinho do Bispo, 3045-016 Coimbra, Portugal

[3] Faculty of Chemistry, Jagiellonian University, 30-060 Krakow, Poland

[4] Bluepharma SA, Ed. Bluepharma, S. Martinho do Bispo, 3045-016 Coimbra, Portugal

[5] Faculty of Biochemistry, Biophysics and Biotechnology, Jagiellonian University, 30-387 Krakow, Poland

2.1. Abstract

The objective of the *in vitro* studies described in this chapter were to evaluate the biological activity of F_2BMet (code name LUZ11) against cancer cells, in the absence of light and after laser irradiation, and its comparison with the performance of the two approved systemic photosensitizers for PDT of cancer, temoporfin (Foscan®) and porfimer sodium (Photofrin®). The PS biological activity against cancer cells was evaluated trough the determination of the cytotoxicity in the absence of light ($IC50_{dark}$) and phototoxicity after laser irradiation ($IC50_{PDT}$). Both parameters are defined by the PS concentration that causes a 50% reduction in cell viability, determined by the resazurin reduction assay. The photosensitizing efficiency (PE), which is defined by the ratio between $IC50_{dark}$ and $IC50_{PDT}$ for a given PS, was employed to compare the performance of the three photosensitizers in two cancer cell lines. In order to generate comparable data, each PS was tested using the exact same protocol parameters, including light dose, fluence and fluence rate. When compared with Photofrin and Foscan, LUZ11 clearly demonstrated the highest photosensitizing efficiency, resulting from its lower toxicity in the absence of light and high phototoxicity after irradiation.

2.2. Introduction

A family of halogenated tetraphenyl bacteriochlorins was screened to evaluate their potential as PS candidates for PDT. Such bacteriochlorins can be economically synthesized [65], exhibit a lower tendency to aggregate [172], combine strong absorptions in the phototherapeutic window with efficient formation of long-lived triplet states [61, 164], bear electron-withdrawing groups that stabilize the macrocycle against oxidation [173] and provide steric protection [174].

It was demonstrated that the interaction between such bacteriochlorins and molecular oxygen can occur both through type I and type II reactions, without compromising photostability, leading to the formation of superoxide ions and hydroxyl radicals in addition to singlet oxygen [168, 175, 176]. The combined effects of these ROS were remarkably efficient in the destruction of tumour cells [68, 165].

The dynamics of the interaction between the photosensitizer triplet state and oxygen determine both the nature of the ROS generated and the stability of the photosensitizer towards such ROS. With LUZ11 it was possible to achieve a delicate balance between a high degree of charge transfer to oxygen and an adequate resistance to oxidation. It is a

perfect example of how the dynamics of the interaction between light, a photosensitizer, and oxygen can be tuned to improve photodynamic efficacy [171].

In vitro studies are still very important screening tools during the early phases of PS development. Even in the artificially controlled conditions of cell culture experiments, they can provide very useful data that contribute to a better characterization of their photodynamic properties in biological systems, and consequently to an early selection of the most promising molecules. During the *in vitro* screening stage the most relevant studies are related to the toxicity in the absence of light, phototoxicity after irradiation, PS cellular accumulation kinetics, intracellular distributions, and mechanisms of cell death induced by PDT [165].

In addition, the comparison of the photodynamic performance of different PS, in the same experimental conditions, can provide preliminary information on the interest of PS candidates for specific PDT applications. Direct comparison between different PS based on literature data is difficult because different cell lines, animal models, and different protocols, are employed. Here, the *in vitro* performance of LUZ11 was directly compared against the most widely used drugs for systemic PDT of cancer: porfimer sodium (generic name of Photofrin®) and temoporfin (generic name of Foscan®). The comparison is focused on the toxicity effects of the three PS in two colon carcinoma cell lines, HT-29 (human) and CT26 (mouse). Literature criteria for photosensitizing efficiency (PE) were employed to evaluate the performance of the three PS [62].

2.3. Material and methods

CHEMICALS

Media for cell culture (RPMI-1640, DMEM high glucose) and resazurin sodium salt were purchased from Sigma-Aldrich (St. Louis, MO, USA). Trypsin/EDTA and penicillin/streptomycin mixture were from Lonza (Verviers, Belgium). Foetal bovine serum (FBS) was from Biochrom (Berlin, Germany) and 4-(2-hydroxyethyl)-1-piperazineethanesulfonic acid (HEPES) was obtained from VWR Chemicals (Leuven, Belgium). The disposable cell culture consumables were from Orange Scientific (Braine-l'Alleud, Belgium) and 96 micro-well plates were purchased from BD Biosciences (Franklin Lakes, NJ, USA). The photosensitizers LUZ11 [163, 164] and temoporfin [177, 178] were synthetized by the Chemistry Research Department (CRD) of Luzitin, SA (Coimbra, Portugal) as described elsewhere. The PS were supplied as weighed amounts in sealed vials under nitrogen atmosphere, and stored at approximately -18ºC, protected from light.

Porfirmer sodium was commercially available as Photofrin® (75 mg of porfimer sodium for injection) from Axcan Pharma (Sittard, The Netherlands).

CELL CULTURE

The cytotoxicity and phototoxicity of PS was evaluated in human lung carcinoma (A549, (ATCC CCL-185), human prostate adenocarcinoma (PC-3, ATCC CRL-1435), human colorectal adenocarcinoma (HT-29, ATCC HTB-38), and mouse colon carcinoma (CT26.WT, ATCC CRL-2638) cell lines (LGC Standards, Middlesex, UK). Cell lines HT-29 and CT26 were cultured in DMEM (high glucose), supplemented with 10 mM of HEPES, and cell lines A549 and PC-3 were cultured in RPMI-1640. Both culture media were also supplemented with 10% heat-inactivated FBS and 100 IU/ml penicillin-100 µg/ml streptomycin mixture. Cell lines were maintained in 75 cm^2 flasks at 37 ºC in humidified atmosphere with 5% CO_2.

PHOTOSENSITIZER STOCK SOLUTIONS

The stock solutions of LUZ11 and temoporfin were prepared by dissolving the PS in propyleneglycol/ethanol (60:40). Complete solubilisation was achieved after three alternated cycles of 1 minute in the ultrasound bath followed by 30 sec of vortex mixing. The stock solution of porfimer sodium was prepared in PBS with 1 minute of vortex mixing for complete solubilisation.

TOXICITY IN THE ABSENCE OF LIGHT

At 80-90% of confluence, cells were counted and seeded in 96-well plates with clear flat-bottom in 100 µl of culture medium at the desired density, and allowed to adhere overnight. The intended PS concentrations were added to the cells (diluted in 100 µl culture medium) and cells were incubated with the drug for 20 h, in the dark at 37 ºC. Control conditions to assess the effect of PS solvent on cell viability were included: cells were incubated (without PS) with the highest percentages of solvent present in the test conditions (typically ≤ 2%). After the incubation period the culture medium was discarded, cells were washed with 200 µl of PBS to remove the non-internalized PS and 200 µl of fresh culture medium were added. Cell viability is evaluated 24 h after medium replacement, using the resazurin reduction assay.

PHOTOTOXICITY AFTER LASER IRRADIATION

At 80-90% of confluence, cells were counted and seeded in black 96-well plates with clear flat bottom in 100 µl of culture medium, and allowed to adhere overnight. The desired

concentrations of PS were added to the cells (diluted in 100 µl culture medium) and cells were incubated with the drug for 20 h, in the dark at 37 ºC. After the incubation period the culture medium was discarded, cells were washed with 200 µl of PBS to remove the non-internalized PS, and 100 µl of fresh culture medium were added. The laser sources employed to illuminate the cells incubated with LUZ11, temoporfin and Photofrin were Lynx external cavity diode lasers TEC 500 powered by PilotPC 500 Laser Controllers (Sacher Lasertechnik, Marburg, Germany) with wavelengths of 748, 652 and 633 nm, respectively. The laser beams were coupled to an optic fibre with an adjustable divergent lens, to ensure that each well was individually and uniformly irradiated. The laser output was tuned to a fluence rate of 8.0 mW/cm^2 at the exit of the lens. The irradiation time was determined as a function of the intended light dose. Two parallel control conditions were included: cells incubated in the dark with the highest dose of drug and were not irradiated, and cells irradiated without PS. After the irradiation 100 µl of fresh culture were added for a final volume of 200 µl/well. Cell viability was evaluated approximately 24 h after the irradiation using the resazurin reduction assay.

Two sets of phototoxicity experiments were performed, one to evaluate the effect of the PS concentration on cell viability (fixed light fluence) and the other to evaluate the effect of the light fluence on cell viability (fixed PS concentration with no toxicity in the absence of light). The details of the experimental conditions used are presented in Table 2.1.

RESAZURIN REDUCTION ASSAY

Cell viability was evaluated using the resazurin reduction assay [179], adapted from the alamarBlue® protocol [180]. The procedure requires a resazurin stock solution (0.1 mg/ml in PBS) that can be stored at -18 ºC in 15 ml tubes. Just before performing the assay, the resazurin stock solution was thawed and diluted to 10% with RPMI culture medium without FBS or antibiotics. Cells in the microplates were washed once with 200 µl of pre-warmed PBS with and 200 µl of the diluted resazurin solution were added to each well. Then 200 µl of RPMI without FBS or antibiotics were added into three empty wells in each plate to be used as blanks. Plates were be incubated for 3 h at 37 ºC and then the absorbance of each well was determined in a microplate reader at 540 and 630nm. Possible interference from porfimer sodium absorbance in the resazurin test was studied in preliminary tests, but no interference was found.

Cell viability in the test wells relative to non-treated controls was determined as the percent difference in resazurin reduction between test and non-treated control wells, using the following equation [180]:

$$Cell\ Viability(\%) = \frac{[(\varepsilon OX)\lambda 2 \times A\lambda 1] - [(\varepsilon OX)\lambda 1 \times A\lambda 2]}{[(\varepsilon OX)\lambda 2 \times A°\lambda 1] - [(\varepsilon OX)\lambda 1 \times A°\lambda 2]} \times 100 \qquad (2.1)$$

Where, Ɛ(OX) are the molar extinction coefficient of the oxidized form of resazurin (blue color) at λ1 (540 nm) 47.619 $M^{-1}cm^{-1}$ and λ2 (630 nm) 34.798 $M^{-1}cm^{-1}$, A is the absorbance of the test well and Aº is the average absorbance of non-treated wells (negative control), at the wavelengths λ1 and λ2. Viability results are plotted as average ± SD relative to the untreated control, of at least 2 independent experiments.

Table 2.1 – Experimental conditions employed in the evaluation of the photodynamic performance of the PS in test. Three distinct studies were performed: evaluation of the toxicity in the absence of light, and the phototoxicity, as a function of the PS concentration or the light dose.

Type of Experiment	Conditions	LUZ11 (μM)	Temoporfin (μM)	Photofrin® (μM)
Toxicity *vs* [PS]	[PS] (μM)	200.0	150.0	150.0
		150.0	100.0	100.0
		125.0	50.0	50.0
		100.0	25.0	25.0
		60.0	10.0	10.0
		20.0	8.0	8.0
		10.0	5.0	5.0
		5.0	3.0	3.0
		1.0	1.0	1.0
		-	0.5	0.5
Phototoxicity *vs* [PS]	Fixed fluence (J/cm^2)	1.0	1.0	1.0
	[PS] (μM)	20.0	5.0	50.0
		15.0	2.5	25.0
		10.0	1.0	10.0
		5.0	0.6	8.0
		1.0	0.4	4.0
		0.5	0.1	1.0
		0.0	0.0	0.0
Phototoxicity *vs* light fluence	Fixed [PS] (μM)	50– HT-29 70 – CT26	1 – HT-29 0.5 – CT26	8 – HT-29 8 – CT26
	Fluence (J/cm^2)		2.00	
			1.50	
			1.25	
			1.00	
			0.75	
			0.50	
			0.25	
			0.10	
			0.00	

PHOTODYNAMIC EFFICIENCY

The *in vitro* comparison between the photosensitizers was based on the photodynamic efficiency (PE) index, adapted from Berlanda, J. *et al.* [62]. PE is given by the ratio between the PS dark cytotoxicity ($IC50_{dark}$) and its phototoxicity ($IC50_{PDT}$), both defined as the concentration of PS that cause a reduction of 50% in cell viability, as given by the following equation:

$$PE = \frac{IC50_{dark}}{IC50_{PDT}} \quad (2.2)$$

2.4. Results and discussion

During the early development stages, the biological activities of the new PS candidates were screened through *in vitro* studies in different tumour cell lines. Such studies were useful to characterize the interaction between PS and cells, and to identify the molecules with higher potential in terms of photodynamic activity (Figure 2.1).

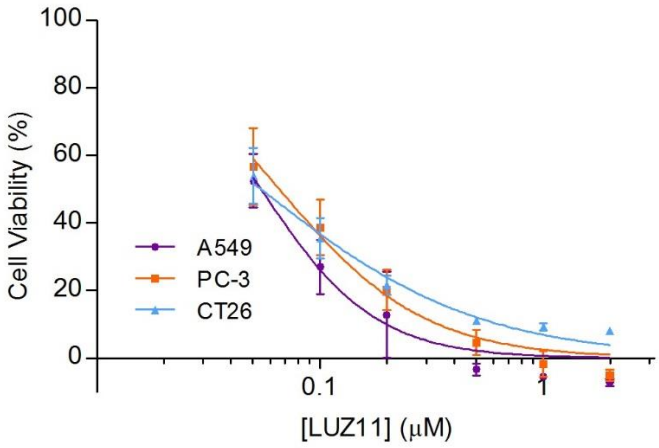

Figure 2.1 – Phototoxicity effect of LUZ11-PDT against different tumour cells lines. Cells were irradiated with 6 J/cm^2 of 748 nm laser light after 20 h of incubation with LUZ11 in the dark. The $IC50_{PDT}$ of LUZ11 in each cell line was calculated through non-linear regression from the respective cell viability results: $IC50_{PDT}$ = 54 nM in A549 and CT26 cells, and $IC50_{PDT}$ = 66 nM in PC-3 cells.

The *in vitro* screening results, together with preliminary *in vivo* efficacy studies of LUZ11-PDT in a mouse tumour model, supported the selection of LUZ11 as the lead compound. LUZ11 was the most photodynamically effective molecule among its family of sulfonamide bacteriochlorins, although its quantum yield of singlet oxygen formation is one of the lowest. This may be compensated by its ability to also produce the superoxide-ion via type I

reactions, which subsequently reacts to form hydrogen peroxide, in a process that is dependent on the amount of excited PS [171]. Hydrogen peroxide and superoxide are further involved in the Haber-Weiss/Fenton reaction that leads to the formation of the hydroxyl radical, a highly reactive species even more cytotoxic than singlet oxygen [168]. This emphasizes the decisive contribution of ROS produced via type I reactions to the photodynamic activity of PS candidates.

The interaction of LUZ11 with cancer cells in culture was studied to evaluate its cellular uptake, to determine the optimal incubation time for phototoxicity experiments, and its subcellular localization to understand which cellular structures will be the most affected by PDT. The time-dependent accumulation of halogenated sulfonamide tetraphenyl bacteriochlorins was evaluated in A549 and S91 (mouse Cloudman melanoma) cells exposed to 5 μM of photosensitizer. The uptake of the bacteriochlorins increased steadily over time and reached a maximum after 18–20 h of incubation in both cell lines. The cellular uptake of the sulfonamide bacteriochlorins seems to be facilitated by their well-balanced amphiphilic character [165]. The hydrophobicity of a compound can be measured by its partition coefficient between *n*-octanol and water (K_{ow}), which can also be expressed as the logarithm to base 10 (Log P_{ow}). The Log P_{ow} is an excellent indicator of a PS affinity to permeate de plasma membrane of cells and of its suitability to be formulated in a vehicle for iv administration. Table 2.3 contains the experimentally-determined Log P_{ow} values for LUZ, temoporfin and porfimer sodium. With a Log P_{ow} of 1.9, LUZ11 has enough hydrophobicity to permeate the plasma membrane of cells, for which also contribute the neutral sulfonamide groups, but not too much that would lead to an extensive aggregation in aqueous biological medium [54].

Intracellular localization was investigated in A549 cells co-incubated with LUZ11 and fluorescent probes specific for lysosomes, mitochondria, and endoplasmic reticulum (ER), using fluorescence confocal microscopy. The topographic profiles of LUZ11 revealed a high degree of localization in the ER, some in the mitochondria, and none in the lysosomes, which is consistent with the results obtained for other halogenated sulfonamide bacteriochlorins [165, 171], and also for Foscan [181] and Photofrin [182]. The intracellular structures where the PS tends to accumulate determine the initial subcellular targets of PDT and may have a decisive contribution to the treatment outcome. The preferential localization of PS in the ER and its ability to generate strong ROS-mediated ER stress has been associated with the induction of immunogenic cancer cell death that may be able to trigger the activation of the host immune system [183, 184].

The cell viability results, in the absence of light and after PDT, for the three PS are presented in Figure 2.2 and Figure 2.3, for the HT-29 and Ct26 cell lines. The correspondent IC50

results, determined through non-linear regression, together with the calculated PE values are presented in Table 2.2.

The results of PS toxicity in the absence of light, in both cell lines, show that LUZ11 is much less toxic than porfimer sodium, which in turn is less toxic than temoporfin. Because of the low toxicity of LUZ11 and its low solubility in aqueous media, it was not possible to reach the IC50 concentration for LUZ11 in the absence of light. Nevertheless, it was possible to estimate the $IC50_{dark}$ of LUZ11 in CT26 cells by extrapolation from the non-linear regression curve. It is clear that, in the dark, LUZ11 is at least 20 times less toxic than temoporfin for both cell lines. Moreover, LUZ11 is at least 4.5 times less toxic than porfimer sodium towards CT26 cells and at least 1.5 times less toxic towards HT-29 cells.

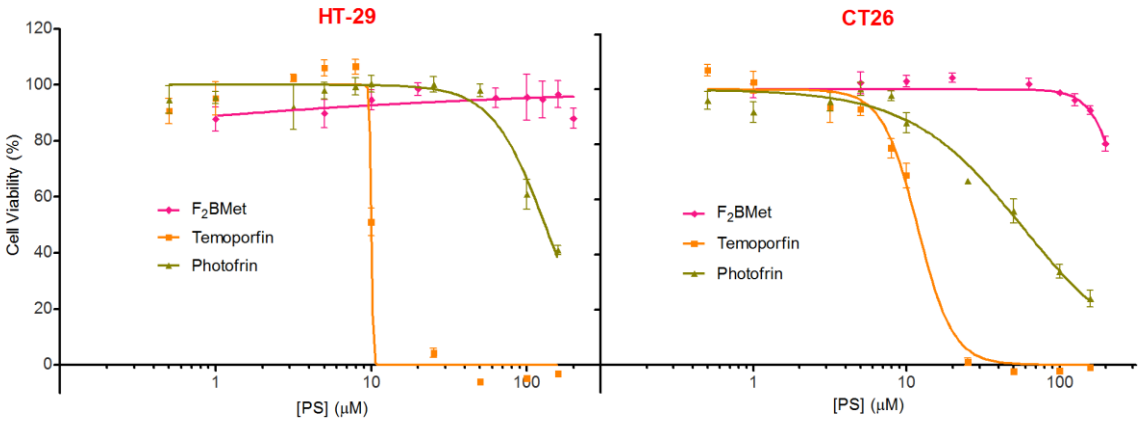

Figure 2.2 – Cell viability as a function of PS concentration, after 20 h incubation in the absence of light.

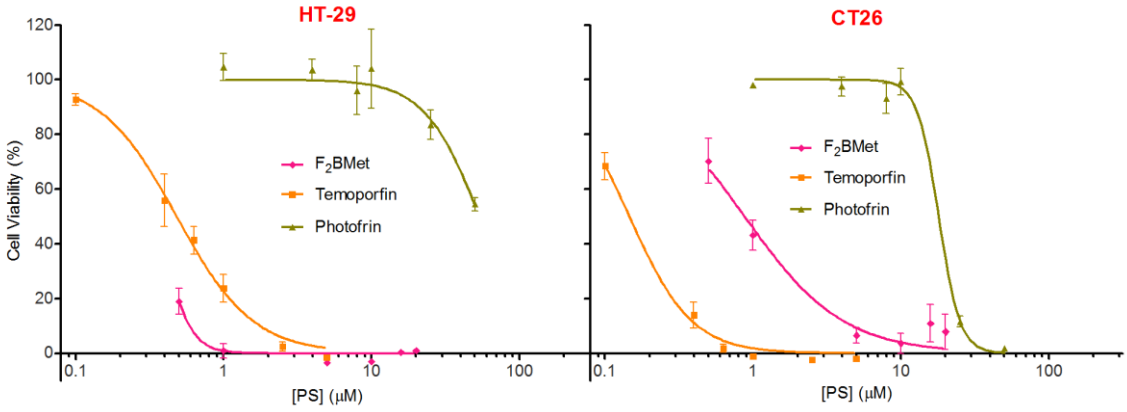

Figure 2.3 – Cell viability as a function of PS concentration after PDT. Cells incubated with each PS, for 20 h in the dark, were irradiated with 1 J/cm^2 of laser light, with the specific wavelength for each PS.

Table 2.2 – Results for toxicity in the absence of light, phototoxicity and photosensitizing efficacy for each PS, in HT-29 and CT26 cell lines.

HT-29	$IC50_{dark}$ (μM)	$IC50_{PDT}$ (μM)	PE	CT26	$IC50_{dark}$ (μM)	$IC50_{PDT}$ (μM)	PE
LUZ11	> 200[a]	0.367	**> 545**	**LUZ11**	273[a,b]	0.878	**311**
Temoporfin	10.0	0.482[c]	**20.7**	**Temoporfin**	11.8	0.146	**80.8**
Photofrin®	131	53.7	**2.44**	**Photofrin®**	57.3	18.0	**3.18**

[a] The limited solubility of LUZ11 in aqueous medium did not allow to reach the concentration needed to attain the $IC50_{dark}$
[b] Calculated by extrapolation from the non-linear regression curve

In terms of photodynamic activity, for a light dose of 1 J/cm^2, LUZ11 is much more effective than porfimer sodium, and is comparable to temoporfin in HT-29 cells and slightly lower in CT26 cells. However, since it is much less toxic in the dark, the phototoxicity of LUZ11 can easily overcome that of temoporfin by increasing the bacteriochlorin concentration, even with a lower light fluence (Figure 2.4), which can be relevant to increase the depth of treatment.

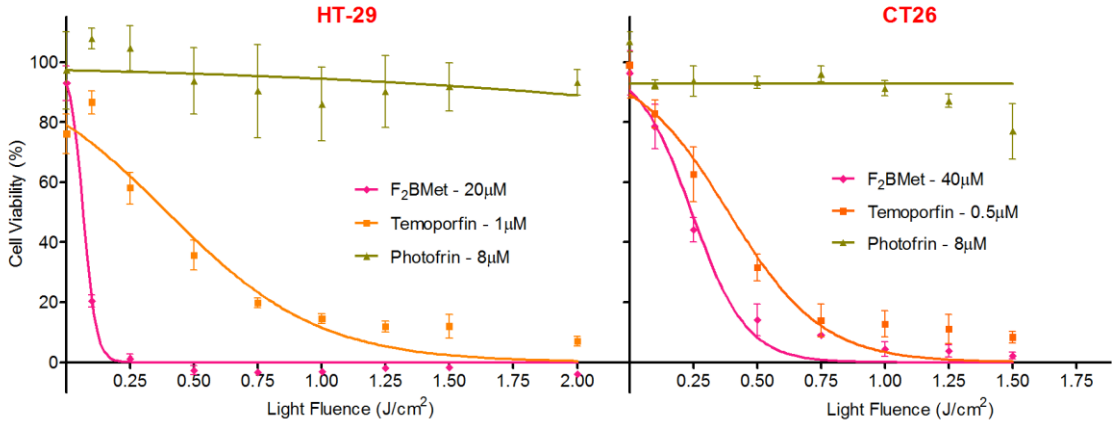

Figure 2.4 – Cell viability as a function of light fluence after PDT. Cells incubated with fixed concentrations of each PS, for 20 h in the absence of light, were irradiated with increasing light fluences.

The photodynamic performance of LUZ11 is evidenced when observing the PE results: more than 100 times higher than that of porfimer sodium (Photofrin®), and around 4 times higher in CT26 cells and at least 25 times higher in HT-29 cells, when compared to temoporfin. The higher PE of LUZ11 is explained by the combination of the lowest toxicity in the dark with high phototoxicity.

Table 2.3 – Comparative data on the properties of photosensitizers LUZ11, Foscan and Photofrin.

Photosensitizer		**LUZ11**	**Foscan** [d]	**Photofrin** [e]
Molecular weight (g/mol)		1135.11	680.74	~ 605
Log P $_{\text{n-octanol/water}}$		1.9	9.2 [f]	0.9 [g]
Absorption [a]	λ_{max} (nm)	743	650	630
	ε_{max} ($M^{-1}.cm^{-1}$)	140000	29600	1170
Triplet [b]	Φ_T	0.65	0.89	0.80
	τ_T (ns)	216	-	-
	k_q ($M^{-1}.s^{-1}$)	2.2	1.8	1.5
$^1O_2$ formation quantum yield (Φ_Δ) [a]		0.43	0.43	0.36
Photodecomposition quantum yield (Φ_{pd})		1.0×10^{-5} [c]	3.3×10^{-5}	5.5×10^{-5}

[a] in ethanol, [b] in air saturated ethanol, [c] PBS/methanol, [d] in methanol from ref. [185, 186], [e] in PBS from ref. [112], [f] from ref. [187], [g] from ref. [188].

These results can be justified by the individual properties of each photosensitizer (Table 2.3). LUZ11 has a much stronger absorption and at longer wavelengths in the phototherapeutic window than Foscan or Photofrin, with a comparable Φ_Δ but with the additional capacity to generate superoxide ion and hydroxyl radical.

The stability of a PS under light irradiation, or photostability, is related to ability of a PS molecule to endure several cycles of photon absorption and ROS production before its oxidative destruction by the locally-generated $^1O_2$ during PDT. This photodegradation, or Photobleaching of a PS, is best described by its photodecomposition quantum yield (Φ_{pd}), determined by the ratio between the rate of PS molecules degradation and the rate of photon absorption. Photodecomposition has a negative impact on local PS availability and, consequently, in treatment efficacy. The photodecomposition of LUZ11 in PBS/methanol ($\Phi_{pd}=1.0\times10^{-5}$) is slower than that of Photofrin in PBS ($\Phi_{pd}=5.5\times10^{-5}$) [189], and in aerated ethanol drops to 6.9×10^{-7}, which is also smaller than that of Foscan in methanol, $\Phi_{pd}=5\times10^{-6}$ [185, 189]. This means that, in comparison to the other two PS, LUZ11 is more efficient in the production of ROS, and it can do so for longer, due to the higher photostability.

2.5. Conclusion

In the early stages of discovery a new family of tetraphenyl halogenated bacteriochlorins was screened to identify the “ideal” photosensitizer candidate for PDT of cancer. LUZ11 is the one that better fulfils the requisites considered critical for the success of PDT, namely

strong absorption at long wavelengths in the phototherapeutic window, high quantum yield of ROS formation, adequate photostability and solubility in biocompatible formulations, low toxicity in the absence of light and high phototoxicity. The combination of these attributes is reflected on the photodynamic performance of LUZ11, when compared against two marketed competitors, Photofrin and Foscan, where it clearly showed the highest photosensitizing efficiency in HT-29 and CT26 cell lines.

Chapter 3

Pharmaceutical Development and Proof-of-Concept

Chapter 3 – Pharmaceutical Development and Proof-of-Concept

The work presented in this chapter was published in:

ChemMedChem (2014) 9(2), 390-398.

Modulation of biodistribution, pharmacokinetics, and photosensitivity with the delivery vehicle of a bacteriochlorin photosensitizer for photodynamic therapy

Saavedra R [1], Rocha LB [2], Dąbrowski JM [3] and Arnaut LG [1,2]

[1] Department of Chemistry, University of Coimbra, Rua Larga, 3004-535 Coimbra, Portugal

[2] Luzitin SA, Rua da Bayer 16, 3045-016 Coimbra, Portugal

[3] Faculty of Chemistry, Jagiellonian University, Ingardena 3, 30-060 Kraków, Poland

3.1. Abstract

Intravenous (iv) formulations with various amounts of organic solvents [PEG400, propylene glycol (PG), Cremophor EL (CrEL)] were used to deliver a fluorinated sulfonamide bacteriochlorin to mice, rats, and minipigs. Biodistribution studies in mice showed that a low-content CrEL formulation combines high bioavailability with high tumour-to-muscle and tumour-to-skin ratios. This formulation was also the most successful in the photodynamic therapy of mice with subcutaneously implanted CT26 murine colon adenocarcinoma tumours. Pharmacokinetic studies in mice and minipigs revealed that with the same low CrEL formulation, the half-life of the photosensitizer in the central compartment was longer in minipigs. Differences in biodistribution with the various formulations, and in pharmacokinetics between the two animal species with the same formulation, are attributed to the interaction of the formulations with low-density lipoproteins (LDL). Skin photosensitivity studies in rats showed that 30 min exposure of the skin to a solar simulator 7 days after iv administration of the fluorinated sulfonamide bacteriochlorin at 1 mg/kg did not elicit significant skin reactions.

3.2. Introduction

Photodynamic therapy (PDT) consists in the use of light to excite a photosensitizer capable of generating reactive oxygen species (ROS) in amounts that are sufficient to kill diseased tissue in the illuminated volume. The closure of peritumoural blood vessels, apoptosis/necrosis of cancer cells, and the activation of antitumour immune response may all contribute to the PDT response [190]. The oxidative stress resulting from PDT depends on the appropriate combination of light, photosensitizer and oxygen. Photosensitizers such as Photofrin® (porfimer sodium for injection) and Foscan® (temoporfin for injection) met with success in the clinical management of solid tumours, whereas Visudyne® (verteporfin for injection) is used in the treatment of age-related macular degeneration. The local ROS dose depends on the nature and number of photosensitizer molecules in the illuminated volume and on the number of photons absorbed. The ability of a photosensitizer to absorb light is measured by its molar absorption coefficient. In this work we use a fluorinated sulfonamide bacteriochlorin (F_2BMet) with a remarkable absorption coefficient in the near infrared, $\varepsilon \approx 1.4 \times 10^5$ M^{-1} cm^{-1} in ethanol [171], a wavelength that penetrates deeply (1-2 cm) in human tissues. Although this photosensitizer strongly absorbs near-infrared photons, its PDT

efficacy will necessarily depend on the presence of photosensitizer molecules in the target tissues at the time of illumination.

A major challenge in PDT is to select a formulation for intravenous (iv) administration of a photosensitizer drug that favours its bioavailability in the target tissue at an appropriate drug-light interval (DLI) – the time interval between the administration of the drug and the illumination of the target tissue. The selective retention of the photosensitizer in solid tumours, often reported in terms of the tumour-to-muscle (T/M) ratio, tends to increase for longer DLI, but its bioavailability for illumination decreases as a function of time because the total amount of photosensitizer in the organism is reduced. Additionally, prolonged skin photosensitivity after treatment is often mentioned as a major inconvenience of PDT. This can be minimized with large tumour-to-skin (T/S) ratios and a rapid drug clearance after the treatment. Thus, the success of PDT is largely dependent on the pharmacokinetics and biodistribution of the photosensitizer, on its dose, on the light dose and on the DLI. The modulation of the bioavailability of various photosensitizers with the delivery vehicle was the subject of a classical review [191]. The relevance of the photosensitizer formulation was further highlighted by recent efforts to improve bioavailability and reduce the skin photosensitivity that complicates the management of PDT patients [27, 142, 192, 193].

This work focuses on the iv delivery of a stable bacteriochlorin photosensitizer, 5,10,15,20-tetrakis(2,6-difluoro-3-*N*-methylsulfamoylphenyl) bacteriochlorin (F_2BMet), characterized by a strong absorption of light at 750 nm, an efficient generation of ROS, a *n*-octanol:water partition coefficient P_{OW} = 80 [171], and practically insoluble in water. We show that the proper formulation for iv administration has a profound impact on PDT efficacy and in the reduction of the skin photosensitivity after PDT.

The iv administration of water-soluble porphyrin-based photosensitizers is conveniently done with aqueous media isotonic with blood. This is the case of Photofrin® [194-197], Tookad®-soluble [53], and 5,10,15,20-tetrakis(2-chloro-5-sulfophenyl)chlorin [198] or the analogous bacteriochlorin [199]. However, F_2BMet is an amphiphilic photosensitizer practically insoluble in water. Such photosensitizers are often administered with drug formulations forming micelles, namely Cremophor EL (CrEL) micelles [200, 201], or liposomes. For example, verteporfin (benzoporphyrin derivative monoacid ring A, BPD) has been formulated in DMSO:PBS and in liposomal suspension [202-204]. Liposomal BPD resulted in a larger proportion of BPD bound to low-density lipoproteins (LDL) and led to more effective PDT treatments with DLI = 3 h. The biodistribution of temoporfin (*m*-tetrahydroxyphenylchlorin, mTHPC,) formulated in ethanol:PEG_{400}:water (2:3:5, v:v:v) [205-211] or more recently in liposomal suspension [142, 192], showed T/S ratios higher than unity in the latter formulation, together with reduced skin photosensitivity. We used a PEG formulation to deliver of 5,10,15,20-tetrakis(2,6-dichloro-3-*N*-ethylsulfamoylphenyl)

bacteriochlorin to DBA mouse bearing the Cloudman S91 melanoma tumours and obtained T/S and T/M ratios higher than 5 one day post-iv [68].

The most extensively used and characterized systems that rely on micelles to deliver drugs are based on CrEL micelles. CrEL spontaneously forms micelles in aqueous solutions and its critical micellar concentration is 0.009% (weight/volume) in protein-free aqueous solution [212]. The role of CrEL delivery in bacteriochlorin-based PDT *in vitro* was recently discussed [213]. It generally reduced aggregation and increased activity up to tenfold (depending on bacteriochlorin). However, CrEL concentrations >0.03% in human serum lead to lipoprotein degradation [201] and hypersensitivity reactions have been associated with CrEL concentrations >0.2% in plasma of cancer patients [214]. Considering that the human blood plasma volume is 35 ml/kg, a total safe dose should be <0.07 ml/kg. A direct comparison between CrEL and liposomal formulations to deliver temocene (the porphycene analogue of temoporfin) revealed that the CrEL formulation (total CrEL dose of 0.24 ml/kg) was more successful in PDT at DLI = 15 min, but the liposomal formulation was better for PDT at DLI = 24 h [193].

We report herein biodistribution, pharmacokinetics, and skin photosensitivity studies as a means to evaluate the adequacy of iv formulations to deliver an amphiphilic photosensitizer. The pitfalls of extrapolating pharmacokinetics from mouse to man motivated a study with minipigs. The impact of the formulations in the long-term tumour response was investigated with the treatment of BALB/c mice bearing subcutaneously implanted CT26 mouse colon carcinoma cells. Four formulations were selected for this work based on the background presented above, their stability and the simplicity of preparation. Special attention is given to the adverse effects expected for high CrEL concentrations and their transfer between species.

3.3. Materials and methods

CHEMICALS

F_2BMet is a new photosensitizer for PDT and its synthesis and characterization is described elsewhere [171]. F_2BMet was provided by Luzitin SA. Medium for cell culture (RPMI, F10) and PBS (phosphate-buffered saline), are from Sigma-Aldrich (St. Louis, MO, USA).

The solubility of F_2BMet in PBS measured preparing a saturated PBS solution of F_2BMet, taking an aliquot of this solution and diluting with DMSO to obtain a 0.5:99.5 PBS:DMSO solution. The fluorescence intensity of this solution was measured at ~750 nm, and its concentration was determined using a calibration curve of known F_2BMet concentrations in

the same solvent mixture but prepared after the initial dissolution of F_2BMet in DMSO. The solubility of F_2BMet in PBS was determined to be 1 mg/L at 25°C.

INTRAVENOUS FORMULATIONS

Table 3.1 compares the contents of organic solvents in the four formulations. Formulations C and D differ in the volume of formulation that is administered for a given dose of F_2BMet: 4 ml/mg in formulation C and 5 ml/mg in formulation D. Consequently, administering 2 mg/kg of F_2BMet leads to a CrEL dose of 0.02 ml/kg in formulation D (1,4 ml CrEL for an average patient) which is less than the CrEl dose currently used in iv delivery of a wide variety of drugs, and a factor of 20 below the CrEL dose administered with Taxol® [215].

Table 3.1 – Relative contents of organic solvents in the formulations, and organic contents per mg of F_2BMet.

Formulation (v/v/v)	EtOH	PEG_{400}	PG	CrEL
A EtOH:PEG:PBS (1:3:5)	0.444	1.332	-	-
B EtOH:PG:PBS (1:2:1)	1.000	-	2.000	-
C CrEL:EtOH:NaCl0.9% (1:1:98)	0.040	-	-	0.040
D CrEL:EtOH:NaCl0.9% (0.2:1:98.8)	0.050	-	-	0.010

BIODISTRIBUTION AND PHARMACOKINETICS IN BALB/C MICE

CT26 cells were cultured as a monolayer in the DMEM medium (high glucose), supplemented with 10 mM of HEPES, 10% heat-inactivated fetal bovine serum and a 100 IU/ml penicillin-100 µg/ml streptomycin mixture. They were maintained at 37 ºC, in humidified atmosphere containing 5% CO_2. The CT26 cells (~$1x10^6$) were taken up in 0.1 ml phosphate buffered saline (PBS) and implanted subcutaneously to the right thigh of female BALB/c mice (Charles River Laboratories®, Barcelona, Spain). The iv administration of the drug formulation was done when the tumour attained a diameter of 5-8 mm in each animal, which usually took 8-10 days after the inoculation.

Each formulation, corresponding to a 2 mg/kg of F_2BMet, was slowly injected in the tail vein of each animal, and the biodistribution was evaluated at 3 time points after administration: 15 min, 24 h and 48 h. At the selected time-points post-injection, the mice were anesthetized with ketamine and xylazine, and sacrificed by cervical dislocation. For each animal, the

following organs and tissue samples were collected separately and weighed: tumour, muscle, skin, liver, spleen, kidneys and blood.

The content of F_2BMet in the tissue samples was determined by fluorescence. In order to extract the pigments, tissue samples were separately homogenized in 0.9 ml of ice-cold solution ethanol:DMSO (75:25) during 1 min, using a tissue homogenizer Ystral Microshaft 6G. The homogenate was centrifuged at 2100*g* for 1 min at 4 ºC, the supernatant was collected and the pellet was re-extracted 4 more times using the procedure described above, to ensure a complete recovery of the drug. The extracts were pooled and the final volume adjusted to 5 ml. The fluorescence analysis of the extracts was done less than 6 h from the harvest. The samples were excited at 505 nm and the fluorescence spectra were recorded in the range between 600 and 800 nm. The amount of F_2BMet in the tissues is reported as the average from 4 animals (exceptionally, for DLI=15 min and formulations A, B, and C only 3 animals were used per group), with the standard error of the mean (SEM).

An extended biodistribution study, covering a dense matrix of times points post-injection, was carried out with formulation D. Plasma pharmacokinetics in mice was obtained after plasma separation. Approximately 500 µl of blood were collected in a tube with heparin (30 IU/ml of blood) as anticoagulant. The tubes were centrifuged at 2100*g* for 10 minutes and then the plasma top layer was transferred for a new tube, weighed, and placed on ice until further analysis.

PHARMACOKINETICS IN MINIPIGS

One female and one male minipig (Instituto Madrileno de Investigacion y Desarrollo Agrario y Alimentario, Aranjuez, Spain), aged ~9 months were used for blood pharmacokinetics. A catheter was surgically implanted in the jugular vein of each animal to facilitate the sequential blood sampling throughout the study. The surgical procedure required the administration of pre-medication (azaperone – Stresnil® – 2 mg/kg, intramuscular injection), induction of anaesthesia (ketamine – Clorketam® – 15 mg/kg, intramuscular injection, plus sodium thiopental 10 mg/kg, iv injection), maintenance of anaesthesia (oxygen + isofluran, 2%), analgesia (carprofen – Norocarp® – 1.4 mg/kg, intramuscular injection in the 1st day), antibiotherapy (amoxicilin – Clamoxyl® LA – 15 mg/kg, intramuscular injection) and two days later an additional dose of antibiotherapy (amoxicillin – Clamoxyl® LA – 15 mg/kg, intramuscular injection). These studies were performed in the Instituto Nacional de Investigação Agrária (Santarem, Portugal) with the assistance of veterinary surgeons.

EXPLORATORY PDT

The BALB/c animal model with the CT26 tumour described above was used in the *in vivo* PDT exploratory study. The tumours were allowed to grow until they reached 5 to 8 mm in diameter. Then, the selected formulations were administered to give a 2 mg/kg dose of F_2BMet. At DLI = 72 h a light dose between 117 and 248 J/cm^2 was delivered with a costumer-made Hamamatsu diode laser, type LA0873, S/N M070301. Alternatively, for the vascular PDT protocol, a 1 mg/kg dose of F_2BMet was administered, and 15 min later, the tumour was illuminated to deliver a light dose of either 73 J/cm^2 or 59 J/cm^2. The laser was controlled with a ThorLabs 500 mA ACC/APC Laser Diode Controller and in-house electronics. The energy of the laser was checked with an Ophir model AN/2E laser power meter before each experiment. The laser delivered 130 mW at 748 nm. The volumes of the tumours was regularly measured until it attained 950 mm^3, at which point the mice were sacrificed. The volumes of the tumours were calculated using the formula $V=LxW^2/2$, where L (length) and W (width) are two perpendicular tumour diameters (W<L). Mice without palpable tumour 60 days after the treatment were considered cured.

SKIN PHOTOSENSITIVITY

Female Wistar rats (Charles River Laboratories®, Barcelona, Spain) were used as animal model to evaluate skin photosensitivity following earlier studies with similar objectives [52, 142]. They were kept in a conventional room with controlled light (12:12, dark: subdued light). The animals were fed with a standard pellet diet and water, both *ad libitum*. Prior to the experiment, the hair from dorsum of the animals was removed using depilatory cream (My Label®). Following the iv administration of F_2BMet (1 mg/kg) in formulation D, 8 circular areas of skin measuring 1 cm of diameter and 1 cm apart were defined in each animal. These areas were exposed to 0, 5 (30 J/cm^2), 15 (90 J/cm^2) and 30 min (180 J/cm^2) of ~100 mW/cm^2 of light from a solar simulator source (Oriel 150 W with global filter AM 1.5) at DLI = 12, 24, 72 or 168 h. A control group was subject to the same illumination procedure, but without the administration of F_2BMet. The visual assessment of the results was made 1, 3, 7, 15 and 30 days after the exposure to light. The visual assessment followed the criteria presented in Table 4.1, which was adapted by Weersink *et al* [52] from Roberts *et al* [216].

3.4. Results and discussion

INTRAVENOUS FORMULATIONS

Formulations A (PEG_{400}:EtOH:PBS, 3:1:5), C (CrEL:EtOH:NaCl 0.9%, 1:1:98) and D (CrEL:EtOH:NaCl 0.9%, 0.2:1:98.8) were well tolerated. Animals administered with formulation B (PG:EtOH:PBS, 3:1:1) suffered mild coordination impairment, which was likely caused by the relatively high content of ethanol in the formulation. Table 3.3 presents the average T/M and T/S ratios for these formulations.

Table 3.2 – Visual skin response scoring chart

Score	Observation
0	No observable effect
1	Mild erythema
2	Moderate erythema
3	Strong erythema
4	Slight oedema
5	Moderate oedema
6	Severe oedema
7	Blistering + oedema
8	Necrosis

In addition to the coordination impairment, formulation B gave the set of lowest T/M and T/S ratios at 48 h post-iv injection. Figure 3.1 shows the relative fluorescence intensities obtained with the other formulations for two DLI. Preferential retention of F_2BMet in the tumours rather than in the muscle or in the skin was observed in all but one case: T/S for formulation C at DLI = 15 min. Figure 3.1 shows that CrEL at a dose of 0.08 ml/kg of body weight (formulation C) leads to the highest bioavailability of F_2BMet, and this may be related to the relatively low amount of F_2BMet found in the liver. However, the T/S and T/M ratios obtained with formulation C were generally lower than those obtained with the PEG_{400} formulation. Formulation D (0.02 mg/kg of CrEL per body weight) combined high bioavailability with large T/M and T/S ratios at long DLI.

The iv administration of amphiphilic photosensitizers is quickly followed by their association with albumin and, especially for the lipophilic photosensitizers, with LDL. The ensuing biodistribution has been related to the increased permeability of tumour vasculature (enhanced permeability and retention, EPR, effect) [217, 218] and to the expression of LDL receptors in different tissues [219-222].

Table 3.3 – Tumour-to-muscle and tumour-to-skin ratios (± SEM) of F_2BMet at various DLI.

DLI	15 min		24 h		48 h	
Formulation	**T/M**	**T/S**	**T/M**	**T/S**	**T/M**	**T/S**
A (PEG_{400})	1.8 ± 0.9	2.4 ± 0.7	4.0 ± 1.7	2.7 ± 1.4	3.9 ± 0.3	3.1 ± 1.1
B (PG)	1.2 ± 0.3	1.7 ± 0.4	6.5 ± 1.7	1.6 ± 0.4	2.1 ± 0.2	1.1 ± 0.3
C (CrEL 1)	1.7 ± 0.6	0.9 ± 0.1	4.0 ± 0.8	1.4 ± 0.2	4.3 ± 0.6	2.1 ± 0.6
D (CrEL 0.2)	1.8 ± 0.3	1.2 ± 0.5	3.8 ± 0.4	2.1 ± 0.2	4.6 ± 1.0	3.3 ± 1.1

The number of LDL receptors is increased in tumour cells compared with their normal counterparts, and this is a relevant factor in the accumulation of porphyrin-based photosensitizers in tumours [217], particularly for photosensitizers with more affinity towards LDL [218].

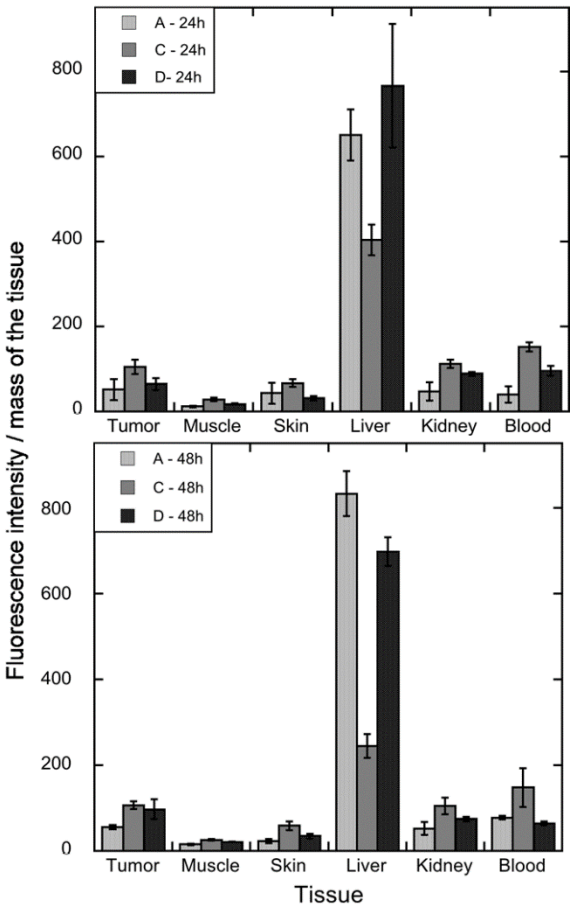

Figure 3.1 – Biodistribution of F_2BMet in relevant tissues with formulations A, C and D, for DLI of 24 and 48 hours. Average values and error bars representing SEM.

It is hypothesized that the amount of CrEL employed in formulation C (0.27% in plasma) could destroy a substantial fraction of the LDL existing in the mice. Although CrEL increased the amount of drug available in the plasma, the small amount of LDL left could not be enough to yield a good biodistribution. The concentration of CrEL in formulation D corresponds to 0.07% in the plasma for the F_2BMet dose of 2 mg/kg. The observation of fast F_2BMet uptake in the liver and in the tumour with formulation D is consistent with the hypothesis that only a small fraction of the LDL existing in the mice is destroyed by CrEL in formulation D. The CrEL content in this formulation is sufficiently high to increase the exposure of the organism to F_2BMet, and yet sufficiently small to allow LDL to drive its biodistribution. Thus, this formulation with a low content of CrEL may give more effective treatments at lower a drug dose, and may also reduce the skin photosensitivity reactions.

BIODISTRIBUTION

The measurement of F_2BMet in tumour, muscle, skin, liver, kidneys, blood heart, spleen, intestines, lungs and brain at times 15 min, 3, 6, 12, 24, 48, 72 and 96 h post-injection with formulation D was performed to provide a complete understanding of the biodistribution and pharmacokinetics of F_2BMet in BALB/c mice with implanted CT26 tumours. The amount of F_2BMet present in the tissues was obtained from the fluorescence intensities per gram of tissue, and is shown in Figure 3.2. Using the dilution factors and a calibration curve, we established that the concentration of F_2BMet in tumour extracts 48 h post-iv was 1.5 mg/kg tissue for a 2 mg/kg administration. This value is in the upper range of tumour uptakes reported in the literature for a variety of photosensitizers [84, 192].

The maximum concentration of F_2BMet in the blood was observed 10 min after bolus injection and is consistent with the good solubilisation of F_2BMet in formulation D. The rapid clearance from the blood is accompanied by an increase of F_2BMet concentration in the liver and in the spleen. Six hours after iv administration, F_2BMet is substantially trapped in the liver, spleen and lungs, which are major contributors to the reticuloendothelial system (RES). The increase of F_2BMet in the liver and the tendency of the T/M and T/S ratios to increase with the decrease of CrEL in the formulation, corroborate the hypothesis that F_2BMet is associated with LDL shortly after iv administration with formulation D and that the preference for tumour localization is mediated by the EPR effect and by the overexpression of LDL receptors in tumour cells.

Extrapolation of biodistribution and pharmacokinetics from mice to human must take into account the fact that the majority of mouse strains (including BALB/c normal and nude mice) have very low LDL levels [81]. Mice generally have LDL levels of 0.2±0.28 mmol/l, whereas

human plasma has 3.9±0.25 mmol/l [81]. The impact of lipoprotein profile in the biodistribution of lutetium texaphyrin was studied in normal and ApoE deficient C57BL/6 mice [219]. The latter strain exhibits a profile more like humans (LDL > HDL) and opposed to that of the normal strain (HDL >> LDL). The T/S ratio increased from 1.9 in the normal strain to 5.3 in the ApoE deficient strain.

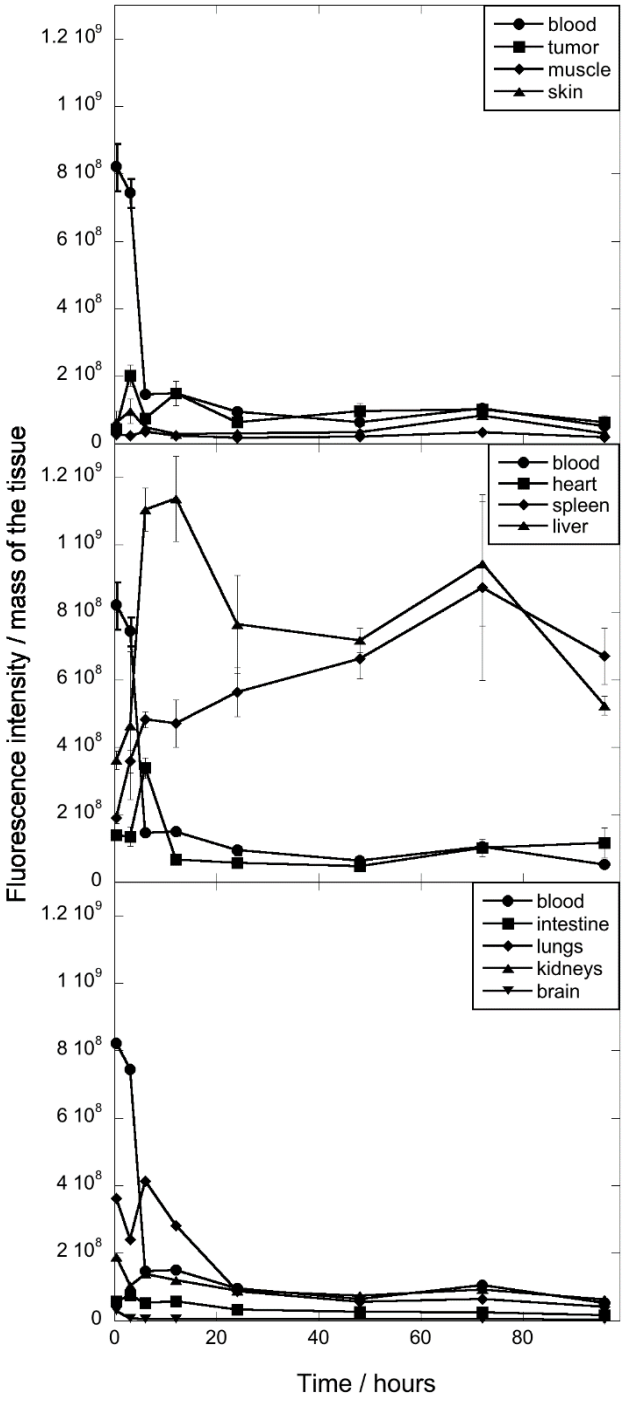

Figure 3.2 – Detailed biodistribution of F_2BMet in relevant tissues with formulation D. Average values and error bars representing the SEM.

The low LDL levels of mice may penalize more strongly CrEL formulations, because CrEL may destroy some of the LDL existing in mice, and it is reasonable to assume that the normal mouse model gives poorer T/S ratios than those expected for humans.
It can be argued that mice, rats and dogs, which are commonly used in preclinical studies, exhibit very low levels of LDL, with the major lipoprotein species represented by HDL [201], and that biodistribution studies in hamsters would be more relevant because they have the same levels of circulating LDL and HDL as humans [220]. We regard this as evidence that photosensitizer biodistribution studies in mice are the worst-case scenario of biodistribution in species with higher levels of LDL. Nevertheless, we addressed the impact of the lipoprotein distribution profile studying the pharmacokinetics of F_2BMet in the CrEL formulation both in BALB/c mice and in minipigs. It is known that pigs have high LDL:HDL ratios, like humans, their LDL levels are 2.3±1.2 mmol/l, and they are an excellent model to study lipid metabolism [221].

PHARMACOKINETICS

The pharmacokinetics of F_2BMet in the plasma of mice after the iv administration of 2 mg/kg in formulation D was studied in detail and is presented in Figure 3.3. The pharmacokinetics of F_2BMet from the initial sampling 10 min post-injection until t = 11 days is very well described by the two-compartment model.
Pharmacokinetic analysis with the two-compartment model describes should be applied to drugs that distribute rapidly from the circulatory system into the peripheral tissues (1st compartment) and then exhibit a gradual decrease attributed to drug metabolism and excretion (2nd compartment) [222]. The drug concentration in the plasma or blood is described by

$$C_p = ae^{-k_1 t} + be^{-k_2 t} \qquad (3.1)$$

Where the initial (t=0) drug concentration is

$$C_{p0} = a + b \qquad (3.2)$$

These equations suffice to determine the volume of distribution of the central compartment

$$V_c = \frac{D}{C_{p0}} \qquad (3.3)$$

(where D is the administered dose) as well as the area under the curve of the drug concentration in the blood as a function of the time as the time tends to infinity

$$AUC_{0-\infty} = \frac{a}{k_1} + \frac{b}{k_2} \quad (3.4)$$

and the blood clearance rate

$$CL = \frac{D}{AUC_{0-\infty}} \quad (3.5)$$

Additionally, the distribution half-life in the first compartment is defined as

$$t_{1/2\ (1)} = \frac{\ln(2)}{k_1} \quad (3.6)$$

and that of the second compartment is

$$t_{1/2\ (2)} = \frac{\ln(2)}{k_2} \quad (3.7)$$

The relevant parameters of this model are presented in Table 3.4. The relatively small value of the volume of distribution is consistent with a high initial retention in the vasculature. The pharmacokinetic profiles of the female and male minigs are very similar. Table 3.4 also presents the pharmacokinetic parameters for minipigs model. The most striking difference between the pharmacokinetics in mice and minipigs is the much longer half-live of F_2BMet in the 1st compartment of the minipigs, although its concentration in the blood drops to a lower value in the minipigs 1-3 days post-iv administration. The initial decrease of F_2BMet level in the blood is characterized by an elimination half-life of 0.5 h in mice and 8.2 h in minipigs.

Table 3.4 – Plasma pharmacokinetic parameters of F2BMet after iv injected dose of 2 mg/kg in formulation D (CrEL:EtOH:NaCl 0.9%, 0.2:1:98.8), calculated using the exponential equations of the two-compartment model.

Pharmacokinetic parameter	Mice	Minipigs
Injected dose (mg/kg)	2.0	2.0
Initial concentration (µg/ml)	39	9.9
Volume of distribution (ml/kg)	52	202
$t_{1/2}$ (1st compartment) (h)	0.5	8.2
$t_{1/2}$ (2nd compartment) (h)	65	121
AUC_∞ (µg h / ml)	763	213
Clearance rate (ml / (kg h))	2.6	9.4

Interestingly, using a two compartment model, it was shown that the half-life of temoporfin in the plasma of mice is 1.3±0.4 h (mean ± SEM) [209] and increases to 2-3 days in Syrian hamsters [208]. This increase was assigned to the different plasma lipoprotein profile of these species [210]. We observe the same trend, but the elimination of F_2BMet from the plasma of mice and minipigs is much faster than the elimination of temoporfin from the plasma of mice and hamsters, respectively. Apparently, the association of the photosensitizer to lipoproteins hinders the kinetics of their elimination by the liver, but with sufficient time they are eliminated more extensively.

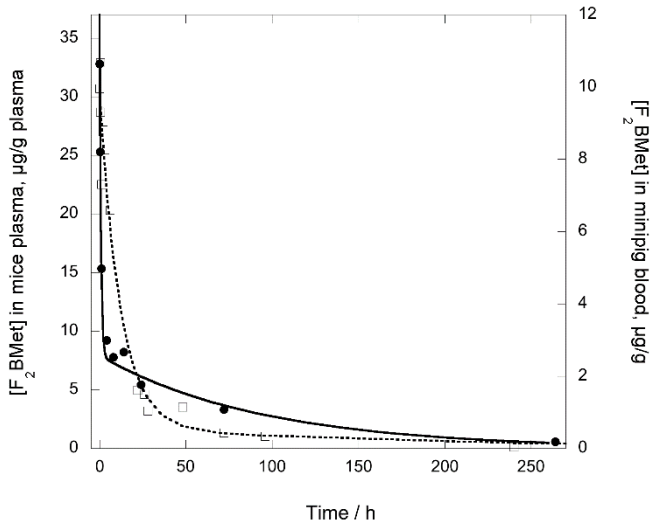

Figure 3.3 – Pharmacokinetics of F_2BMet in the plasma of mice (left axis, circles) and in the blood of minipigs (right axis, squares) after the administration of 2 mg/kg of F_2BMet in formulation D (CrEL:EtOH:NaCl 0.9%, 0.2:1:98.8).

It is insightful to draw an analogy between the differences in biodistribution observed with formulations C and D in mice and the differences in pharmacokinetics observed between mice and minipigs. Figure 3.1 shows that 1-2 days after the administration of F_2BMet in mice, its content in the blood is lower with formulation D than with formulation C, and the opposite is observed for the liver. We assign these differences to the ability of more LDL to resist degradation by CrEL in formulation D, which gives a higher LDL/CrEL ratio than formulation C. Thus, with formulation D more LDL are available to distribute the photosensitizer to the RES. Figure 3.3 shows that 1-2 days after the administration of F_2BMet in formulation D, its content in the blood of minipigs is reduced by a larger fraction than in the plasma of mice. We presume that this observation is originated from the same fact: the higher LDL/CrEL level in minipig blood relative to mice blood increases the initial exposure of the minipigs to F_2BMet and the opportunity for sequestration by the RES.

PDT TREATMENT

Formulations A, B and D were also evaluated in terms of the responses elicited after PDT treatment of BALB/c mice with subcutaneous CT26 tumour. Groups of 4 to 6 animals, with tumours measuring around 5-8 mm in diameter, were injected with these formulations containing F_2BMet (2 mg/kg) and the tumours were irradiated after DLI=72h with light doses between of 117-248 J/cm^2. This DLI maximizes the T/M ratio of formulation D and should minimize damage to healthy tissues while treating the tumour. The concern for preserving normal tissues during PDT was also present in early developments of PDT and motivated the definition of a therapeutic index (TI) in terms of the cross-sectional area of tumour necrosis per depth of visible injury to normal tissue at a control site [223]. This TI increased as the DLI was prolonged up to 5 days and was generally related to the T/M ratio. However, this definition of TI does not take into consideration the long-term tumour response. Figure 3.4 presents the local tumour control after PDT with this conservative protocol.

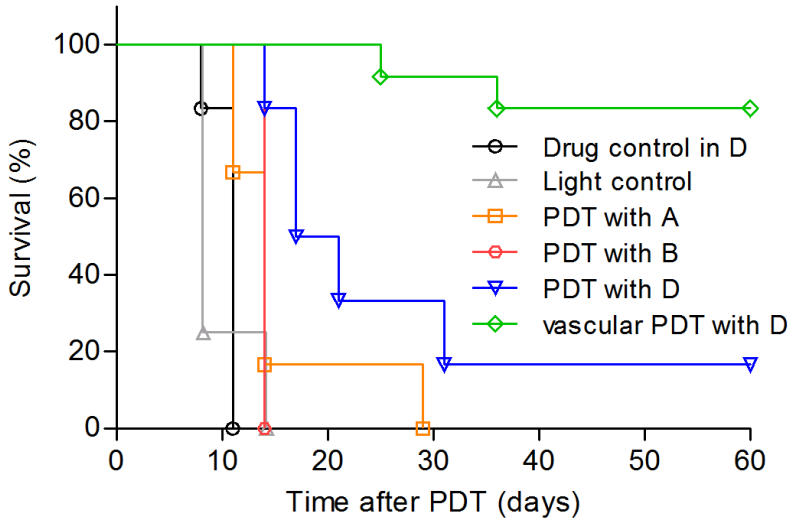

Figure 3.4 – Kaplan-Meier survival plot of the groups treated with PDT using different F_2BMet formulations and DLI = 72 h or 15 min (vascular PDT). Group median survival times: Drug control – 11 days; Light control – 8 days; PDT with formulation A (PEG:EtOH:PBS, 3:1:5, 2 mg/kg F_2BMet) and 179 J/cm^2 – 14 days; PDT with formulation B (PG:EtOH:PBS, 3:1:1, 2 mg/kg F_2BMet) and 248 J/cm^2 – 14 days; PDT with formulation D (CrEL:EtOH:NaCl0.9%, 0.2:1:98.8, 2 mg/kg F_2BMet) and 117 J/cm^2 – 21 days. Vascular PDT with formulation D (1 mg/kg F_2BMet) and either 59 or 73 J/cm^2 – 83% of tumour remissions.

As shown in Figure 3.4, formulation D followed 72 h later by irradiation was responsible for a significant increase in the median survival time relative to control (from 11 to 21 days, log-rank test p<0.001), and in one case the mouse remained without tumour 60 days after the PDT treatment and was considered cured. The good performance of this formulation can be assigned to the higher exposure of the tumour to the drug at the time of irradiation. This

higher exposure was partially compensated by an increase in the light dose used with formulations A and B, but this did not offset the difference between the formulations. The conservative protocol employed in these studies led to a large oedema and to a small necrotic scab at the irradiation site, which resolved in a few days.

Figure 3.4 also presents a study with formulation D and DLI = 15 min, in which illumination was performed while all F_2BMet was confined in the vasculature (vascular PDT). The bioavailability is higher at 15 min than at 72 h because the concentration of F_2BMet in the blood decreases by one order of magnitude in this DLI. Overdosing at 15 min was avoided by reducing the drug dose to 1 mg/kg and the light dose to 73 J/cm^2 (one group of 6 animals) or to 59 J/cm^2 (another group of 6 animals). The results obtained with the two groups of 6 animals were the same: 5 out of the 6 animals remained free of tumour for at least 60 days. This remarkable long-term tumour response is accompanied by extensive necrosis in all the area illuminated. Although the acute local response was very strong, the animals maintained their normal behaviour, the necrotic scab eventually disappeared, and a good cosmetic effect was generally observed.

SKIN PHOTOSENSITIVITY

Skin photosensitivity is a major clinical adverse effect caused by current photosensitizers. The comparison between their skin photosensitivity requires the use of similar experimental conditions and comparable criteria to classify the adverse effects. We used the criteria previously described by Weersink *et al* [52] and reproduced in Table 3.2, to evaluate the results of exposure to similar light sources and light doses, as it was also adopted in a study with Foscan® [142]. Figure 3.5 shows the skin responses of circumscribed areas of the skin of Wistar rats after exposure to different light doses and their evolution over time. The light doses were delivered with a solar simulator 12, 24, 72 or 168 h after the iv administration of 1 mg/kg of F_2BMet in formulation D. The scores are the average of 4 independent experiments. As expected, the strongest skin reactions were observed for longer exposure times and shorter times after the administration of F_2BMet. However, 7 days after the administration of F_2BMet the exposure to the solar simulator elicited at most a mild erythema. Figure 3.6 presents the scoring 3 days after the exposure to light, when it is at its maximum.

For comparison, it is interesting to note that the exposure of Wistar rat skin to a similar light source 7 days after the iv administration of 0.3 mg/kg of temoporfin in Foscan® gave a scores of 5.0±0.8 for an exposure times of 30 min, whereas for 1 mg/kg of F2BMet in formulation D the corresponding score is 0.5±0.3.It is also interesting to note that the iv administration of 4 mg/kg of Photofrin® followed 72 h later to exposure to 94.5 J/cm2 of

broad spectrum light elicited oedema, inflammation and eschar formation (the equivalent of a score of 5 according to the criteria adopted in this work) in the depilated back of DBA/2J mice [226]. For a similar light dose and DLI, F2BMet at 1 mg/kg gave a score of 1.5±0.3.

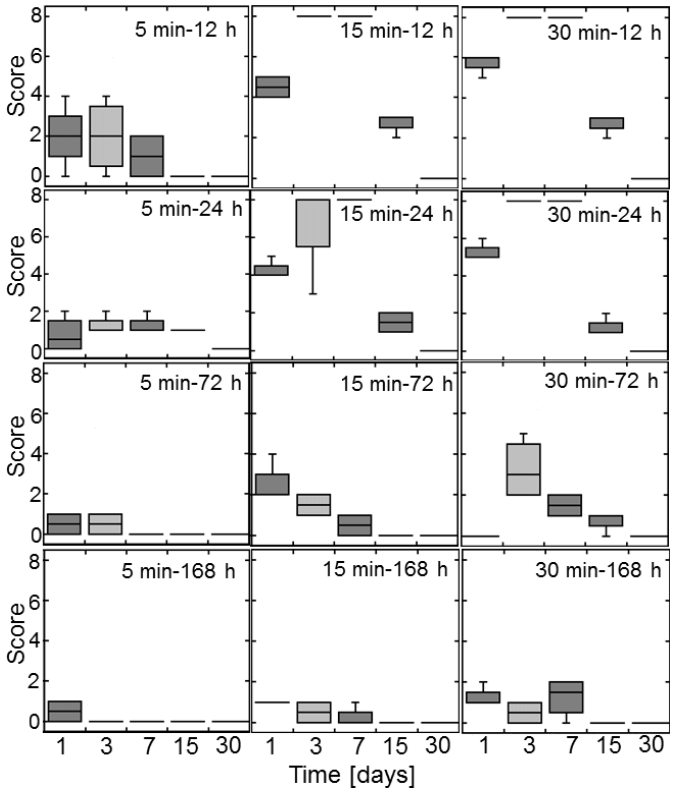

Figure 3.5 – Evolution of the skin reactions over time, in Wistar rats exposed to 5, 15 and 30 min of 100 mW/cm^2 light from a solar simulator after DLI = 12, 24, 72 and 168 h post iv administration of F_2BMet (1 mg/kg) in formulation D.

3.5. Conclusion

The ideal drug formulation should lead to high T/S and T/M ratios and to high bioavailability. Additionally, PDT photosensitizers should be rapidly eliminated from the organism after the therapy to reduce the risk of adverse skin reactions. The ideal drug formulation should also be simple to prepare and have a long shelf life.

We showed that a formulation containing 0.08 ml of CrEL per kg body weight (0.27% in plasma), formulation C, reduces the amount of F_2BMet in the liver in the first days and increases the bioavailability of this photosensitizer with respect to other formulations. Formulation C helps F_2BMet bypass the RES tissues, but this also erodes the T/M and T/S ratios with respect to those of other formulations. Both these effects may be assigned to a lower transfer of F_2BMet to LDL in formulation C, aggravated by the low level of LDL in BALB/c mice. Reducing the CrEL content to 0.02 ml/kg body weight (0.07% in plasma) in formulation D, maintains a relatively high exposure of the mice to F_2BMet but preserves the

LDL, which improves the delivery of F_2BMet to tumours. The content of CrEL in this formulation is a factor of 3 below the level known to elicit adverse effects, if F_2BMet is used at a dose of 2 mg/kg.

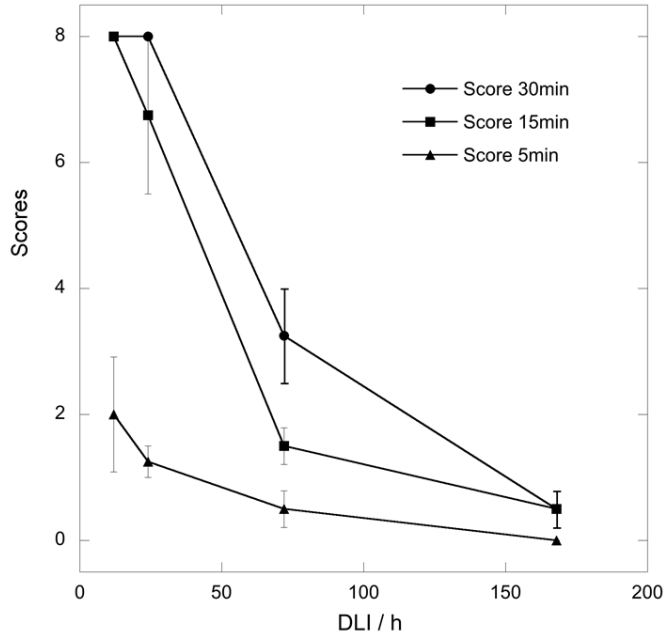

Figure 3.6 – Scores of skin reaction in Wistar rats exposed to 5, 15 and 30 min of 100 mW/cm^2 light from a solar simulator as a function of the interval between the iv administration of F_2BMet (1 mg/kg) in formulation D and the exposure to the solar simulator. The scoring was made 3 days after the exposure to light.

The pharmacokinetic profiles obtained with mice and minipigs are consistent with a good solubilisation of F_2BMet and high bioavailability even at times very close to the administration time. This allows for testing various PDT modalities, namely taking advantage of the vascular effect. On the other hand, the T/M ratio in mice is high 12 h after administration and remains high for several days. This favours a selective and more conservative therapy protocol, presumably capable of destroying the tumours while sparing the surrounding tissue. An exploratory PDT study with 2 mg/kg of F_2BMet and DLI = 72 h led to the cure of one animal out of 6, and confirmed the superiority of formulation D for PDT with F_2BMet. Vascular PDT with DLI=15 min lead to the cure of 10 out of 12 animals. This extraordinary result was associated with a very strong local response. Future work will focus on the development of treatment protocols for different modes of action of PDT and on the study of long-term tumour responses.

We obtained T/S ratios larger than unit, which should reduce the skin photosensitivity associated with PDT. Indeed, exposure of the skin of rats to the light of a solar simulator 7 days after the iv administration of 1 mg/kg of F_2BMet did not elicit important skin reactions. Moreover, minipigs subject to F_2BMet doses of 2 mg/kg and exposed to normal indoors

lighting did not show adverse reactions. This is a substantial reduction in skin photosensitivity with respect to the photosensitizers approved for PDT of cancer in the USA and Europe.

In summary, the favourable biodistribution and pharmacokinetics of F_2BMet in a formulation with a low content of CrEL led to good tumour responses for a conservative therapy (DLI=72 h), and to a cure rate of 83% for the more aggressive vascular PDT (DLI=15 min). This formulation leads to only a minor skin photosensitivity. Although CrEL formulations are very convenient to deliver amphiphilic photosensitizers, the CrEL dose must be low to minimize lipoprotein degradation and allow LDL to drive biodistribution.

Chapter 4

Nonclinical Safety Evaluation

Chapter 4 – Nonclinical Safety Evaluation

The work presented in this chapter will be submitted for publication (manuscript in preparation):

Evaluation of intravenous single-dose toxicity of redaporfin PDT in rodents

Luis B. Rocha [1,2], Fábio Schaberle [1], Janusz M. Dąbrowski [3] and Luis G. Arnaut [4]

[1] Luzitin SA, S. Martinho do Bispo, 3045-016 Coimbra, Portugal

[2] Bluepharma – Indústria Farmacêutica, SA, S. Martinho do Bispo, 3045-016 Coimbra, Portugal

[3] Faculty of Chemistry, Jagiellonian University, 30-060 Krakow, Poland

[4] Chemistry Department, University of Coimbra, 3004-535 Coimbra, Portugal

3

4.1. Abstract

Safety evaluation of drug candidates in animal models is a pre-requisite for their successful development, namely to reach clinical trials. Thus, the objective of this study was to explore the tolerability and safety of a single dose of LUZ11 formulated in Cremophor® EL/Ethanol/NaCl 0.9%, administered iv to mice and rats.

The study was divided in two parts that focused on two distinct approaches to evaluate the acute toxicity of drug candidates that are referred in the ICH M3(R2) guideline for the nonclinical safety studies for pharmaceuticals. The first part, a dose escalation Study in mice, aimed to evaluate the maximum tolerated dose (MTD) of LUZ11 formulation administered intravenously. LUZ11 formulation was well tolerated by the animals, in the dose range from 20 mg/kg to 100 mg/kg, and no signs of adverse reactions were detected at the site of injection. There were no noticeable changes in body weight, behaviour or physical condition, in comparison with the control group. No signs of photosensitivity reactions were observed and the animals did not show light avoidance behaviour during the course of the study.

For the second part, a safety toxicology study in Wistar rats, a single well tolerated dose of LUZ11 with expected clinical relevance was selected for iv administration, followed or not by laser irradiation, to evaluate possible signs of systemic toxicity through the analysis of haematology and serum biochemistry parameters. The results showed that LUZ11 was very well tolerated. No relevant changes or trends were verified, except for a significant but transient increases in hepatic function and muscle integrity markers, and also on neutrophils counts, observed after the application of a PDT protocol. No visible abnormalities were apparent, including reactions at the injection site. No skin photosensitivity reactions occurred during the study, even though the animals were maintained in normal indoor lighting.

4.2. Introduction

Photodynamic Therapy is generally recognized as a safe and effective strategy to treat some forms of cancers. To ensure that new PS under development present acceptable profiles of tolerability and safety and guarantee the lowest possible level of risk for the participants in the first clinical trial, they must be subjected to an extensive nonclinical toxicology programme. The general requirements for these toxicology studies are described in the harmonized guideline ICH M3(R2), and are further detailed in the comprehensive set

of guidelines related to safety (S guidelines), specific for each type of study [224]. These studies are distributed throughout the several development stages in order to deliver the results that are the most relevant in each stage. The exploratory characterization of potential toxic effects of new drug candidates should start in the early development stages to allow the identification and elimination of molecules with unacceptable safety profiles, thus avoiding the waste of precious resources on their development. This guideline states that "the goals of the nonclinical safety evaluation generally include a characterisation of toxic effects with respect to target organs, dose dependence, relationship to exposure, and when appropriate, potential reversibility." The evidences produced at this stage will support the estimation of a safe starting dose and dose range for the first-in-man clinical trial and will allow the identification of clinical markers that should be monitored to foresee potential adverse effects. In addition, the decision to advance into the next clinical development stage should be supported by non-clinical and clinical evidences that demonstrate adequate safety, as they become available [224].

The requirements for safety evaluation of drug candidates are also applied to the nonclinical development of PS candidates for PDT application, however the potential adverse reactions in those cases can either be intrinsically related to the PS or its formulation, or can be a consequence of the irradiation protocol. These specificities associated to the PDT protocol must be taken in consideration in the design of the safety evaluation studies for PS candidates [225, 226]. Thus, for a preliminary nonclinical evaluation of the safety of LUZ11 in its formulation, two studies were performed, a dose escalation study to evaluate the Maximum Tolerated Dose, without irradiation in mice, and a systemic toxicity screening with and without irradiation in rats. The goal is for the LUZ11-PDT in the clinic to be effective with only one treatment, so both studies focused on the acute reactions elicited by a single session of PDT.

4.3. Materials and methods

CHEMICALS

The test substance LUZ11 was supplied by the CRD of Luzitin, S.A. in sealed vials with weighed amounts under nitrogen atmosphere, and was stored at approximately -18 ºC, in the dark. All procedures involving the handling of LUZ11, either as a solid or in solution, were performed in conditions of reduced luminosity (in the absence of direct light).

Cremophor® EL was purchased from Sigma-Aldrich (St. Louis, MO, USA). Absolute ethanol and NaCl were obtained from Merck (Darmstadt, Germany).

ANIMALS

The studies involving the use of laboratory animals were authorized by the Portuguese Veterinary Authority (DGAV) – project authorization number 0420/000/000/2011.
BALB/c female mice with 8 weeks of age and female Wistar Han rats with 10 weeks of age were supplied by Charles River Laboratories (Barcelona, Spain). They were maintained with free access to food and water in a room with controlled cycle of 12 hours light/dark. At the end of the study, animals were anaesthetised with a mixture of ketamine 100 mg/kg (Clorketam 1000, Vetoquinol, Barcarena, Portugal) and xylazine 10mg/kg (Rompun 2%, Bayer, Carnaxide, Portugal) and sacrificed by cervical dislocation.

DOSE ESCALATION STUDY

LUZ11 FORMULATIONS

Each test dose of LUZ11 (20, 28, 35, 40, 50 and 100 mg/kg) was prepared as an individual formulation for iv administration. The formulation was the same for all doses and was a modified version of the one developed and optimized in the previous chapter, containing CrEL/EtOH/NaCl 0.9%. For this study the relative proportions of CrEL and EtOH in relation to LUZ11 had to be significantly increased, to allow the complete solubilisation of the necessary amount of PS to reach the defined maximum dose of 100 mg/kg, but were kept within the recommended limits for iv administration in mice [227, 228]. The modified formulation CrEL/EtOH/NaCl 0.9% (5:10:85) was prepared according to the following steps:

The defined amount of LUZ11 was weighed into a 2 ml microtube and dissolved in the appropriated volumes of CrEL and absolute ethanol through alternated cycles of 30 sec of vortex mixing followed by 5 min in an ultra-sound bath. Then, the solution was transferred to another tube containing the appropriated volume of NaCl 0.9% and was homogenised through vortex mixing, resulting in a limpid dark green solution. The complete solubilisation of LUZ11 was confirmed by the absence of precipitate after a 5 min centrifugation at 4000 rpm.
As expected, the difficulties in the solubilisation of LUZ11 in the CrEL/EtOH mixture increased dramatically with the concentration of the molecule. Consequently, the formulation for 100 mg/kg of LUZ11 (10 mg/ml) was the maximum feasible dose.

INTRAVENOUS INJECTION

The final formulations listed in Table 4.1 were slowly injected in the mice tail vein using a syringe with a 26G needle in a proportion of 200 µl per 20 g of mouse body weight. The first

6 groups (G0 to G5) were administered and followed in the first stage of the study. After the end of this first stage, group G6 was then administered and followed.

Table 4.1 – Summary of the study groups and the correspondent administered LUZ11 iv formulations

Test Group	n	LUZ11 (mg/kg)	LUZ11 (mg/mL)	CrEL (mg)	EtOH (µl)	NaCl 0.9% (µl)
G0 (Control)	5	0	0.0	78.8	150	1275
G1		20	2.0			
G2		28	2.8			
G3		35	3.5			
G4		40	4.0			
G5		50	5.0			
G6	4	100	10.0			

MICE FOLLOW-UP

After administration, mice condition was evaluated at least once a week during 5 weeks, where the following observations were registered: body weight, local reactions at the site of injection, light sensitivity/avoidance and general condition.

SAFETY TOXICOLOGY STUDY

LUZ11 FORMULATION

The formulation with CrEL/EtOH/NaCl 0.9% described in Chapter 3 was used for the iv administration of 2 mg/kg of LUZ11, with adjustment on the content of NaCl to allow the administration of a suitable volume for Wistar rats. The final formulation was obtained by diluting a solution of LUZ11 (16.67 mg/ml) in CrEL/EtOH (16.7:83.3, v:v) in NaCl 0.9%, to a final concentration of 1.15 mg/ml of LUZ11. For the iv administration of 20 mg/kg of LUZ11 the final formulation was obtained by diluting a solution of LUZ11 (32.94 mg/ml) in CrEL/EtOH (16.7:83.3, v:v) in NaCl 0.9%, to a final concentration of 11.15 mg/ml of LUZ11. The method to prepare LUZ11 formulation was the following:

The defined amount of LUZ11 was weighed and completely dissolved in the appropriated volumes of CrEL and absolute ethanol, using alternated cycles of 30 sec of vortex mixing followed by 5 min in an ultra-sound bath. Then, the previous solution was transferred to a tube containing the appropriated volume of NaCl 0.9%, and was carefully homogenised, resulting in a limpid dark green solution. The complete solubilisation of LUZ11 was confirmed by the absence of precipitate after a 5 min centrifugation at 4000 rpm.

INTRAVENOUS INJECTION, PDT AND BLOOD COLLECTION

Seven groups of animals were randomly organized (n=4): 4 non-irradiated groups – non-treated control; LUZ11 2 mg/kg, LUZ11 20 mg/kg and vehicle (the same vehicle used in the 20 mg/kg formulation, which contained the higher amounts of CrEL and EtOH); and 3 groups that received LUZ11 2 mg/kg followed by laser irradiation (DLI=15 min, 74 J/cm^2, Ø 10 mm). Rats from these 3 groups were irradiated in the muscle of the right thigh, previously shaved, using Hamamatsu diode laser, type LA0873, S/N M070301 controlled with a ThorLabs 500 mA ACC/APC Laser Diode Controller and in-house electronics, emitting 130 mW at 748 nm, which was hand-held during the irradiation. The time-points for the terminal blood collection were 24 h, 72 h, and 1 week after PDT for the irradiated groups, and 24 h after the administration for the other groups. Due to the volume of blood needed for the haematological and biochemistry tests the procedure for blood collection was terminal. For the administration, irradiation and blood collection rats were anesthetised with an ip injection of a mixture of ketamine 75 mg/kg and xylazine 10 mg/kg. At the defined time-points 2 – 2.5 ml of blood were drawn from the abdominal aorta and immediately after the animals were sacrificed by cervical dislocation.

BLOOD ANALYSIS

Blood tests (haematology and serum biochemistry) were outsourced to the Clinical Analysis Laboratory from the Faculty of Pharmacy of the University of Coimbra and were performed using standard clinical procedures and equipment.

Immediately after collection, each blood sample was fractioned: 1 ml was transferred to an haematology tube containing EDTAK_3 and gently homogenised, and the remaining, for serum biochemistry, was dispensed into a 2 ml microtube and was allowed to cloth at ambient temperature during 30 min. Serum was separated by centrifugation at 4000 rpm for 10 min, and 0.5 ml of supernatant were transferred to a new tube.

Blood for haematology and serum were stored at 2-8 ºC and analysed in the same day. For manual leukocyte differential counts, a blood smear was prepared for each blood sample after blood collection, using a drop of EDTA-anticoagulated blood from the haematology

tube. When dry, the smear was fixed with methanol for 3 min, and then left to dry in vertical position. Slides were stored at ambient temperature until processing and analysis.

The haematology test evaluated the following parameters:

- Red Blood Cells ($x10^{12}$/L)
- Reticulocytes (%)
- Haemoglobin (g/dL)
- Haematocrit (%)
- Mean Corpuscular Volume (fL)
- Mean Corpuscular Haemoglobin (pg)
- Mean Corpuscular Haemoglobin Concentration (g/L)
- Red Cell Distribution Width (%)
- Platelets ($x10^{9}$/L)
- Mean Platelet Volume (fL)
- Plateletcrit (%)
- Platelet Distribution Width (%)
- White Blood Cells ($x10^{9}$/L)
- White Blood Cells Differential Count

The serum biochemistry test evaluated the following parameters:

- Glucose (mg/dL)
- Urea (mg/dL)
- Total Protein (g/L)
- Cholesterol (mg/dL)
- Triglycerides (mg/mL)
- Aspartate Aminotransferase (IU/L)
- Alanine Aminotransferase (IU/L)
- *gamma*-Glutamyl Transpeptidase (IU/L)
- Alkaline Phosphatase (IU/L)
- Ureic Nitrogen (mg/dL)
- Creatine Kinase (IU/L)
- Lactate Dehydrogenase (IU/L)
- Creatinine (mg/dL)
- Bilirubin (mg/dL)

Results are presented for each group and time-point as average±SD. Differences between test and control groups were evaluated by one-way ANOVA, using GraphPad Prism

software (V5.01), with Tukey's post hoc test for multiple pair-wise comparisons. Differences were considered statistically significant for $p<0.05$.

4.4. Results and discussion

DOSE ESCALATION STUDY

Throughout the study, no apparent variations were observed between the average body weight (BW) of any of the study group, including the control group that received vehicle alone. The BW evolution over time after the administration for each group is summarised in Table 4.2.

The eyes, tail and paws of the animals were observed at the time of weighing and no changes were detected in comparison to the beginning of the study. No signs of photosensitivity were observed and the animals did not show light avoidance behaviour during the handling procedures. In addition, there were no signs of local reaction at the site of injection. There were also no alterations in overall condition or behaviour of the mice throughout the study.

Mice from group G6 (100 mg/kg) started the study 8 weeks after the other groups, once it was concluded that the injected LUZ11 formulations up to 50 mg/kg did not cause any observable reaction in mice. This time gap accounts for the higher average body weight observed in the 100 mg/kg dose group as compared to the other groups.

Table 4.2 – Body weight (g) over time after the iv injection of LUZ11 formulation for each study group (average ± SD)

Group Code	LUZ11 (mg/kg)	Days after injection									
		0	4	7	11	14	16	21	28	35	46
G0	0	21.9±0.6	-	21.9±0.8	-	-	22.2±1.0	-	22.1±1.2	22.4±0.8	-
G1	20	22.0±0.7	-	21.8±0.6	-	-	22.4±0.6	-	22.9±0.5	23.1±0.6	-
G2	28	22.0±1.0	-	21.7±0.8	-	-	22.1±0.9	-	22.3±1.0	22.1±1.1	-
G3	35	21.4±0.5	-	20.8±0.7	-	-	21.0±0.7	-	21.9±1.1	21.7±0.4	-
G4	40	22.8±0.9	-	22.5±0.9	-	-	22.6±1.0	-	22.3±0.9	23.4±1.0	-
G5	50	21.9±1.2	-	21.5±1.0	-	-	21.7±1.0	-	21.8±1.3	22.2±1.0	-
G6	100	24.4±1.7	23.9±1.6	24.2±1.7	24.2±1.6	24.2±1.6	-	24.5±1.8	25.5±1.6	-	25.3±1.7

SAFETY TOXICOLOGY STUDY

All animals enrolled in this study survived until the time-point defined for blood collection, without any observable signs of adverse reactions that could be associated with the iv administration of LUZ11 formulation, the vehicle alone or the PDT protocol. Changes in the general condition or behaviour of the animals were not detected, even in the group that received 20 mg/kg or in the irradiated groups. There was no reaction when they were exposed to the normal illumination of the animal laboratory, which indicates the absence of light sensitivity.

Table 4.3 – Results of the haematology tests from all study groups.

Haematology	Control	2 mg/kg	2 mg/kg PDT 24h	2 mg/kg PDT 72h	2 mg/kg PDT 1Week	20 mg/kg	Vehicle
RBC (x10^{12}/L)	6.5±0.3	7.2±0.3	6.7±0.3	6.1±0.2	6.2±0.4	6.4±0.2	6.5±0.3
Retic (%)	1.3±0.1	1.3±0.1	1.2±0.1	1.3±0.1	NP	1.4±0.1	1.4±0.1
Hg (g/L)	13.4±0.5	14.1±0.2	13.8±0.1	12.0±0.2	12.6±0.7	13.1±0.2	13.5±0.2
HCT (%)	36.3±2.0	39.7±1.0	39.5±0.7	34.6±1.1	35.5±1.8	35.1±0.6	36.3±0.6
MCV (fL)	56.1±1.7	55.2±1.3	59.5±2.0	56.9±1.8	57.1±1.0	55.0±1.3	55.1±1.8
MCH (pg)	20.8±0.8	19.6±0.9	20.7±1.0	19.8±0.5	20.2±0.3	20.6±0.7	20.6±1.1
MCHC (g/L)	37.1±0.8	35.5±0.8	34.9±0.5	34.8±0.6	35.4±0.6	37.4±0.5	37.3±0.8
RDW (%)	12.0±0.4	12.3±1.3	11.2±0.6	11.9±0.9	13.0±1.3	12.7±1.0	12.3±1.1
PLT (x10^{9}/L)	740±62	801±56	615±167	610±34	NM	654±83	629±90
MPV (fL)	5.8±0.2	5.4±0.1	6.1±0.4	5.7±0.2	5.7±0.2	5.7±0.2	5.6±0.3
PCT (%)	42.7±2.4	43.4±2.4	37.4±8.6	35.0±1.0	67.3±9.4	37.4±6.1	35.0±3.4
PDW (%)	17.0±0.2	16.9±0.8	17.2±0.4	16.7±0.3	16.6±0.3	16.8±0.5	16.7±0.6
WBC (x10^{9}/L)	5.1±0.6	7.0±2.0	6.9±1.7	5.4±0.8	4.8±0.5	3.6±0.4	3.5±0.7
NE (%)	16.0±6.4	11.0±5.0	53.3±10.2	28.3±7.8	NP	20.7±9.3	14.0±3.5
NE	0.8±0.2	0.8±0.5	3.7±1.0	1.5±0.4	NP	0.8±0.4	0.5±0.1
LY (%)	82.0±6.3	85.3±5.0	41.3±10.0	66.0±7.5	NP	76.0±9.5	84.3±3.4
LY (x10^{9}/L)	4.2±0.7	5.9±1.6	2.9±1.2	3.6±0.7	NP	2.7±0.2	3.0±0.6
MO (%)	1.8±1.5	3.0±0.8	5.3±0.6	5.0±2.2	NP	3.3±1.5	1.8±2.1
MO (x10^{9}/L)	0.1±0.1	0.2±0.1	0.4±0.1	0.3±0.1	NP	0.1±0.1	0.1±0.1
EO (%)	0.3±0.5	0.8±1.0	0.0±0.0	0.8±1.0	NP	0.0±0.0	0.0±0.0
EO (x10^{9}/L)	0.0±0.0	0.1±0.1	0.0±0.0	0.0±0.1	NP	0.0±0.0	0.0±0.0
BA (%)	0.0±0.0	0.0±0.0	0.0±0.0	0.0±0.0	NP	0.0±0.0	0.0±0.0
BA (x10^{9}/L)	0.0±0.0	0.0±0.0	0.0±0.0	0.0±0.0	NP	0.0±0.0	0.0±0.0

Values are presented as average ± SD. Abbreviations: RBC = red blood cells, Retic = reticulocytes, Hb = haemoglobin, HCT = haematocrit, MCV = mean corpuscular volume, MCH = mean corpuscular haemoglobin, MCHC = mean corpuscular haemoglobin concentration, RDW = red blood cell distribution width, PLT = platelets, MPV = mean platelet volume, PCT = plateletcrit, PDW = platelet distribution width, WBC = white blood cells, NE = neutrophils, LY = lymphocytes, MO = monocytes, EO = eosinophils, BA = basophils. NP = Not performed due to sample degradation during blood smear processing, NM = Not measurable – out of range.

The three groups irradiated 15 min after the administration of the PS, on the following day, presented a significant inflammatory response in the irradiated leg, indicated by a large oedema, although it did not interfere with their movements. In addition, a necrotic eschar covering the irradiated area was visible 72 h after PDT in all animals from the irradiated groups. Possible signs of systemic toxicity were accessed by a standard set of clinical blood tests at selected time-points, post-administration/irradiation. Those tests are routinely performed to evaluate acute and chronic toxicity reactions through the measurement of haematological parameters and biochemistry markers, and are very useful in the non-clinical evaluation of the safety profile of new drug candidates, including PS [229, 230]. Generally they provide relevant information about the circulatory homeostasis, liver and renal function or muscle injury [231].

The detailed results of the blood tests performed for all study groups are presented in Table *4.3* (haematology) and Table 4.4 (serum biochemistry). The values determined for the non-treated control group were found to be in the normal ranges for female Wistar rats with similar age, indicated in the supplier technical documents [232]. The haematology and serum biochemistry results obtained for the three non-irradiated groups, which received vehicle alone, LUZ11 at 2 mg/kg or 20 mg/kg, show that there was no significant difference in comparison to the non-treated control group. This demonstrate that a single iv administration of the LUZ11 formulation, even at a dose of 20 mg/kg, doesn't cause a significant impact on the clinical blood parameters, and therefore there are no signs of systemic toxicity.

The comparison between the serum biochemistry results of the irradiated groups and the control group revealed significant differences on the markers for liver function and muscle damage. The results show that 24 h after the irradiation there was a significant increase in the levels of the hepatic transaminases, AST and ALT, while ALP remained unchanged (Figure 4.1). Together with the significant rise in LDH and CK, which are normally associated with muscle damage [233], these results were probably a consequence of the destruction of skeletal muscle in the irradiated area caused by the photodynamic effect of the LUZ11-PDT. Nevertheless, 72 h after PDT the levels of all four markers had already decreased, and only AST and ALT remained significantly higher than in the control group. One week after PDT all the altered biochemistry parameters have returned to their levels pre-PDT, indicating that the changes in liver function were transitory and probably a consequence of muscle damage, associated with the observed local tissue destruction caused by the PDT protocol. There were no significant alterations on the levels of renal function, like urea, blood urea nitrogen, creatinine or total protein, which is a good indication that the kidneys were not affected by LUZ11 and its formulation, nor by the photodynamic reaction elicited by the PDT protocol.

Regarding the haematology results, all parameters from all test groups were largely unaffected in comparison to the control group, with only two statistically significant exceptions: a drastic increase in the number of circulating neutrophils observed 24 h after PDT, and a decrease in the haemoglobin level 72 h after PDT. In addition, 24 h after PDT there was a significant decrease in the lymphocyte population relative to 2 mg/kg group, but not significant in relation to the control group (Figure 4.2).

Table 4.4 – Results of the serum biochemistry tests from all study groups.

Biochemistry	Control	2 mg/kg	2 mg/kg PDT 24h	2 mg/kg PDT 72h	2 mg/kg PDT 1Week	20 mg/kg	Vehicle
GLU(mg/dl)	229±54	217±46	174±47	171±21	191±34	222±9	218±17
Urea (mg/dl)	42±3	33±4	30±2	40±8	44±2	32±5	33±2
CHOL (mg/dl)	52±7	51±4	68±12	54±4	55±8	41±7	43±7
TG (mg/ml)	114±45	120±62	61±16	58±14	117±53	66±20	84±9
AST (U/L)	73±11	76±10	968±317	555±123	78±12	178±100	73±13
ALT (U/L)	27±5	29±2	165±47	106±13	25±3	38±13	24±3
CRE (mg/dl)	0.47±0.02	0.45±0.01	0.48±0.07	0.43±0.02	0.49±0.03	0.44±0.05	0.44±0.03
ɣ-GT (U/L)	NM	NM	NM	NM	NM	NM	NM
ALP (U/L)	88±15	93±37	97±38	56±13	60±8	90±12	54±6
BIL (mg/dl)	0±0	0±0	0.1±0.1	0.1±0.1	0.1±0.0	0.1±0.1	0.1±0.0
TP (g/L)	5.6±0.2	5.3±0.2	4.7±0.3	5.3±0.1	5.6±0.1	5.6±0.3	5.2±0.3
CK (U/L)	352±105	272±142	4314±496	347±84	301±74	416±169	230±58
BUN (mg/dl)	20±1	15±2	14.2±1.0	18.6±3.7	20.5±0.7	15.1±2.2	15.3±0.8
LDH (U/L)	552±97	355±127	1625±483	376±217	513±185	698±227	372±104

Values are presented as average±SD. Abbreviations: GLU = glucose, CHOL = total cholesterol, TG = triglycerides, AST = aspartate aminotransferase, ALT = alanine aminotransferase, CRE = creatinine, ɣ-GT = Gamma-glutamyl transferase, ALP = alkaline phosphatase, BIL = total bilirubin, TP = total protein, CK= creatine kinase, BUN = blood urea nitrogen, LDH= lactate dehydrogenase. NM = Not measurable – out of range.

The increase of the neutrophil population in circulation can be associated with the innate immune system response to a local insult, which triggers an acute inflammatory response [48]. This response was clearly observed in the form of a large oedema that extended through the whole leg of the animals, on the days that followed the irradiation. On the third day after irradiation the population of circulating neutrophils was already decreasing, which can be an indication of there are moving from the circulation into the damaged tissues [87]. One week after PDT the number of neutrophils in the blood had already returned to the levels pre-PDT.

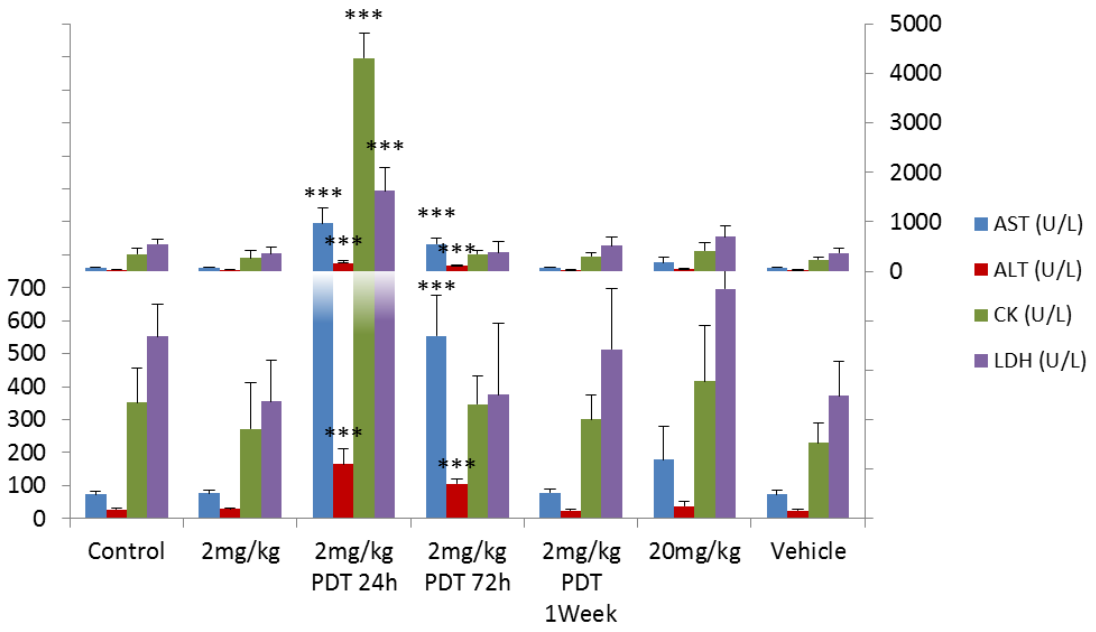

Figure 4.1 – Summary of the most relevant results from serum biochemistry of Wistar rats, presented as average±SD. (*** difference relative to the control group – p<0.001). The graph is composed by two panels that present the same results in different scales to highlight the inter-group differences.

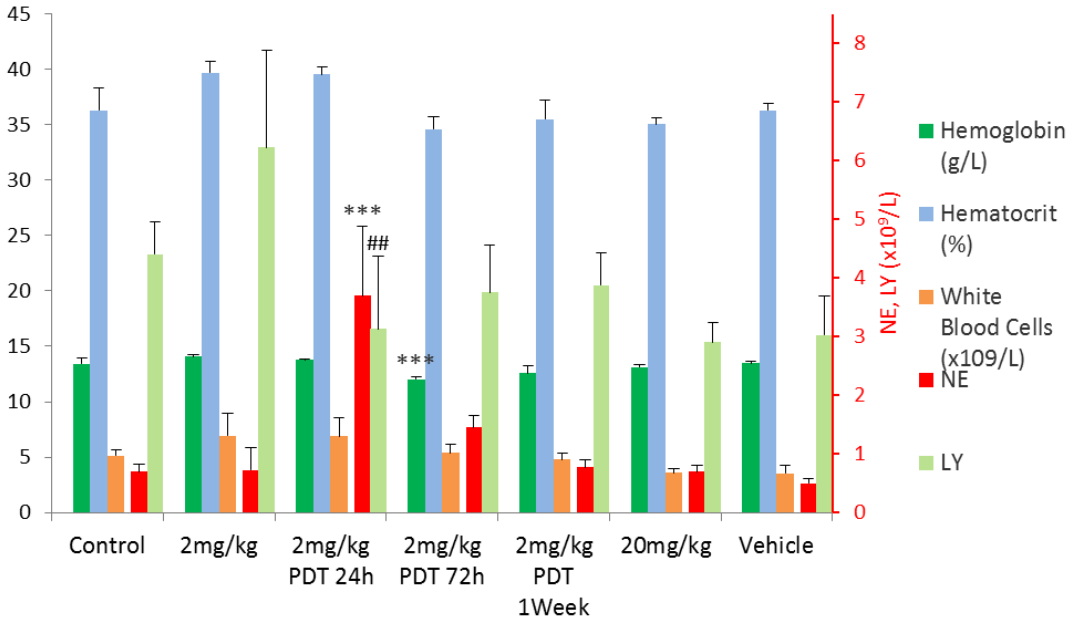

Figure 4.2 – Summary of the most relevant results from Wistar rats haematology, presented as average±SD. The values for the neutrophils (NE) and lymphocytes (LY) populations are presented in the secondary vertical axis. (*** difference relative to the control group – p<0.001; ## difference relative to the 2 mg/kg group – p<0.01).

4.5. Conclusion

The LUZ11 formulations administered intravenously to mice without irradiation, even at the highest dose of 100 mg/kg, seem to be very well tolerated by the animals. There were no observable signs of local irritation at the injection site, and no signs of photosensitivity appeared in any of the groups.

The *in vivo* efficacy results of a non-optimized PDT protocol with 1 mg/kg of LUZ11, presented in the previous chapter, already showed a highly significant antitumour effect. Thus, the highest dose tested without visible adverse reactions (100 mg/kg), could be at least 100 times higher than the therapeutic dose.

These results give important indications on the safety of LUZ11 and its formulation, confirming the very low toxicity in the absence of light determined during the *in vitro* screening stage, and give a comfortable safety margin in relation to the expected therapeutic dose.

In the safety toxicology study in rats, LUZ11 formulation was administered intravenously to evaluate possible signs of systemic toxicity, through the assessment of clinical blood markers after LUZ11 administration and at different time-points after PDT. Once again, there were no visible signs of irritation at the injection site, and no light-avoidance behaviour was observed in any animal, even in the 20 mg/kg group. The results confirmed that the LUZ11 formulation, either at 2 mg/kg or at 20 mg/kg, without the application of a PDT protocol is very well tolerated by the animals and does not cause significant alterations on the baseline levels of the evaluated parameters. The scenario was different when a vascular-PDT protocol was applied. This protocol led to a strong local inflammatory response in and around the irradiated area, and by the formation of a necrotic scab covering perfectly the illuminated tissue. In addition to these macroscopic observations some of the clinical markers for the hepatic function and muscle integrity showed dramatically increases 24 h after PDT, which were attributed to the considerable destruction of skeletal muscle caused by LUZ11-PDT. On the day after PDT there was also a significant but transient increase of the population of neutrophils in circulation, which could be a result of their recruitment in response to the local inflammatory reaction to infiltrate the affected tissues. Nevertheless, these acute changes were temporary, as demonstrate by their attenuation 72 h after the irradiation, and after one week returned to their levels before PDT. Other PS described in literature showed a much lower tolerance level than LUZ11. These reactions to LUZ11 iv administration are far less significant than those reported for the approved systemic photosensitizer Foscan, on the scientific discussion document from the European Medicines Agency (EMA). In mice and rats exposed only normal light conditions, for doses as low as 0.85 mg/kg of Foscan by iv, without irradiation, several adverse reaction were

described including phototoxicity reactions on exposed areas of the skin and systemic toxicity characterized by significant changes in haematological and haematopoietic parameters and increased spleen and liver weights [234].

Although the character of the dose escalation and toxicology studies here presented had been exploratory, the results obtained demonstrate the low toxicity potential of LUZ11 and its formulation, even when combined with a biologically effective PDT protocol. These results were later confirmed and complemented with other toxicology studies in rat and dog, performed by a CRO in accordance to all regulatory GLP requisites.

Chapter 5

Towards a clinical protocol

Chapter 5 – Towards a clinical protocol

The work presented in this chapter was published in:

European Journal of Cancer (2015) 51, 1822 -1830.

Elimination of primary tumours and control of metastasis with rationally designed bacteriochlorin photodynamic therapy regimes

Luis B. Rocha[1], Lígia C. Gomes-da-Silva[2], Janusz M. Dąbrowski[3] and Luis G. Arnaut[2]

[1] Luzitin SA, R. Bayer, S. Martinho do Bispo, 3045-016 Coimbra, Portugal

[2] Chemistry Department, University of Coimbra, 3004-535 Coimbra, Portugal

[3] Faculty of Chemistry, Jagiellonian University, 30-060 Krakow, Poland

5.1. Abstract

Photodynamic therapy (PDT) with current photosensitizers focuses on local effects and these are limited by light penetration in tissues. We employ a stable near-infrared (NIR) absorbing bacteriochlorin with around 8 h of plasma half-live to increase the depth of the treatment and elicit strong systemic (immune) responses. Primary tumour growth delays and cures of BALB/c and nude mice bearing CT26 mouse colon carcinoma are related to the parameters that control PDT efficacy. The systemic antitumour protection elicited by the optimized PDT regime is assessed by tumour rechallenges and by resistance to the establishment of metastasis after intravenous injection of CT26 cells. The optimized treatment regime offered 86% cure rate in BALB/c mice but no cures in BALB/c nude mice. Cured mice rechallenged over 3 months later with CT26 cells rejected the tumour cells in 67% of the cases. PDT of a subcutaneous CT26 tumour 5 days after the additional intravenous injection of CT26 cells very significantly reduced lung metastasis. The PDT regime optimized for the bacteriochlorin leads to remarkable long-term survival rates, effective immune memory and control of lung metastasis.

5.2. Introduction

Photodynamic therapy (PDT) is a promising cancer treatment owing to its selectivity and absence of adverse drug reactions [24]. PDT is based on the photosensitizer administration, its accumulation in tumours and then illumination with light. Photosensitizers absorbing light in the NIR, where tissues have higher optical penetration depths (δ=2.3 mm at 750 nm) [58], increase the treatment depth. Excited photosensitizer molecules transfer energy or electrons to oxygen leading to singlet oxygen or hydroxyl radicals [38, 235], respectively, that trigger various biological mechanisms (vascular shutdown [108, 236], apoptosis/necrosis of tumour cells [20, 237] and immunogenic cell death [48, 236]) eventually leading to tumour remission.

Photosensitizers characterized by long plasma half-lives, such as temoporfin, $t_{1/2}$=45.4 h, are prescribed with drug-light intervals (DLI) of 4–6 days [220, 238]. Long exposure to temoporfin is associated with high tumour selectivity but prolonged skin photosensitivity. The period of photosensitivity is reduced using verteporfin ($t_{1/2}$=5-6 h) [239]. Verteporfin, first used in age-related macular degeneration (AMD), is currently in clinical trials on pancreatic cancer [240]. Verteporfin is irradiated at DLI=15 min in AMD or 60-90 min in pancreatic cancer treatments. Table 5.1 presents this and other factors that contribute to

the treatment outcome. Finding the best combination of drug dose, light dose, DLI, radiant exposure R, irradiance E, and tumour margin is crucial for primary tumour destruction. Additionally the PDT protocol may determine antitumour immune responses [241]. Thus, the success of PDT depends on the development of photosensitizers and treatment regimes.

Table 5.1 – Factors that limit the range of the parameters controlled in PDT.

Parameter	Lower limit range	Higher limit range
DLI	Selectivity	Drug clearance
Irradiance	Sub-lethal damage	Oxygen depletion
Light dose	Depth of treatment	Photosensitizer bleaching
Drug dose	Photosensitizer bleaching	Inner filter
Margins	Re-supply of nutrients	PDT-induced lethality

We recently described a photostable bacteriochlorin (LUZ11, redaporfin) with intense infrared absorption, high yield of ROS generation, high phototoxicity [171], low skin photosensitivity and favourable pharmacokinetics [54, 242]. This work uncovers relationships between PDT regimes, cure rates, antitumour immune memory and resistance to metastasis using redaporfin. Our results supported to regulatory approval to conduct a phase I/II clinical study of redaporfin (ClinicalTrials.gov identifier: NCT02070432).

5.3. Materials and methods

CHEMICALS

5,10,15,20-*Tetrakis*(2,6-difluoro-3-*N*-methylsulfamoylphenyl) bacteriochlorin (redaporfin) was provided by Luzitin SA (Coimbra, Portugal) as a powder in a sealed amber glass vial under N_2 atmosphere. The drug doses were calculated from the weighted amount and the content of the redaporfin sample (75%) given by Luzitin SA. In earlier studies (presented in the previous chapters) the purity was not known exactly and the reported doses were calculated only from the weighted amount of the redaporfin sample.

INTRAVENOUS FORMULATION

Redaporfin for intraveoknous (iv) injection was formulated in CrEL:EtOH:NaCl 0.9% (0.2:1:98.8). This bacteriochlorin has a molar absorption coefficient ε = 125.000 $M^{-1}cm^{-1}$ at

748 nm in this formulation [171]. The appropriate volume of the PS formulation (200 µl for 20 g of mouse body weight) was slowly injected in the tail vein of each animal, to administer the desired drug dose. Redaporfin is readily soluble in CrEL:EtOH, which forms micelles when added to the saline solution. This administration vehicle has been selected on the basis on the detailed biodistribution studies [54]. It is well tolerated and prevents the precipitation of the photosensitizer in the organism.

TUMOUR CELL LINE

Medium for cell culture (Dulbecco's Modified Eagle Medium, high glucose), PBS (phosphate-buffered saline) and Cremophor EL® (CrEL), were purchased from Sigma-Aldrich Corp. (St. Louis, MO, USA). Absolute ethanol (EtOH) was obtained from Fisher Scientific (Leicester, UK), NaCl from Merck (Darmstadt, Germany) and 4-(2-hydroxyethyl)-1-piperazineethanesulfonic acid (HEPES) from VWR Chemicals (Leuven, Belgium). Foetal bovine serum (FBS) was purchased from Biochrom GmbH (Berlin, Germany) and penicillin/ streptomycin mixture was obtained from Lonza (Walkersville, MD, USA). CT26 (mouse colon carcinoma) cells (CRL-2638™, ATCC-LCG Standards, Barcelona, Spain) were cultured as a monolayer in the DMEM medium (high glucose), supplemented with 10 mM of HEPES, 10% heat-inactivated FBS and a 100 IU/ml penicillin-100 µg/ml streptomycin mixture. They were maintained at 37 ºC, in humidified atmosphere containing 5% CO_2. When subcutaneously injected into BALB/c mice, CT26 colon carcinoma cells originate subcutaneous tumours that are considered minimally to moderately immunogenic tumours [243].

MOUSE TUMOUR MODEL

The animal studies (DGAV authorization no. 0420/000/000/2011) employed female BALB/c mice (Charles River Laboratories®, Barcelona, Spain) with 8 to 10 weeks of age, weighing 17-22 grams, which were organized in the pilot study groups of Table 5.2. For tumour establishment 350.000 CT26 cells were taken up in 0.1 ml PBS and inoculated subcutaneously in the right thigh of each mouse. The tumours were treated 8-10 days after the inoculation. The larger diameters of the tumours in the studies with controlled illumination area ranged from 3.7 to 9.2 mm, with an average of 5.51 mm and a standard deviation of 0.85 mm.

LIGHT DELIVERY DEVICES

The first studies employed a Hamamatsu diode laser, type LA0873, S/N M070301 controlled with a ThorLabs 500 mA ACC/APC Laser Diode Controller and in-house electronics, which was hand-held during the illumination of the tumour.

The final studies employed an Omicron (Rodgau, Germany) diode laser system, model LDM750.300.CWA.L.M with laser head 1201-07-D and 1201-08-D, maximum output power of 300 mW and wavelength of 749 nm ± 3 nm, connected to a glass optical fibre with microlens tip from Medlight (Ecublens, Switzerland), model FD with 2 mm of diameter and 4 m of overall length, which was held in a fixed position and directed perpendicularly to the tumour to produce an illumination circle concentric with the tumour. This customized laser is equipped with a <5 mW aiming laser emitting at 640±10 nm that provides the same illumination field as the 750 nm laser. The energies of the lasers were checked with an Ophir model AN/2E laser power meter or a Newport (Irvine, CA, USA) power meter model 1916-R and sensor 818P-010-12 or with a LaserCheck (Coherent Inc, Santa Clara, CA, USA) handheld power meter. When the Hamamatsu laser was used it was held by hand during the illumination of the tumour (the mouse was restrained using the other hand without anaesthesia), small oscillations around the centre of the tumour were made to ensure that the light dose was delivered proportionally to the tumour mass. When the Omicron laser was used, the position of the optical fibre was fixed relative to the mouse and the microlens produced an illumination circle concentric with the tumour. The mice were restrained by hand without anaesthesia and held in a fixed position under the laser beam. The duration of the irradiation was defined for each study group in order to obtain the desired light dose.

PDT REGIMES

The treatments with a specific diameter of the laser spot used the aiming beam of the Omicron laser to establish the diameter of the illuminated field. Tumour dimensions were determined before the illumination, and then twice a week until the largest diameter attained Ø≥15 mm, at which point the mice were sacrificed. Mice without palpable tumour 60 days after the treatment were considered cured. No significant correlation was found between tumour sizes and cures for the range of tumour sizes used.

ANTITUMOUR IMMUNE MEMORY

Mice cured with the optimized PDT protocol were subcutaneously rechallenged with 350.000 CT26 cells in the contralateral thigh more than 90 days after the treatment. An age-matched group of BALB/c mice with CT26 tumours was subjected to surgery to remove the tumour. The surgery was performed in aseptic conditions with the animals under general anaesthesia. The mice that after the surgery remained tumour free >90 days and an age-matched control group of naïve BALB/c mice were also inoculated with 350.000 CT26 cells and followed as in the treatment groups.

Table 5.2 - Pilot studies of PDT regimes with redaporfin, exploring drug-light intervals, drug and light doses, tumour margins and laser fluence (or radiant exposure), using N mice in each group.

Group	DLI (h)	Drug Dose (mg/kg)	Laser power (mW)	Light Dose (J)	Diameter (cm)	Radiant exposure (J/cm^2)	N	Survivals	Cured	Efficacy (%)
C	NA	0.0	0	0	NA	0	6	6	0	0
C+L	NA	0.0	130	179	Manual	-	7	7	0	0
1	0.25	0.37	130	31	1.4	20	10	10	1	10
2	0.25	0.37	130	44	1.2	39	6	6	0	0
3	0.25	0.37	130	78	Manual	-	6	6	3	50
4	0.25	0.37	65	78	Manual	-	4	4	1	25
5	0.25	0.52	130	44	1.2	39	6	6	0	0
6	0.25	0.52	185	63	1.2	56	7	7	2	29
7	0.25	0.52	130	78	1.2	69	7	7	2	29
8	0.25	0.75	130	47	Manual	-	6	6	5	83
9	0.25	0.75	130	59	Manual	-	6	6	5	83
10	0.25	0.75	130	44	1.2	39	7	7	2	29
11	0.25	0.75	130	60	1.2	53	7	7	4	57
12	0.25	0.75	130	≈73	1.1	74	19	19	10	53
13a	**0.25**	**0.75**	**173**	**67**	**1.3**	**50**	**8**	**8**	**7**	**88**
13b	**0.25**	**0.75**	**173**	**67**	**1.3**	**50**	**6**	**6**	**5**	**83**
14	0.25	0.75	185	75	1.4	49	4	2	2	50
15	0.25	0.75	185	81	1.4	53	6	4	~~4~~	67
16	0.25	0.75	173	85	1.4	50	7	6	4	57
17	0.25	1.5	130	47	Manual	-	6	**5**	2	33
18	0.25	1.5	130	59	Manual	-	8	6	6	75
19	0.25	1.5	130	78	Manual	-	6	1	0	0
20	0.25	1.5	130	117	Manual	-	6	0	0	0
21	12	0.75	65	59	Manual	-	5	5	0	0
22	12	1.5	130	59	Manual	-	6	1	0	0
23	12	1.5	130	94	Manual	-	6	1	0	0
24	24	1.5	130	94	Manual	-	9	4	0	0
25	48	1.5	130	94	Manual	-	6	5	0	0
26	72	1.5	130	94	Manual	-	6	6	1	17
27	72	2.2	130	94	Manual	-	6	6	0	0
28	72	1.5	130	119	1.2	105	9	7	0	0
29	72	1.5	130	140	Manual	-	6	5	1	17

VASCULAR-PDT IN BALC/C NUDE MICE

BALB/c nude female mice (Charles River Laboratories®, Barcelona, Spain) with 8 to 10 weeks were inoculated subcutaneously with 350.000 CT26 colon tumour cells. After 8-10 days of tumour cells inoculation, nude mice were then treated with redaporfin vascular-PDT using the same conditions as the wild type animals.

LUNG METASTASIS

BALB/c mice were subcutaneously inoculated with 350.000 CT26 cells and 7 days later 500.000 CT26 cells were injected in the tail vein. On day 12, one group with subcutaneous tumours was submitted to the optimized PDT regime, and 11 days later all the mice were sacrificed, the lungs were harvested, fixed with Bouin´s solution, weighted and the metastases were counted by two researchers.

IMMUNOHISTOCHEMISTRY

Four micrometre paraffin slices from tumours were deparanized and hydrated. Antigen retrieval was done in 0.1 M citrate buffer upon microwave treatment. Samples were blocked with 10% goat serum and incubated, overnight at 4 ºC, with a CD3 antibody (Dako). After washing, sections were incubated with anti-rabbit EnVision+ Systen-HRP Labelled Polymer (Dako), revealed with 3,3'-diaminobenzidine (DAB), counterstained with Harris' Haematoxylin and examined by light microscopy.

5.4. Results

Intermediate DLI have low phototherapeutic indexes

Table 5.2 reveals that the protocol parameters tested for vascular-PDT (DLI = 0.25 h) covered observations ranging from the absence of cures to 100% PDT-induced lethality. High light doses (>70 J) associated with large drug doses (≥ 0.75 mg/kg) delivered to large areas (>1 cm^2) led to lethality in the two days after treatment. For comparable doses (1.5 mg/kg, 78 or 95 J), PDT-induced lethality and efficacy decreased as the DLI increased, which is related with the photosensitizer clearance. Although the concentration of redaporfin in the tumour equals that in the plasma at DLI=12 h [16], this did not improve PDT efficacy. The therapeutic index of the regimes using DLI=12, 24 and 48 h is narrow, with no cures and lethality. It is again possible to obtain cures without lethality for a drug dose of 1.5 mg/kg when DLI is increased to 72 h, although this bears a high safety risk.

Factors that improve PDT outcome

Increasing the irradiance from 65 to 130 mW/cm^2 in groups 3 and 4 (0.37 mg/kg, 78 J) increased efficacy from 25% to 50%. The difference between these groups is not statistically significant but the lower efficacy at lower irradiances suggests that oxygen depletion in the tissues is not a limiting factor in vascular-PDT. The irradiance was not increased above 164 mW/cm^2 (group 6) to avoid photothermal effects. PDT efficacy did not respond to the increased light dose in groups 1 and 2 (0.37 mg/kg, 31 or 44 J) or in groups 6 and 7 (0.52 mg/kg, 63 and 78 J) suggesting that photobleaching becomes a limiting factor for 0.37 mg/kg with light doses >35 J and for 0.52 mg/kg with light doses >60 J. The groups 10 and 11, with DLI=0.25 h and 0.75 mg/kg, show a positive response to the light dose increase (Figure 5.1A).

The compensation of a lower photosensitizer dose by a higher light dose indicates that the photosensitizer dose is sufficiently high to be insensitive to photobleaching at the light dose used [244]. The median tumour delay after treatment in groups 27 (2.2 mg/kg, 94 J) and 29 (1.5 mg/kg, 140 J) at DLI=72 h and the unchanged PDT efficacy in groups 6 (0.52 mg/kg, 63 J) and 10 (0.75 mg/kg, 44 J) at DLI=0.25 h insures that photobleaching is not a limiting factor at these dose ranges. Thus, the full potential of vascular-PDT is attained for a drug dose of 0.75 mg/kg and a radiant exposure of 50 J/cm^2.

The evaluation of inner filter effects, where the photosensitizer concentration is sufficiently high to compromise the light penetration depth and PDT efficacy, is obscured by the onset of lethality at high drug doses in groups 17-20.

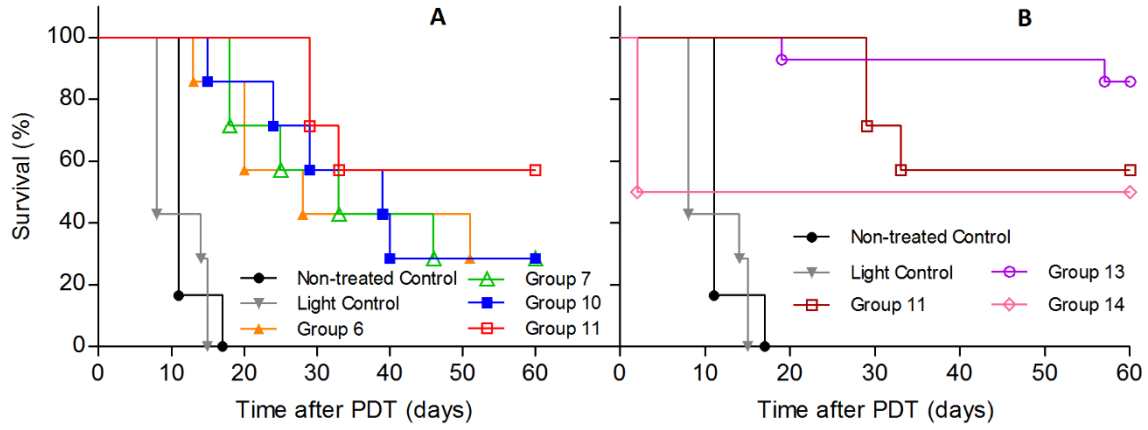

Figure 5.1 - Kaplan–Meier plots for survival times of mice with untreated tumours or after photodynamic therapy (PDT) at DLI = 0.25 h. (A) Photobleaching is an efficacy-limiting factor for PS doses lower than 0.75 mg/kg when combined with light doses higher than 60 J. (B) Effect of tumour margin in long-term PDT efficacy.

Figure 5.1B shows that for a 0.75 mg/kg dose and a 51±2 J/cm^2 radiant exposure, the PDT-efficacy increases with the tumour margin. The onset PDT-induced lethality for an illuminated field ≥1.5 cm^2 limits the success of this protocol. Group 13 corresponds to the optimized protocol for BALB/c mice where 86% of the mice were cured after PDT. This protocol was repeated (groups 13a and 13b) with consistent results.

PDT at DLI=72 h leads to a small eschar within 72 h of the treatment, and DLI=0.25 h leads to tissue destruction, with eschar formation in 48 h. The local response to vascular-PDT is very strong, but the animals maintained their normal behaviour, and the necrotic eschar disappeared and a good cosmetic effect was observed. Significantly larger oedemas were observed with DLIs 0.25 h and 12 h than with 72 h and 48 h. On the other hand, larger erythemas were observed with DLI=72 h than 0.25 h. The larger oedemas doubled the diameter of the mice leg in the vicinity of the tumour.

Vascular-PDT generates antitumour immunity

Mice cured with PDT, mice with surgically removed tumours and a control group of naïve animals were inoculated again 3 or more months later with CT26 cells into the contralateral thigh. Figure 5.2 shows that 67% of the mice cured with the optimized PDT protocol rejected the rechallenged with CT26 cells and remained tumour free for at least 70 days. When the rechallenge results of all PDT-cured mice are pooled together (43 mice), the rate of tumour rejection dropped to 40%. This indicates that the optimized protocol is especially effective in stimulating the immune system, presumably because it leads to a very strong local reaction.

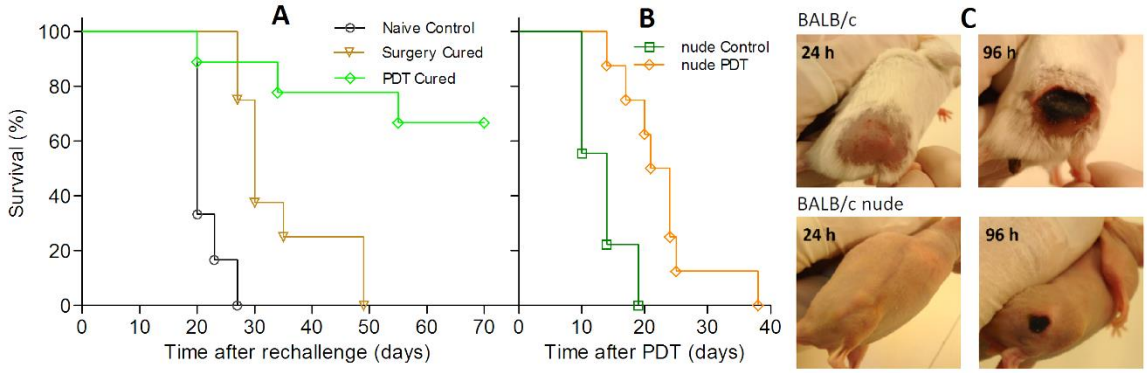

Figure 5.2 – Kaplan–Meier plots. (A) Survival times of BALB/c mice after rechallenge with CT26 cells of mice cured with vascular-photodynamic therapy (V-PDT) (0.75 mg/kg, drug-light interval (DLI) = 0.25 h, 50 J/cm^2, 130 mW/cm^2, Ø 13 mm) (n=9) or cured by surgical removal of the CT26 tumour (n=8), compared with a group of naïve animals with the same age (n=6), never exposed to such tumour cells; log-rank test for PDT cured vs. naïve p = 0.0005. PDT cured vs. surgery cured: p = 0.0031. (B) Survival times of BALB/c nude mice with untreated tumours (control) (n=8) or after vascular- PDT (0.75 mg/kg, DLI = 0.25 h, 50 J/cm^2, 130 mW/cm^2, Ø 13 mm) (n=9); log-rank test for naïve PDT treated vs. naïve control: p = 0.0006. (C) Photographs of typical local reactions at 24 and 96 h after PDT.

To test the hypothesis that T cells mediated the adaptive immune response, we performed the optimized redaporfin-PDT protocol in BALB/c nude mice. Figure 5.2 shows that the cure rate dropped from 86% to zero when changing to nude mice. Moreover, the oedema and eschar after the treatment of the normal mice are much larger than in the nude mice. The difference between normal and nude mice unveils the role played by the stimulation of the adaptive immune system, and of the presence of functional T cells, in long-term PDT efficacy.

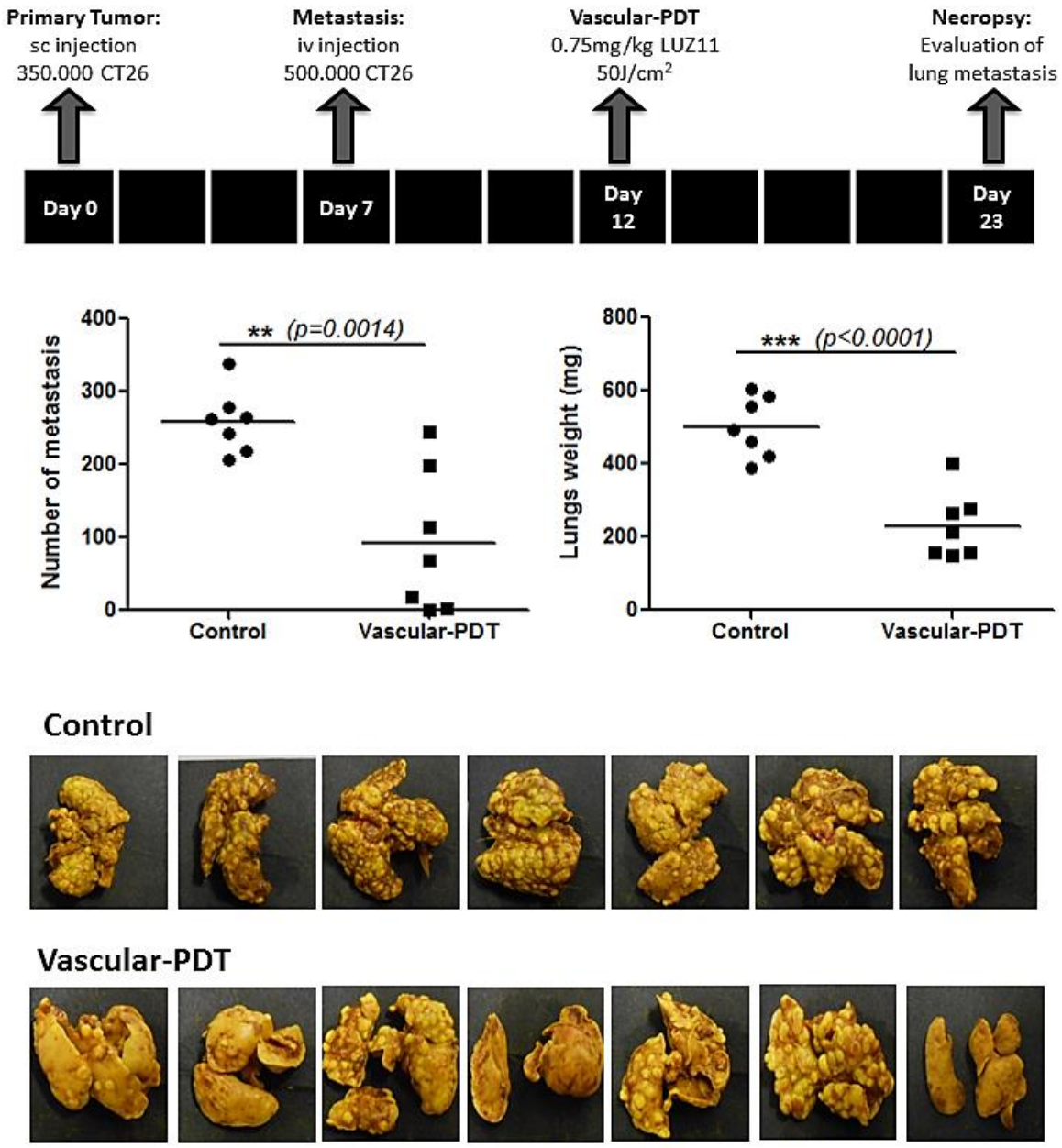

Figure 5.3 – Impact of vascular-photodynamic therapy (PDT) (0.75 mg/kg, DLI = 0.25 h, 50 J/cm^2, 130 mW/cm^2, Ø 13 mm) on distant metastasis evaluated in terms of the number of lung metastasis

and weight of the lungs. The photographs show the lungs stained with Bouin's solution in control and PDT-treated groups.

Systemic antitumour protection against metastasis

The systemic antitumour protection after PDT was further assessed combining subcutaneous and intravenous injection of CT26 cells. The subcutaneous tumour was induced as in the other experiments and after 7 days, 500,000 CT26 cells were injected in the tail vein. The subcutaneous tumour develops, while the cells injected produce lung metastasis. The observation of deaths in the control group 23 days after inoculation, due to the lung metastasis, dictated the end of the experiment at that point, and the animals treated with the optimized PDT regime were sacrificed 12 days after inoculation. The treatment regime and its outcome are presented in Figure 5.3. Necropsies revealed multiple tumour foci in the lungs of control mice but 2 of the 7 treated animals were free of lung metastasis at the time of the sacrifice. Two-tail unpaired t-test gave an extremely statistically significant difference between treated and control groups.

Recruitment of lymphocytes

CD3+ is a general T-lymphocyte marker and its infiltration in tumours is associated with a positive effect on survival [245]. Figure 5.4 shows that CD3+ cells were observed in untreated tumours, which evidenced the chronic inflammatory status typical of cancer. Six hours after tumour irradiation, these cells were almost completely absent of the tumour mass, presumably due to the treatment. This effect might be beneficial as these T cells are commonly immunosupressor T regulatory cells. In contrast, 24 h post-treatment, CD3+ cells significantly increased, reaching levels superior to the ones observed in untreated tumours. This T cell infiltration may be mediated by the signals emitted by the tumour cells killed by PDT, which recruit lymphocytes from the blood stream into the tumour with especially incidence to the tumour periphery. Such infiltrations have been observed in studies with vascular PDT [246].

5.5. Discussion

Various authors reported systemic PDT-induced antitumour immune responses [118, 247-249], including cases of vascular-PDT of BALB/c mice bearing CT26 tumours when verteporfin [120] or Pd-bacteriopheophorbide WST11 [246] were used. However, PDT with verteporfin failed to cure in mice bearing wild-type CT26 tumours. Only mice with

CT26.CL25 tumours expressing the tumour antigen β-galactosidase could be cured and acquired immune memory [120]. Cures in BALB/c mice bearing CT26 tumours with verteporfin-PDT required the preliminary administration of cyclophosphamide, an anticancer drug that selectively depletes Treg cells in mice, and this combination produces a greater local oedema than PDT alone [138]. Vascular-PDT with WST11 resulted in cure of 70% BALB/c and 19% BALB/c nude mice with implanted CT26 tumours [246]. The cured mice challenged two weeks later with injection of CT26 cells resisted the development of lung metastases, which were observed in control mice.

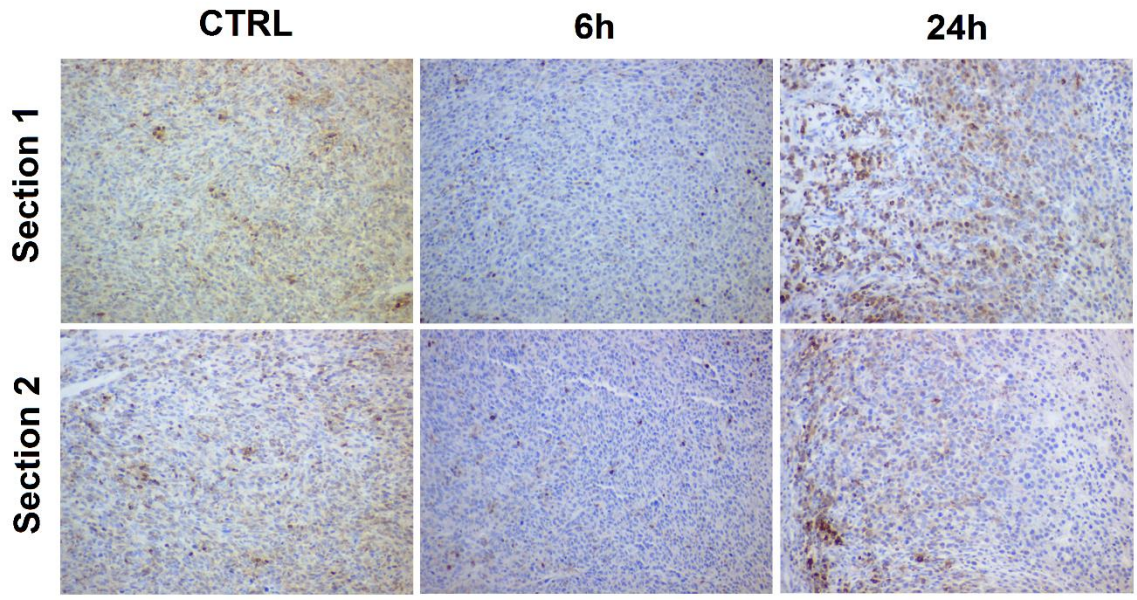

Figure 5.4 – T cells (CD3+) infiltration into CT26 sc tumours. Images of two sections (distance of ~600 µm) of a representative tumour from each group: control, 6 and 24 h post treatment. T cells (CD3+) can be visualised in brown (10x magnification) while the nuclei of tumour cells are in blue.

The optimized redaporfin-PDT regime (0.75 mg/kg, 0.25 h, 50 J/cm^2, 130 mW/cm^2, Ø= 13 mm), that emerged from our studies cured 12 out of 14 mice in two independent experiments. The overall cure rate of 86% is particularly remarkable because CT26 were the most resistant cells in vitro [171]. The antitumour immune memory of mice cured with the optimized PDT regime was compared with that of an age-matched group cured by surgery. All the mice in the surgery groups developed tumours when rechallenged with CT26 cells in the contralateral thigh, whereas 67% of the mice treated with the optimized redaporfin-PDT regime remained tumour-free more than 70 days later. This unprecedented immune memory with a minimally to moderately immunogenic tumour model reveals that the optimized treatment regime was effective in the stimulation the immune system.

The systemic response was further explored in a pseudo-metastatic model. Figure 5.3 shows that PDT of established tumours controlled lung metastasis resulting from CT26 cells

injection five days before the treatment. The photographs of the lungs illustrate that vascular-PDT with redaporfin is an effective photodynamic-immunotherapy. The drop in cure rates from normal to nude BALB/c mice, from 86% to 0%, together with the T cell infiltration in the tumour mass illustrated in Figure 5.4 strongly suggested that our optimized protocol activates T cell adaptive immunity. The protocol optimized for redaporfin elicits an immune response against CT26 tumours that is only paralleled by other photosensitizers when strongly immunogenic models are used [118].

Vascular-PDT with redaporfin led to a large oedema and eschar formation, mounted a high local inflammation and was very efficient in controlling the primary tumour and protecting from tumour rechallenges. This agrees with expected relation between high inflammation and durable immune responses but challenges the view that high-inflammation PDT regimes are less efficient in primary tumour control than low-inflammation PDT regimes [127, 241]. For the tumours with thicknesses of 3-4 mm used in this study, the 3-4 mm margin should be associated with an irradiance at a depth z=7 mm capable of producing ROS above the therapeutic threshold.

The threshold concentration for tissue necrosis by singlet oxygen was estimated as $[^1O_2]$=0.9 mM from the necrosis of rat liver with Photofrin [109]. The estimate of the $[^1O_2]$ threshold for skin necrosis is substantially higher, 93 mM, because of the lack of sensitivity of normal epidermal cells to PDT [250]. According to the AAPM, a typical threshold dose for necrosis is 17 mM and the amount of ROS produced per unit volume of tissue is given by [107]:

$$[ROS]_{local} = \phi_{ROS} \cdot \left(\frac{\lambda \cdot 1000}{h \cdot c \cdot N_A}\right) \cdot E \cdot \varepsilon \cdot [PS]_{local} \quad (1.2)$$

Which can be reduced to $[ROS]_{local}$= 460$R$$[LUZ11]_{local}$ using the parameters of redaporfin and where R=t_{irr}E is the radiant exposure in J/cm^2. From the pharmacokinetic data of redaporfin in mice, at DLI=0.25 h we have $[redaporfin]_{plasma}$=13 μM for a 0.75 mg/kg drug dose and [ROS]=0.3 M at the tumour surface when R_0=50 J/cm^2. At a depth of z=7 mm, where $R=R_0\ exp^{(-z/\delta)}$, for the optimized regime with illumination at 750 nm we obtain [ROS]=14 mM, which should produce tissue necrosis. Thus, the success of the optimized regime is related with the three-dimensional tumour margin of 3-4 mm.

Gomer reported a tumour margin of 1-2 mm for PDT and a resection margin of 4 mm in surgical excision of the same tumours [251], whereas Hamblin used tumour margins of 2-3 mm [135, 252]. Increasing the illuminated surface may improve the PDT outcome. This depends on δ and on the photosensitizer photodecomposition. The drug-light dose compensation observed in the range of the values of the optimized protocol shows that the

redaporfin photodecompostion does not limit the depth of the treatment under these conditions.

Hypoxia in tissues during PDT may also diminish the amount of ROS produced. Indeed, high irradiances curb the median survival time of mice bearing tumours when the photosensitizer is predominately localized in the tumour cells (DLI>6 h) [74, 253, 254], although exceptions were observed [255, 256]. A study using 10 mg/kg of motexafin lutetium irradiated at DLI=3 h concluded that the outcome of the treatment was not related with the oxygenation [257]. The abundance of oxygen in the vasculature, the long-lived triplet state of redaporfin and its participation in Type I reactions, circumvent oxygen depletion effects in vascular-PDT even at the highest irradiance tested (E=164 mW/cm^2). The higher irradiances in vascular-PDT even improved the outcome of the therapy, because they produce an acute vascular response at a greater tumour depth and enable strong hypoxia after PDT, which is correlated with PDT efficacy [108].

The protocols with DLI between 12 and 48 h have a narrow phototherapeutic index that is related with pharmacokinetics because ~80% of redaporfin is cleared from the plasma in 12 h post-iv administration [54]. PDT with DLI=72 h (1.5 mg/kg, 100 J/cm^2) is the most selective, but considering that the final goal must be eliciting a favourable long-term tumour response, vascular-PDT (0.75 mg/kg, DLI=0.25 h, 50 J/cm^2, tumour margin of 4 mm) is preferable because it provides the highest cures rates and long-lasting systemic antitumour immunity.

5.6. Conclusion

The PDT regime optimized with redaporfin combines local oxidative stress in the target tissue capable of eliminating the primary tumour, with a systemic immune response that controls metastasis. The success of the treatment is related with the three-dimensional margin >3 mm and with the strong immune response triggered by the high local inflammation after PDT, evidenced by the recruitment of lymphocytes. The clinical implications of this study are currently being explored in a Phase I/II clinical trial with redaporfin (LUZ11) using an adaptation of the optimized regime.

Chapter 6

General Conclusion and Future Perspectives

Chapter 6 – General Conclusion and Future Perspectives

The primary motivation behind this ambitious project was the rational design a new family of photosensitizers with improved photodynamic and pharmacological properties for application in PDT of cancer. The goal was to achieve a significant improvement, in terms of safety and efficacy, over the alternatives in the market and to contribute to the choice of PDT as a first line anticancer strategy, hoping that this will contribute to the well-being of cancer patients. The long project timeline has steadily been punctuated with an impressive collection of achievements, one of the most important being the selection of redaporfin as the lead compound. This critical step was supported by solid nonclinical results that unveiled the near-ideal properties of this molecule and warranted its further development as a drug candidate for PTD of cancer.

Redaporfin demonstrated low toxicity in the absence of light and high photodynamic activity after laser irradiation, against several cancer cells lines. These results account for a Photosensitizing Efficiency far superior than those obtained in the same conditions for the marketed systemic PS for cancer treatment, Photofrin and Foscan. This observation strengthened the potential of redaporfin for PDT applications.

The evaluation of the biological activity of redaporfin in vivo required the development of a suitable formulation to allow for its intravenous administration. An aqueous based formulation with low Cremophor EL content was able to yield favourable PS biodistribution and pharmacokinetics profiles that were characterized by immediate bioavailability and good tumour/muscle and tumour/skin ratios for longer DLI. This was translated *in vivo* into high antitumour efficacy in a mouse tumour model, with good tumour responses to a selective-PDT protocol (DLI=72h) and an excellent long-term cure rate of 83% for a vascular-PDT protocol (DLI=15min). Moreover, the formulation developed and optimized is simple to prepare, well tolerated and leads only to low skin photosensitivity on the first days following PS administration, which disappeared completely 7 days after the administration.

One of the most critical stages in drug development is the demonstration of the safety of the molecule and its formulation. As effective as a drug candidate may be, it will never obtain regulatory approval if its safety is not conveniently demonstrated, through a favourable risk-benefit analysis. The results of the nonclinical safety toxicology and pharmacology studies are the base for a first-in-man clinical trial approval, since they have to clearly show that the patients or healthy volunteers that first receive drug candidate are not exposed to

unnecessary health risks. The preliminary safety evaluation of the redaporfin iv formulation showed that it is very well tolerated in mice and rats, up to 100 and 20 mg/kg respectively, without signs of toxicity or skin photosensitivity. When combined with a PDT protocol it led, as expected, to a strong local inflammatory response and to significant, but transient, alterations on some clinical blood markers, which returned to their levels pre-PDT within one week after the irradiation.

The last stage of this project was dedicated to the optimization of a PDT protocol in a mouse tumour model and the evaluation of the immune system response induced by PDT. It was by far the longest and most challenging part of the project, but the results obtained were unparalleled and highly promising. The PDT protocol optimization was performed in mice with a subcutaneous tumour by exploring PS and light doses, tumour margins and light fluences, while addressing the different modes of action of PDT by testing drug-light intervals from 15 min up to 72 h. Despite the significant antitumour effect observed by several tested protocols, the optimal compromise between safety and efficacy was obtained with only one application of a vascular acting protocol with 15 min DLI that produced an impressive long term efficacy rate of 86%. This level of nonclinical efficacy was never reported before for any PS in the same tumour model, and its observation with a protocol using a very short DLI is another important advantage in the clinical setting, since it can be performed in only one session and in an outpatient basis, with positive impact on the budget and resource management of the healthcare systems.

The effect of PDT on the host immune system has since long been reported and explored because of its potential contribution to systemic tumour control. In addition to the high efficacy against the primary tumour, this type of immune response was also found in mice treated with the optimized redaporfin vascular-PDT protocol. It was triggered by the strong local inflammatory response, and revealed by the recruitment of lymphocytes to the tumour tissue and the absence of long term cures in immunosuppressed mice. Further *in vivo* studies showed a sustained and systemic antitumour immune response that allowed 67% of the PDT-cured mice to reject a second rechallenge with the same tumour cells, and was capable of significantly reduce the development of lung metastasis.

The potential impact of these findings on the future of PDT and cancer therapy can be enormous. Redaporfin vascular-PDT may represent an important contribution to combine local and systemic (immune-mediated) effects and initiate the new era of photodynamic-immunotherapy of cancer.

The nonclinical results presented in this thesis together with GLP-compliant studies subcontracted to a CRO represent a crucial part of the clinical trial application approved by

the national regulatory agency for medicines. The ongoing Phase I/II clinical trial in advanced head & neck cancer patients aims to explore the clinical implications of redaporfin using an adaptation of the optimized protocol [69]. The clinical results already obtained in the trial are in close agreement with the findings of the nonclinical studies, revealing the absence of significant treatment-related adverse reactions, a favourable PK profile of redaporfin, and a dose-dependent antitumour effect. The local effect on the primary tumour closely parallels that reported in this thesis raising the expectations of a successful trial.

Additional studies on the mechanisms behind the antitumour immune response induced by redaporfin vascular-PDT and on strategies for its modulation are warranted and may enable powerful PDT-immunotherapy combinations. Further developments of redaporfin-PDT for other cancer indications, namely using interstitial irradiation, are also envisioned.

7.1. References

[1] International Agency for Research on Cancer and Cancer Research UK, *World Cancer Factsheet*, 2012, Cancer Research UK: London.

[2] R. Stahel, J. Bogaerts, F. Ciardiello, D. de Ruysscher, P. Dubsky, M. Ducreux, S. Finn, P. Laurent-Puig, S. Peters, M. Piccart, E. Smit, C. Sotiriou, S. Tejpar, E. Van Cutsem, and J. Tabernero. *Optimising translational oncology in clinical practice: Strategies to accelerate progress in drug development. Cancer treatment reviews*, 2014,

[3] B.J. Coventry and M.L. Ashdown. *Complete clinical responses to cancer therapy caused by multiple divergent approaches: a repeating theme lost in translation. Cancer management and research*, 2012, 4(1), 137-49.

[4] J. Bergh. *Quo vadis with targeted drugs in the 21st century? Journal of clinical oncology : official journal of the American Society of Clinical Oncology*, 2009, 27(1), 2-5.

[5] S.H. Ibbotson. *An overview of topical photodynamic therapy in dermatology. Photodiagnosis Photodyn Ther*, 2010, 7(1), 16-23.

[6] C. Hopper, C. Niziol, and M. Sidhu. *The cost-effectiveness of Foscan mediated photodynamic therapy (Foscan-PDT) compared with extensive palliative surgery and palliative chemotherapy for patients with advanced head and neck cancer in the UK. Oral Oncol*, 2004, 40(4), 372-82.

[7] Z. Matějka, V. Adámková, R. Šmucler, J. Svobodová, and H. Hubálková. *Photodynamic therapy (PDT) for disinfection of oral wounds. In vitro study. centeurjmed*, 2012, 7(1), 118-123.

[8] J.P. Celli, B.Q. Spring, I. Rizvi, C.L. Evans, K.S. Samkoe, S. Verma, B.W. Pogue, and T. Hasan. *Imaging and photodynamic therapy: mechanisms, monitoring, and optimization. Chemical reviews*, 2010, 110(5), 2795-838.

[9] J. Soriano, A. Villanueva, J.C. Stockert, and M. Canete. *Regulated necrosis in HeLa cells induced by ZnPc photodynamic treatment: a new nuclear morphology. International journal of molecular sciences*, 2014, 15(12), 22772-85.

[10] R. Ackroyd, C. Kelty, N. Brown, and M. Reed. *The history of photodetection and photodynamic therapy. Photochemistry and photobiology*, 2001, 74(5), 656-69.

[11] M.D. Daniell and J.S. Hill. *A history of photodynamic therapy. The Australian and New Zealand journal of surgery*, 1991, 61(5), 340-8.

[12] R.R. Allison and C.H. Sibata. *Oncologic photodynamic therapy photosensitizers: a clinical review. Photodiagn Photodyn Ther*, 2010, 7(2), 61-75.

[13] M. Triesscheijn, P. Baas, J.H.M. Schellens, and F.A. Stewart. *Photodynamic Therapy in Oncology. The Oncologist*, 2006, 11(9), 1034-1044.

[14] T.J. Dougherty, G.B. Grindey, R. Fiel, K.R. Weishaupt, and D.G. Boyle. *Photoradiation therapy. II. Cure of animal tumors with hematoporphyrin and light. Journal of the National Cancer Institute*, 1975, 55(1), 115-21.

[15] T.J. Dougherty, J.E. Kaufman, A. Goldfarb, K.R. Weishaupt, D. Boyle, and A. Mittleman. *Photoradiation therapy for the treatment of malignant tumors. Cancer research*, 1978, 38(8), 2628-35.

[16] F. Canada-Canada, A. Bautista-Sanchez, M. Taverna, P. Prognon, P. Maillard, D.S. Grierson, and A. Kasselouri. *Simple sensitive and simultaneous high-performance liquid chromatography method of glucoconjugated and non-glucoconjugated porphyrins and chlorins using near infra-red fluorescence detection. Journal of chromatography B, Analytical technologies in the biomedical and life sciences*, 2005, 821(2), 166-72.

[17] A.F. Cruess, G. Zlateva, A.M. Pleil, and B. Wirostko. *Photodynamic therapy with verteporfin in age-related macular degeneration: a systematic review of efficacy, safety, treatment modifications and pharmacoeconomic properties. Acta ophthalmologica*, 2009, 87(2), 118-32.

[18] I. Yoon, J.Z. Li, and Y.K. Shim. *Advance in photosensitizers and light delivery for photodynamic therapy. Clinical endoscopy*, 2013, 46(1), 7-23.

[19] Z. Huang, H. Xu, A.D. Meyers, A.I. Musani, L. Wang, R. Tagg, A.B. Barqawi, and Y.K. Chen. *Photodynamic therapy for treatment of solid tumors--potential and technical challenges. Technology in cancer research & treatment*, 2008, 7(4), 309-20.

[20] A.P. Castano, T.N. Demidova, and M.R. Hamblin. *Mechanisms in photodynamic therapy: part one—photosensitizers, photochemistry and cellular localization. Photodiagn Photodyn Ther*, 2004, 1(4), 279-293.

[21] P.G. Calzavara-Pinton, M. Venturini, and R. Sala. *Photodynamic therapy: update 2006. Part 1: Photochemistry and photobiology. Journal of the European Academy of Dermatology and Venereology : JEADV*, 2007, 21(3), 293-302.

[22] C.S. Foote. *Definition of type I and type II photosensitized oxidation. Photochemistry and photobiology*, 1991, 54(5), 659.

[23] S. Yano, S. Hirohara, M. Obata, Y. Hagiya, S.-i. Ogura, A. Ikeda, H. Kataoka, M. Tanaka, and T. Joh. *Current states and future views in photodynamic therapy. Journal of Photochemistry and Photobiology C: Photochemistry Reviews*, 2011, 12(1), 46-67.

[24] P. Agostinis, K. Berg, K.A. Cengel, T.H. Foster, A.W. Girotti, S.O. Gollnick, S.M. Hahn, M.R. Hamblin, A. Juzeniene, D. Kessel, M. Korbelik, J. Moan, P. Mroz, D. Nowis, J. Piette, B.C. Wilson, and J. Golab. *Photodynamic therapy of cancer: an update. CA: a cancer journal for clinicians*, 2011, 61(4), 250-81.

[25] J.E. Moulder and S. Rockwell. *Tumor hypoxia: its impact on cancer therapy. Cancer metastasis reviews*, 1987, 5(4), 313-41.

[26] P. Nowak-Sliwinska, A. Karocki, M. Elas, A. Pawlak, G. Stochel, and K. Urbanska. *Verteporfin, photofrin II, and merocyanine 540 as PDT photosensitizers against melanoma cells. Biochemical and biophysical research communications*, 2006, 349(2), 549-55.

[27] H. Ding, H. Yu, Y. Dong, R. Tian, G. Huang, D.A. Boothman, B.D. Sumer, and J. Gao. *Photoactivation switch from type II to type I reactions by electron-rich micelles for improved photodynamic therapy of cancer cells under hypoxia. Journal of controlled release : official journal of the Controlled Release Society*, 2011, 156(3), 276-80.

[28] K. Plaetzer, B. Krammer, J. Berlanda, F. Berr, and T. Kiesslich. *Photophysics and photochemistry of photodynamic therapy: fundamental aspects. Lasers in medical science*, 2009, 24(2), 259-68.

[29] D.V. Sakharov, A. Bunschoten, H. van Weelden, and K.W. Wirtz. *Photodynamic treatment and H2O2-induced oxidative stress result in different patterns of cellular protein oxidation. European journal of biochemistry / FEBS*, 2003, 270(24), 4859-65.

[30] F.H. Sakamoto, J.D. Lopes, and R.R. Anderson. *Photodynamic therapy for acne vulgaris: A critical review from basics to clinical practice: Part I. Acne vulgaris: When and why consider photodynamic therapy? Journal of the American Academy of Dermatology*, 2010, 63(2), 183-193.

[31] T.J. Dougherty. *An update on photodynamic therapy applications. Journal of clinical laser medicine & surgery*, 2002, 20(1), 3-7.

[32] Food and Drug Administration (FDA) - Center for Drug Evaluation and Research. *Approved Drug Products*. [cited 2015 12-02-2015]; Available from: http://www.accessdata.fda.gov/scripts/cder/drugsatfda/index.cfm.

[33] European Medicines Agency (EMA). *Human Medicines*. [cited 2015 12-02-2015]; Available from: http://www.ema.europa.eu/ema/index.jsp?curl=pages/medicines/landing/epar_search.jsp&mid=WC0b01ac058001d124.

[34] T.C. Zhu and J.C. Finlay. *The role of photodynamic therapy (PDT) physics. Medical physics*, 2008, 35(7), 3127-36.

[35] U.S. National Institutes of Health. *ClinicalTrials.gov*. [cited 2015 18-09-2015]; Available from: https://clinicaltrials.gov/ct2/results?term=photodynamic+therapy&recr=Open&no_unk=Y&cond=cancer&rcv_s=01%2F01%2F2011&pg=1.

[36] A. Ormond and H. Freeman. *Dye Sensitizers for Photodynamic Therapy. Materials*, 2013, 6(3), 817-840.

[37] E. Buytaert, M. Dewaele, and P. Agostinis. *Molecular effectors of multiple cell death pathways initiated by photodynamic therapy. Biochimica et biophysica acta*, 2007, 1776(1), 86-107.

[38] L.G. Arnaut, *Design of porphyrin-based photosensitizers*, in *Advances in Inorganic Chemistry*, Volume 63, E. Rudi van and S. Grażyna, Editors. 2011, Academic Press. p. 187-233.

[39] S.B. Brown, E.A. Brown, and I. Walker. *The present and future role of photodynamic therapy in cancer treatment. The Lancet Oncology*, 2004, 5(8), 497-508.

[40] A.P. Castano, T.N. Demidova, and M.R. Hamblin. *Mechanisms in photodynamic therapy: Part three—Photosensitizer pharmacokinetics, biodistribution, tumor localization and modes of tumor destruction. Photodiagnosis and Photodynamic Therapy*, 2005, 2(2), 91-106.

[41] H. Maeda, H. Nakamura, and J. Fang. *The EPR effect for macromolecular drug delivery to solid tumors: Improvement of tumor uptake, lowering of systemic toxicity, and distinct tumor imaging in vivo. Advanced Drug Delivery Reviews*, 2013, 65(1), 71-9.

[42] J. Moan and K. Berg. *The photodegradation of porphyrins in cells can be used to estimate the lifetime of singlet oxygen. Photochemistry and photobiology*, 1991, 53(4), 549-53.

[43] I. Postiglione, A. Chiaviello, and G. Palumbo. *Enhancing Photodynamyc Therapy Efficacy by Combination Therapy: Dated, Current and Oncoming Strategies. Cancers*, 2011, 3(2), 2597-2629.

[44] J. Barge, T. Glanzmann, M. Zellweger, D. Salomon, H. van den Bergh, and G. Wagnieres. *Correlations between photoactivable porphyrins' fluorescence, erythema and the pain induced by PDT on normal skin using ALA-derivatives. Photodiagnosis Photodyn Ther*, 2013, 10(4), 683-93.

[45] N. Ikeda, J. Usuda, H. Kato, T. Ishizumi, S. Ichinose, K. Otani, H. Honda, K. Furukawa, T. Okunaka, and H. Tsutsui. *New aspects of photodynamic therapy for central type early stage lung cancer. Lasers in surgery and medicine*, 2011, 43(7), 749-754.

[46] L.K. Martin, G.A. Otterson, and T. Bekaii-Saab. *Photodynamic Therapy (PDT) May Provide Effective Palliation in the Treatment of Primary Tracheal Carcinoma: A Small Case Series. Photomedicine and Laser Surgery*, 2012, 30(11), 668-671.

[47] P.S. Thong, K.W. Ong, N.S. Goh, K.W. Kho, V. Manivasager, R. Bhuvaneswari, M. Olivo, and K.C. Soo. *Photodynamic-therapy-activated immune response against distant untreated tumours in recurrent angiosarcoma. The Lancet Oncology*, 2007, 8(10), 950-2.

[48] A.P. Castano, P. Mroz, and M.R. Hamblin. *Photodynamic therapy and anti-tumour immunity. Nature reviews Cancer*, 2006, 6(7), 535-45.

[49] T.G. St Denis, K. Aziz, A.A. Waheed, Y.-Y. Huang, S.K. Sharma, P. Mroz, and M.R. Hamblin. *Combination approaches to potentiate immune response after photodynamic therapy for cancer. Photochemical & photobiological sciences : Official journal of the European Photochemistry Association and the European Society for Photobiology*, 2011, 10(5), 792-801.

[50] T.J. Dougherty, M.T. Cooper, and T.S. Mang. *Cutaneous phototoxic occurrences in patients receiving Photofrin. Lasers in surgery and medicine*, 1990, 10(5), 485-8.

[51] P. Mlkvy, H. Messmann, J. Regula, M. Conio, M. Pauer, C.E. Millson, A.J. MacRobert, and S.G. Bown. *Photodynamic therapy for gastrointestinal tumors using three photosensitizers--ALA induced PPIX, Photofrin and MTHPC. A pilot study. Neoplasma*, 1998, 45(3), 157-61.

[52] R.A. Weersink, J. Forbes, S. Bisland, J. Trachtenberg, M. Elhilali, P.H. Brún, and B.C. Wilson. *Assessment of Cutaneous Photosensitivity of TOOKAD (WST09) in Preclinical Animal Models and in Patients¶. Photochemistry and photobiology*, 2005, 81(1), 106-113.

[53] O. Mazor, A. Brandis, V. Plaks, E. Neumark, V. Rosenbach-Belkin, Y. Salomon, and A. Scherz. *WST11, a novel water-soluble bacteriochlorophyll derivative; cellular uptake, pharmacokinetics, biodistribution and vascular-targeted photodynamic activity using melanoma tumors as a model. Photochemistry and photobiology*, 2005, 81(2), 342-51.

[54] R. Saavedra, L.B. Rocha, J.M. Dabrowski, and L.G. Arnaut. *Modulation of biodistribution, pharmacokinetics, and photosensitivity with the delivery vehicle of a bacteriochlorin photosensitizer for photodynamic therapy. ChemMedChem*, 2014, 9(2), 390-8.

[55] L. Brancaleon and H. Moseley. *Laser and non-laser light sources for photodynamic therapy. Lasers in medical science*, 2002, 17(3), 173-86.

[56] R. Tong and D.S. Kohane. *Shedding light on nanomedicine. Wiley interdisciplinary reviews Nanomedicine and nanobiotechnology*, 2012, 4(6), 638-62.

[57] J. Trachtenberg, R.A. Weersink, S.R. Davidson, M.A. Haider, A. Bogaards, M.R. Gertner, A. Evans, A. Scherz, J. Savard, J.L. Chin, B.C. Wilson, and M. Elhilali. *Vascular-targeted photodynamic therapy (padoporfin, WST09) for recurrent prostate cancer after failure of external beam radiotherapy: a study of escalating light doses. BJU international*, 2008, 102(5), 556-62.

[58] A.N. Bashkatov, E.A. Genina, V.I. Kochubey, and V.V. Tuchin. *Optical properties of human skin, subcutaneous and mucous tissues in the wavelength range from 400 to 2000 nm. Journal of Physics D: Applied Physics*, 2005, 38(15), 2543.

[59] M.S. Patterson, B.C. Wilson, and R. Graff. *In vivo tests of the concept of photodynamic threshold dose in normal rat liver photosensitized by aluminum chlorosulphonated phthalocyanine. Photochemistry and photobiology*, 1990, 51(3), 343-9.

[60] J.M. Dabrowski, M.M. Pereira, L.G. Arnaut, C.J. Monteiro, A.F. Peixoto, A. Karocki, K. Urbanska, and G. Stochel. *Synthesis, photophysical studies and anticancer activity of a new halogenated water-soluble porphyrin. Photochemistry and photobiology*, 2007, 83(4), 897-903.

[61] E.l.G. Azenha, A.C. Serra, M. Pineiro, M.M. Pereira, J. Seixas de Melo, L.G. Arnaut, S.J. Formosinho, and A.M.d.A. Rocha Gonsalves. *Heavy-atom effects on metalloporphyrins and polyhalogenated porphyrins. Chemical Physics*, 2002, 280(1–2), 177-190.

[62] J. Berlanda, T. Kiesslich, V. Engelhardt, B. Krammer, and K. Plaetzer. *Comparative in vitro study on the characteristics of different photosensitizers employed in PDT. Journal of photochemistry and photobiology B, Biology*, 2010, 100(3), 173-80.

[63] Y.M. Riyad, S. Naumov, S. Schastak, J. Griebel, A. Kahnt, T. Haupl, J. Neuhaus, B. Abel, and R. Hermann. *Chemical modification of a tetrapyrrole-type photosensitizer: tuning application and photochemical action beyond the singlet oxygen channel. The journal of physical chemistry B*, 2014, 118(40), 11646-58.

[64] N. Betrouni, R. Lopes, P. Puech, P. Colin, and S. Mordon. *A model to estimate the outcome of prostate cancer photodynamic therapy with TOOKAD Soluble WST11. Phys Med Biol*, 2011, 56(15), 4771-83.

[65] M.M. Pereira, C.J.P. Monteiro, A.V.C. Simões, S.M.A. Pinto, A.R. Abreu, G.F.F. Sá, E.F.F. Silva, L.B. Rocha, J.M. Dąbrowski, S.J. Formosinho, S. Simões, and L.G. Arnaut. *Synthesis and photophysical characterization of a library of photostable halogenated bacteriochlorins: an access to near infrared chemistry. Tetrahedron*, 2010, 66(49), 9545-9551.

[66] J.M. Dabrowski, L.G. Arnaut, M.M. Pereira, C.J. Monteiro, K. Urbanska, S. Simoes, and G. Stochel. *New halogenated water-soluble chlorin and bacteriochlorin as photostable PDT sensitizers: synthesis, spectroscopy, photophysics, and in vitro photosensitizing efficacy. ChemMedChem*, 2010, 5(10), 1770-80.

[67] M.M. Pereira, C.J.P. Monteiro, A.V.C. Simões, S.M.A. Pinto, L.G. Arnaut, G.F.F. Sá, E.F.F. Silva, L.B. Rocha, S. Simões, and S.J. Formosinho. *Synthesis and photophysical properties of amphiphilic halogenated bacteriochlorins: new opportunities for photodynamic therapy of cancer. Journal of Porphyrins and Phthalocyanines*, 2009, 13(04n05), 567-573.

[68] J.M. Dabrowski, L.G. Arnaut, M.M. Pereira, K. Urbanska, and G. Stochel. *Improved biodistribution, pharmacokinetics and photodynamic efficacy using a new photostable sulfonamide bacteriochlorin. MedChemComm*, 2012, 3(4), 502-505.

[69] U.S. National Institutes of Health. *Photodynamic Therapy With LUZ11 in Advanced Head and Neck Cancer*. [cited 2015 13-02-2015]; Available from: https://clinicaltrials.gov/ct2/show/NCT02070432?term=photodynamic+therapy&recr=Open&rank=37.

[70] J.H. Woodhams, A.J. Macrobert, and S.G. Bown. *The role of oxygen monitoring during photodynamic therapy and its potential for treatment dosimetry. Photochemical & photobiological sciences : Official journal of the European Photochemistry Association and the European Society for Photobiology*, 2007, 6(12), 1246-56.

[71] L. Yang, Y. Wei, D. Xing, and Q. Chen. *Increasing the efficiency of photodynamic therapy by improved light delivery and oxygen supply using an anticoagulant in a solid tumor model. Lasers in surgery and medicine*, 2010, 42(7), 671-679.

[72] E. Blake, J. Allen, and A. Curnow. *The effects of protoporphyrin IX-induced photodynamic therapy with and without iron chelation on human squamous carcinoma cells cultured under normoxic, hypoxic and hyperoxic conditions. Photodiagnosis and Photodynamic Therapy*, 2013, 10(4), 575-582.

[73] H. Schouwink, M. Ruevekamp, H. Oppelaar, R. Van Veen, P. Baas, and F.A. Stewart. *Photodynamic Therapy for Malignant Mesothelioma: Preclinical Studies for Optimization of Treatment Protocols¶. Photochemistry and photobiology*, 2001, 73(4), 410-417.

[74] B.W. Henderson, T.M. Busch, and J.W. Snyder. *Fluence rate as a modulator of PDT mechanisms. Lasers in surgery and medicine*, 2006, 38(5), 489-493.

[75] S. Anand, B.J. Ortel, S.P. Pereira, T. Hasan, and E.V. Maytin. *Biomodulatory approaches to photodynamic therapy for solid tumors. Cancer letters*, 2012, 326(1), 8-16.

[76] A. Maier, F. Tomaselli, U. Anegg, P. Rehak, B. Fell, S. Luznik, H. Pinter, and F.M. Smolle-Juttner. *Combined photodynamic therapy and hyperbaric oxygenation in carcinoma of the esophagus and the esophago-gastric junction. European journal of cardio-thoracic surgery : official journal of the European Association for Cardio-thoracic Surgery*, 2000, 18(6), 649-54; discussion 654-5.

[77] Q. Chen, Z. Huang, H. Chen, H. Shapiro, J. Beckers, and F.W. Hetzel. *Improvement of tumor response by manipulation of tumor oxygenation during photodynamic therapy. Photochemistry and photobiology*, 2002, 76(2), 197-203.

[78] European Medicines Agency. *The European Union Clinical Trials Register*. [cited 2015 19-09-2015]; Available from: https://www.clinicaltrialsregister.eu/ctr-search/search?query=Photodynamic+therapy&status=ongoing&dateFrom=2009-01-01.

[79] Z. Ji, G. Yang, V. Vasovic, B. Cunderlikova, Z. Suo, J.M. Nesland, and Q. Peng. *Subcellular localization pattern of protoporphyrin IX is an important determinant for its photodynamic efficiency of human carcinoma and normal cell lines. Journal of photochemistry and photobiology B, Biology*, 2006, 84(3), 213-20.

[80] C.A. Robertson, D.H. Evans, and H. Abrahamse. *Photodynamic therapy (PDT): a short review on cellular mechanisms and cancer research applications for PDT. Journal of photochemistry and photobiology B, Biology*, 2009, 96(1), 1-8.

[81] M. Triesscheijn, M. Ruevekamp, R. Out, T.C. Van Berkel, J. Schellens, P. Baas, and F. Stewart. *The pharmacokinetic behavior of the photosensitizer meso-tetra-hydroxyphenyl-chlorin in mice and men. Cancer Chemotherapy and Pharmacology*, 2007, 60(1), 113-122.

[82] W.W. Chin, P.W. Heng, P.S. Thong, R. Bhuvaneswari, W. Hirt, S. Kuenzel, K.C. Soo, and M. Olivo. *Improved formulation of photosensitizer chlorin e6 polyvinylpyrrolidone for fluorescence diagnostic imaging and photodynamic therapy of human cancer. European journal of pharmaceutics and biopharmaceutics : official journal of Arbeitsgemeinschaft fur Pharmazeutische Verfahrenstechnik eV*, 2008, 69(3), 1083-93.

[83] R.R. Allison, H.C. Mota, V.S. Bagnato, and C.H. Sibata. *Bio-nanotechnology and photodynamic therapy--state of the art review. Photodiagnosis Photodyn Ther*, 2008, 5(1), 19-28.

[84] Y.N. Konan, R. Gurny, and E. Allemann. *State of the art in the delivery of photosensitizers for photodynamic therapy. Journal of photochemistry and photobiology B, Biology*, 2002, 66(2), 89-106.

[85] A.P. Castano, T.N. Demidova, and M.R. Hamblin. *Mechanisms in photodynamic therapy: part two—cellular signaling, cell metabolism and modes of cell death. Photodiagnosis and Photodynamic Therapy*, 2005, 2(1), 1-23.

[86] J. Kim, O.A. Santos, and J.H. Park. *Selective photosensitizer delivery into plasma membrane for effective photodynamic therapy. Journal of controlled release : official journal of the Controlled Release Society*, 2014, 191(98-104.

[87] P. Mroz, A. Yaroslavsky, G.B. Kharkwal, and M.R. Hamblin. *Cell Death Pathways in Photodynamic Therapy of Cancer. Cancers*, 2011, 3(2), 2516-2539.

[88] D. Kessel. *More Adventures in Photodynamic Therapy. International journal of molecular sciences*, 2015, 16(7), 15188-93.

[89] M.F. Wei, M.W. Chen, K.C. Chen, P.J. Lou, S.Y. Lin, S.C. Hung, M. Hsiao, C.J. Yao, and M.J. Shieh. *Autophagy promotes resistance to photodynamic therapy-induced apoptosis selectively in colorectal cancer stem-like cells. Autophagy*, 2014, 10(7), 1179-92.

[90] J.J. Reiners, Jr., P. Agostinis, K. Berg, N.L. Oleinick, and D. Kessel. *Assessing autophagy in the context of photodynamic therapy. Autophagy*, 2010, 6(1), 7-18.

[91] A.D. Garg, D. Nowis, J. Golab, and P. Agostinis. *Photodynamic therapy: illuminating the road from cell death towards anti-tumour immunity. Apoptosis*, 2010, 15(9), 1050-1071.

[92] D. Kessel. *Apoptosis and associated phenomena as a determinants of the efficacy of photodynamic therapy. Photochemical & photobiological sciences : Official journal of the European Photochemistry Association and the European Society for Photobiology*, 2015,

[93] J. Karch and J.D. Molkentin. *Regulated Necrotic Cell Death: The Passive Aggressive Side of Bax and Bak. Circulation research*, 2015, 116(11), 1800-1809.

[94] R.R. Allison and K. Moghissi. *Photodynamic Therapy (PDT): PDT Mechanisms. Clinical endoscopy*, 2013, 46(1), 24-9.

[95] N. Asare, M. Lag, D. Lagadic-Gossmann, M. Rissel, P. Schwarze, and J.A. Holme. *3-Nitrofluoranthene (3-NF) but not 3-aminofluoranthene (3-AF) elicits apoptosis as well as programmed necrosis in Hepa1c1c7 cells. Toxicology*, 2009, 255(3), 140-50.

[96] M. Baritaud, H. Boujrad, H.K. Lorenzo, S. Krantic, and S.A. Susin. *Histone H2AX: The missing link in AIF-mediated caspase-independent programmed necrosis. Cell Cycle*, 2010, 9(16), 3166-73.

[97] L. Galluzzi, I. Vitale, J.M. Abrams, E.S. Alnemri, E.H. Baehrecke, M.V. Blagosklonny, T.M. Dawson, V.L. Dawson, W.S. El-Deiry, S. Fulda, E. Gottlieb, D.R. Green, M.O. Hengartner, O. Kepp, R.A. Knight, S. Kumar, S.A. Lipton, X. Lu, F. Madeo, W. Malorni, P. Mehlen, G. Nunez, M.E. Peter, M. Piacentini, D.C. Rubinsztein, Y. Shi, H.U. Simon, P. Vandenabeele, E. White, J. Yuan, B. Zhivotovsky, G. Melino, and G.

Kroemer. *Molecular definitions of cell death subroutines: recommendations of the Nomenclature Committee on Cell Death 2012. Cell death and differentiation*, 2012, 19(1), 107-20.

[98] A. Casas, G. Di Venosa, T. Hasan, and B. Al. *Mechanisms of resistance to photodynamic therapy. Current medicinal chemistry*, 2011, 18(16), 2486-515.

[99] G. Szakacs, J.K. Paterson, J.A. Ludwig, C. Booth-Genthe, and M.M. Gottesman. *Targeting multidrug resistance in cancer. Nature reviews Drug discovery*, 2006, 5(3), 219-34.

[100] A. Bebes, T. Nagy, Z. Bata-Csorgo, L. Kemeny, A. Dobozy, and M. Szell. *Specific inhibition of the ABCG2 transporter could improve the efficacy of photodynamic therapy. Journal of photochemistry and photobiology B, Biology*, 2011, 105(2), 162-6.

[101] H.M. Lee, C.W. Chung, C.H. Kim, H. Kim do, T.W. Kwak, Y.I. Jeong, and D.H. Kang. *Defensive mechanism in cholangiocarcinoma cells against oxidative stress induced by chlorin e6-based photodynamic therapy. Drug design, development and therapy*, 2014, 8(1451-62.

[102] B.C. Wilson and M.S. Patterson. *The physics, biophysics and technology of photodynamic therapy. Phys Med Biol*, 2008, 53(9), R61-109.

[103] R.R. Allison and K. Moghissi. *Oncologic photodynamic therapy: clinical strategies that modulate mechanisms of action. Photodiagnosis Photodyn Ther*, 2013, 10(4), 331-41.

[104] K.K. Wang, J.C. Finlay, T.M. Busch, S.M. Hahn, and T.C. Zhu. *Explicit dosimetry for photodynamic therapy: macroscopic singlet oxygen modeling. J Biophotonics*, 2010, 3(5-6), 304-18.

[105] S. Lee, D.H. Vu, M.F. Hinds, S.J. Davis, A. Liang, and T. Hasan. *Pulsed diode laser-based singlet oxygen monitor for photodynamic therapy: in vivo studies of tumor-laden rats. J Biomed Opt*, 2008, 13(6), 064035.

[106] U. Sunar. *Monitoring photodynamic therapy of head and neck malignancies with optical spectroscopies. World journal of clinical cases*, 2013, 1(3), 96-105.

[107] General Medical Physics Committee of the Science Council, *Photodynamic Therapy Dosimetry*, 2005, American Association of Physicists in Medicine.

[108] M. Krzykawska-Serda, J.M. Dabrowski, L.G. Arnaut, M. Szczygiel, K. Urbanska, G. Stochel, and M. Elas. *The role of strong hypoxia in tumors after treatment in the outcome of bacteriochlorin-based photodynamic therapy. Free radical biology & medicine*, 2014, 73(239-51.

[109] T.J. Farrell, B.C. Wilson, M.S. Patterson, and R. Chow. *Dependence of photodynamic threshold dose on treatment parameters in normal rat liver in vivo*. 1991.

[110] I. Georgakoudi, M.G. Nichols, and T.H. Foster. *The mechanism of Photofrin photobleaching and its consequences for photodynamic dosimetry. Photochemistry and photobiology*, 1997, 65(1), 135-44.

[111] R. Bonnett, P. Charlesworth, B. D. Djelal, S. Foley, D. J. McGarvey, and T. George Truscott. *Photophysical properties of 5,10,15,20-tetrakis(m-hydroxyphenyl)porphyrin (m-THPP), 5,10,15,20-tetrakis(m-hydroxyphenyl)chlorin (m-THPC) and 5,10,15,20-tetrakis(m-hydroxyphenyl)bacteriochlorin (m-THPBC): a comparative study. Journal of the Chemical Society, Perkin Transactions 2*, 1999, 2), 325-328.

[112] C. Tanielian, C. Wolff, and M. Esch. *Singlet Oxygen Production in Water: Aggregation and Charge-Transfer Effects. The Journal of Physical Chemistry*, 1996, 100(16), 6555-6560.

[113] B. Krammer and T. Verwanger. *Molecular response to hypericin-induced photodamage. Current medicinal chemistry*, 2012, 19(6), 793-8.

[114] C. Abels. *Targeting of the vascular system of solid tumours by photodynamic therapy (PDT). Photochemical & photobiological sciences : Official journal of the European Photochemistry Association and the European Society for Photobiology*, 2004, 3(8), 765-71.

[115] B. Chen, B.W. Pogue, P.J. Hoopes, and T. Hasan. *Vascular and cellular targeting for photodynamic therapy. Critical reviews in eukaryotic gene expression*, 2006, 16(4), 279-305.

[116] J.M. Dabrowski and L.G. Arnaut. *Photodynamic therapy (PDT) of cancer: from local to systemic treatment. Photochemical & Photobiological Sciences*, 2015,

[117] W.R. Chen, W.-G. Zhu, J.R. Dynlacht, H. Liu, and R.E. Nordquist. *Long-term tumor resistance induced by laser photo-immunotherapy. International Journal of Cancer*, 1999, 81(5), 808-812.

[118] E. Kabingu, L. Vaughan, B. Owczarczak, K.D. Ramsey, and S.O. Gollnick. *CD8+ T cell-mediated control of distant tumours following local photodynamic therapy is independent of CD4+ T cells and dependent on natural killer cells. British journal of cancer*, 2007, 96(12), 1839-48.

[119] S.O. Gollnick and C.M. Brackett. *Enhancement of anti-tumor immunity by photodynamic therapy. Immunol Res*, 2010, 46(1-3), 216-26.

[120] P. Mroz, A. Szokalska, M.X. Wu, and M.R. Hamblin. *Photodynamic Therapy of Tumors Can Lead to Development of Systemic Antigen-Specific Immune Response. PloS one*, 2010, 5(12),

[121] E. Kabingu, A.R. Oseroff, G.E. Wilding, and S.O. Gollnick. *Enhanced systemic immune reactivity to a Basal cell carcinoma associated antigen following photodynamic therapy. Clinical cancer research : an official journal of the American Association for Cancer Research*, 2009, 15(13), 4460-6.

[122] P. Mroz and M.R. Hamblin. *The immunosuppressive side of PDT. Photochemical & Photobiological Sciences*, 2011, 10(5), 751-758.

[123] M. Ferracini, R.P. Sahu, K.A. Harrison, R.A. Waeiss, R.C. Murphy, S. Jancar, R.L. Konger, and J.B. Travers. *Topical Photodynamic Therapy Induces Systemic Immunosuppression via Generation of Platelet-Activating Factor Receptor Ligands. J Invest Dermatol*, 2015, 135(1), 321-323.

[124] G.A. Frost, G.M. Halliday, and D.L. Damian. *Photodynamic Therapy-Induced Immunosuppression in Humans Is Prevented by Reducing the Rate of Light Delivery. Journal of Investigative Dermatology*, 2011, 131(4), 962-968.

[125] S.M. Thanos, G.M. Halliday, and D.L. Damian. *Nicotinamide reduces photodynamic therapy-induced immunosuppression in humans. The British journal of dermatology*, 2012, 167(3), 631-6.

[126] G. Evangelou, M.D. Farrar, L. Cotterell, S. Andrew, A.D. Tosca, R.E. Watson, and L.E. Rhodes. *Topical photodynamic therapy significantly reduces epidermal Langerhans cells during clinical treatment of basal cell carcinoma. The British journal of dermatology*, 2012, 166(5), 1112-5.

[127] B.W. Henderson, S.O. Gollnick, J.W. Snyder, T.M. Busch, P.C. Kousis, R.T. Cheney, and J. Morgan. *Choice of oxygen-conserving treatment regimen determines the inflammatory response and outcome of photodynamic therapy of tumors. Cancer research*, 2004, 64(6), 2120-6.

[128] A.D. Garg, D.V. Krysko, P. Vandenabeele, and P. Agostinis. *Hypericin-based photodynamic therapy induces surface exposure of damage-associated molecular patterns like HSP70 and calreticulin. Cancer immunology, immunotherapy : CII*, 2012, 61(2), 215-21.

[129] R.E. Voll, M. Herrmann, E.A. Roth, C. Stach, J.R. Kalden, and I. Girkontaite. *Immunosuppressive effects of apoptotic cells. Nature*, 1997, 390(6658), 350-1.

[130] J. Piette. *Signalling pathway activation by photodynamic therapy: NF-kappaB at the crossroad between oncology and immunology. Photochemical & photobiological sciences : Official journal of the European Photochemistry Association and the European Society for Photobiology*, 2015,

[131] A.D. Garg, D.V. Krysko, P. Vandenabeele, and P. Agostinis. *DAMPs and PDT-mediated photo-oxidative stress: exploring the unknown. Photochemical & photobiological sciences : Official journal of the European Photochemistry Association and the European Society for Photobiology*, 2011, 10(5), 670-80.

[132] E. Panzarini, V. Inguscio, and L. Dini. *Immunogenic cell death: can it be exploited in PhotoDynamic Therapy for cancer? BioMed research international*, 2013, 2013(482160.

[133] A.D. Garg and P. Agostinis. *ER stress, autophagy and immunogenic cell death in photodynamic therapy-induced anti-cancer immune responses. Photochemical & photobiological sciences : Official journal of the European Photochemistry Association and the European Society for Photobiology*, 2014, 13(3), 474-87.

[134] H. Saji, W. Song, K. Furumoto, H. Kato, and E.G. Engleman. *Systemic antitumor effect of intratumoral injection of dendritic cells in combination with local photodynamic therapy. Clinical cancer research : an official journal of the American Association for Cancer Research*, 2006, 12(8), 2568-74.

[135] A.P. Castano, P. Mroz, M.X. Wu, and M.R. Hamblin. *Photodynamic therapy plus low-dose cyclophosphamide generates antitumor immunity in a mouse model. Proceedings of the National Academy of Sciences of the United States of America*, 2008, 105(14), 5495-500.

[136] Y.G. Qiang, C.M. Yow, and Z. Huang. *Combination of photodynamic therapy and immunomodulation: current status and future trends. Medicinal research reviews*, 2008, 28(4), 632-44.

[137] M. Kwitniewski, A. Juzeniene, R. Glosnicka, and J. Moan. *Immunotherapy: a way to improve the therapeutic outcome of photodynamic therapy? Photochemical & photobiological sciences : Official journal of the European Photochemistry Association and the European Society for Photobiology*, 2008, 7(9), 1011-7.

[138] E. Reginato, P. Mroz, H. Chung, M. Kawakubo, P. Wolf, and M.R. Hamblin. *Photodynamic therapy plus regulatory T-cell depletion produces immunity against a mouse tumour that expresses a self-antigen. British journal of cancer*, 2013, 109(8), 2167-74.

[139] P. Mroz, A.P. Castano, and M.R. Hamblin, in *Biophotonics and Immune Responses IV*, W.R. Chen, Editor 2009, SPIE: San Jose, CA, USA. p. 717803-717803.

[140] S.A. de Visscher, P.U. Dijkstra, I.B. Tan, J.L. Roodenburg, and M.J. Witjes. *mTHPC mediated photodynamic therapy (PDT) of squamous cell carcinoma in the head and neck: a systematic review. Oral Oncol*, 2013, 49(3), 192-210.

[141] A.S.L. Derycke and P.A.M. de Witte. *Liposomes for photodynamic therapy. Advanced Drug Delivery Reviews*, 2004, 56(1), 17-30.

[142] M.J. Bovis, J.H. Woodhams, M. Loizidou, D. Scheglmann, S.G. Bown, and A.J. Macrobert. *Improved in vivo delivery of m-THPC via pegylated liposomes for use in photodynamic therapy. Journal of controlled release : official journal of the Controlled Release Society*, 2012, 157(2), 196-205.

[143] J.R. Starkey, A.K. Rebane, M.A. Drobizhev, F. Meng, A. Gong, A. Elliott, K. McInnerney, and C.W. Spangler. *New two-photon activated photodynamic therapy sensitizers induce xenograft tumor regressions after near-IR laser treatment through the body of the host mouse. Clinical cancer research : an official journal of the American Association for Cancer Research*, 2008, 14(20), 6564-73.

[144] M.S. Mathews, E. Angell-Petersen, R. Sanchez, C.-H. Sun, V. Vo, H. Hirschberg, and S.J. Madsen. *The effects of ultra low fluence rate single and repetitive photodynamic therapy on glioma spheroids. Lasers in surgery and medicine*, 2009, 41(8), 578-584.

[145] P. Mroz, J.T. Hashmi, Y.-Y. Huang, N. Lang, and M.R. Hamblin. *Stimulation of anti-tumor immunity by photodynamic therapy. Expert Review of Clinical Immunology*, 2011, 7(1), 75-91.

[146] M. Korbelik. *Cancer vaccines generated by photodynamic therapy. Photochemical & Photobiological Sciences*, 2011, 10(5), 664-669.

[147] F. Ades, D. Zardavas, C. Senterre, E. de Azambuja, A. Eniu, R. Popescu, M. Piccart, and F. Parent. *Hurdles and delays in access to anti-cancer drugs in Europe. Ecancermedicalscience*, 2014, 8(482.

[148] R. Mahajan and K. Gupta. *Food and drug administration's critical path initiative and innovations in drug development paradigm: Challenges, progress, and controversies. Journal of pharmacy & bioallied sciences*, 2010, 2(4), 307-13.

[149] C.P. Adams and V.V. Brantner. *Spending on new drug development1. Health economics*, 2010, 19(2), 130-41.

[150] P.S. Jones and D. Jones. *New regulatory framework for cancer drug development. Drug discovery today*, 2012, 17(5-6), 227-31.

[151] R.A. Roberts, S.L. Kavanagh, H.R. Mellor, C.E. Pollard, S. Robinson, and S.J. Platz. *Reducing attrition in drug development: smart loading preclinical safety assessment. Drug discovery today*, 2014, 19(3), 341-7.

[152] V. Ahuja and S. Sharma. *Drug safety testing paradigm, current progress and future challenges: an overview. Journal of applied toxicology : JAT*, 2014, 34(6), 576-94.

[153] J. Woodcock and R. Woosley. *The FDA critical path initiative and its influence on new drug development. Annual review of medicine*, 2008, 59(1-12.

[154] A.I. Graul. *Promoting, improving and accelerating the drug development and approval processes. Drug news & perspectives*, 2008, 21(1), 36-43.

[155] J.M. Reichert, S.L. Rochon, and B.D. Zhang. *Finding value in the U.S. Food and Drug Administration's Fast Track program. Drug news & perspectives*, 2009, 22(1), 53-8.

[156] International Conference on Harmonisation (ICH), *Guideline S9 - Nonclinical Evaluation for Anticancer Pharmaceuticals*, 2009.

[157] R. Ponce. *ICH S9: Developing anticancer drugs, one year later. Toxicologic pathology*, 2011, 39(6), 913-5.

[158] Y. Vakrat-Haglili, L. Weiner, V. Brumfeld, A. Brandis, Y. Salomon, B. McLlroy, B.C. Wilson, A. Pawlak, M. Rozanowska, T. Sarna, and A. Scherz. *The microenvironment effect on the generation of reactive oxygen species by Pd-bacteriopheophorbide. Journal of the American Chemical Society*, 2005, 127(17), 6487-97.

[159] A.L. Gryshuk, Y. Chen, W. Potter, T. Ohulchansky, A. Oseroff, and R.K. Pandey. *In vivo stability and photodynamic efficacy of fluorinated bacteriopurpurinimides derived from bacteriochlorophyll-a. Journal of medicinal chemistry*, 2006, 49(6), 1874-81.

[160] E.D. Sternberg, D. Dolphin, and C. Brückner. *Porphyrin-based photosensitizers for use in photodynamic therapy. Tetrahedron*, 1998, 54(17), 4151-4202.

[161] A.M.d.A.R. Gonsalves, J.M.T.B. Varejão, and M.M. Pereira. *Some new aspects related to the synthesis of meso-substituted porphyrins. Journal of Heterocyclic Chemistry*, 1991, 28(3), 635-640.

[162] A.M.d.A. Rocha Gonsalves, R. A. W. Johnstone, M. M. Pereira, A. M. P. De Santana, A. C. Serra, A. J. F. N. Sobral and P. A. Stocks. *New procedures for the synthesis and analysis of 5,10,15,20-tetrakis(sulphophenyl)porphyrins and derivatives through chlorosulphonation. Heterocycles*, 1996, 43(9.

[163] M.M. Pereira, A.R. Abreu, N.P.F. Goncalves, M.J.F. Calvete, A.V.C. Simoes, C.J.P. Monteiro, L.G. Arnaut, M.E. Eusebio, and J. Canotilho. *An insight into solvent-free diimide porphyrin reduction: a versatile approach for meso-aryl hydroporphyrin synthesis. Green Chemistry*, 2012, 14(6), 1666-1672.

[164] M. Pineiro, M.M. Pereira, S.J. Formosinho, and L.G. Arnaut. *New Halogenated Phenylbacteriochlorins and Their Efficiency in Singlet-Oxygen Sensitization‡. The Journal of Physical Chemistry A*, 2002, 106(15), 3787-3795.

[165] J.M. Dabrowski, L.G. Arnaut, M.M. Pereira, K. Urbanska, S. Simoes, G. Stochel, and L. Cortes. *Combined effects of singlet oxygen and hydroxyl radical in photodynamic therapy with photostable bacteriochlorins: evidence from intracellular fluorescence and increased photodynamic efficacy in vitro. Free radical biology & medicine*, 2012, 52(7), 1188-200.

[166] C.J. Monteiro, M.M. Pereira, M.E. Azenha, H.D. Burrows, C. Serpa, L.G. Arnaut, M.J. Tapia, M. Sarakha, P. Wong-Wah-Chung, and S. Navaratnam. *A comparative study of water soluble 5,10,15,20-tetrakis(2,6-dichloro-3-sulfophenyl)porphyrin and its metal complexes as efficient sensitizers for photodegradation of*

phenols. Photochemical & photobiological sciences : Official journal of the European Photochemistry Association and the European Society for Photobiology, 2005, 4(8), 617-24.

[167] C.J.P. Monteiro, M.M. Pereira, S.M.A. Pinto, A.V.C. Simões, G.F.F. Sá, L.G. Arnaut, S.J. Formosinho, S. Simões, and M.F. Wyatt. *Synthesis of amphiphilic sulfonamide halogenated porphyrins: MALDI-TOFMS characterization and evaluation of 1-octanol/water partition coefficients. Tetrahedron*, 2008, 64(22), 5132-5138.

[168] E.F. Silva, C. Serpa, J.M. Dabrowski, C.J. Monteiro, S.J. Formosinho, G. Stochel, K. Urbanska, S. Simoes, M.M. Pereira, and L.G. Arnaut. *Mechanisms of singlet-oxygen and superoxide-ion generation by porphyrins and bacteriochlorins and their implications in photodynamic therapy. Chemistry*, 2010, 16(30), 9273-86.

[169] WO2006/053707(A1), *Nouveaux derives de porphyrine, notamment chlorines et/ou bacteriochlorines et leurs applications en therapie photodynamique*, 2005.

[170] WO2010/047611(A1), *Process for preparing chlorins and their pharmaceutical uses*, 2008.

[171] L.G. Arnaut, M.M. Pereira, J.M. Dabrowski, E.F. Silva, F.A. Schaberle, A.R. Abreu, L.B. Rocha, M.M. Barsan, K. Urbanska, G. Stochel, and C.M. Brett. *Photodynamic therapy efficacy enhanced by dynamics: the role of charge transfer and photostability in the selection of photosensitizers. Chemistry*, 2014, 20(18), 5346-57.

[172] T.P.G. Sutter, R. Rahimi, P. Hambright, J.C. Bommer, M. Kumar, and P. Neta. *Steric and inductive effects on the basicity of porphyrins and on the site of protonation of porphyrin dianions: radiolytic reduction of porphyrins and metalloporphyrins to chlorins or phlorins. Journal of the Chemical Society, Faraday Transactions*, 1993, 89(3), 495-502.

[173] S.I. Yang, J. Seth, J.-P. Strachan, S. Gentemann, D. Kim, D. Holten, J.S. Lindsey, and D.F. Bocian. *Ground and Excited State Electronic Properties of Halogenated Tetraarylporphyrins: Tuning the Building Blocks for Porphyrin-based Photonic Devices. Journal of Porphyrins and Phthalocyanines*, 1999, 03(02), 117-147.

[174] A.M.S. Silva, M.G.P.M.S. Neves, R.R.L. Martins, J.A.S. Cavaleiro, T. Boschi, and P. Tagliatesta. *Photo-oxygenation of meso-Tetraphenylporphyrin Derivatives: the Influence of the Substitution Pattern and Characterization of the Reaction Products. Journal of Porphyrins and Phthalocyanines*, 1998, 02(01), 45-51.

[175] E. Yang, J.R. Diers, Y.-Y. Huang, M.R. Hamblin, J.S. Lindsey, D.F. Bocian, and D. Holten. *Molecular Electronic Tuning of Photosensitizers to Enhance Photodynamic Therapy: Synthetic Dicyanobacteriochlorins as a Case Study. Photochemistry and photobiology*, 2013, 89(3), 605-618.

[176] E.F. da Silva, B.W. Pedersen, T. Breitenbach, R. Toftegaard, M.K. Kuimova, L.G. Arnaut, and P.R. Ogilby. *Irradiation- and sensitizer-dependent changes in the lifetime of intracellular singlet oxygen produced in a photosensitized process. The journal of physical chemistry B*, 2012, 116(1), 445-61.

[177] R. Bonnett, S. Ioannou, R. White, U.-J. Winfield, and M. Berenbaum. *Meso-Tetra (hydroxyphenyl) porphyrins, as Tumour Photosensitisers: Chemical and Photochemical Aspects. Photobiochemical Photobiophysics (suppl)*, 1997, 45–56.

[178] R. Bonnett, R.D. White, U.J. Winfield, and M.C. Berenbaum. *Hydroporphyrins of the meso-tetra(hydroxyphenyl)porphyrin series as tumour photosensitizers. The Biochemical journal*, 1989, 261(1), 277-80.

[179] J. O'Brien, I. Wilson, T. Orton, and F. Pognan. *Investigation of the Alamar Blue (resazurin) fluorescent dye for the assessment of mammalian cell cytotoxicity. European journal of biochemistry / FEBS*, 2000, 267(17), 5421-6.

[180] *alamarBlue® Cell Viability Assay Protocol - Invitrogen Corporation*. 22-06-2015]; Available from: http://tools.lifetechnologies.com/content/sfs/manuals/PI-DAL1025-1100_TI%20alamarBlue%20Rev%201.1.pdf.

[181] M.H. Teiten, L. Bezdetnaya, P. Morliere, R. Santus, and F. Guillemin. *Endoplasmic reticulum and Golgi apparatus are the preferential sites of Foscan localisation in cultured tumour cells. British journal of cancer*, 2003, 88(1), 146-52.

[182] Y.J. Hsieh, J.S. Yu, and P.C. Lyu. *Characterization of photodynamic therapy responses elicited in A431 cells containing intracellular organelle-localized photofrin. J Cell Biochem*, 2010, 111(4), 821-33.

[183] D.V. Krysko, A.D. Garg, A. Kaczmarek, O. Krysko, P. Agostinis, and P. Vandenabeele. *Immunogenic cell death and DAMPs in cancer therapy. Nature reviews Cancer*, 2012, 12(12), 860-875.

[184] A.D. Garg, D.V. Krysko, T. Verfaillie, A. Kaczmarek, G.B. Ferreira, T. Marysael, N. Rubio, M. Firczuk, C. Mathieu, A.J.M. Roebroek, W. Annaert, J. Golab, P. de Witte, P. Vandenabeele, and P. Agostinis, *A novel pathway combining calreticulin exposure and ATP secretion in immunogenic cancer cell death*. Vol. 31. 2012. 1062-1079.

[185] R. Bonnett, B.D. Djelal, P.A. Hamilton, G. Martinez, and F. Wierrani. *Photobleaching of 5,10,15,20-tetrakis(m-hydroxyphenyl)porphyrin (m-THPP) and the corresponding chlorin (m-THPC) and bacteriochlorin(m-THPBC). A comparative study. Journal of Photochemistry and Photobiology B: Biology*, 1999, 53(1–3), 136-143.

[186] R.W. Redmond and J.N. Gamlin. *A compilation of singlet oxygen yields from biologically relevant molecules. Photochemistry and photobiology*, 1999, 70(4), 391-475.

[187] M. Chen, X. Liu, and A. Fahr. *Skin penetration and deposition of carboxyfluorescein and temoporfin from different lipid vesicular systems: In vitro study with finite and infinite dosage application. Int J Pharm*, 2011, 408(1-2), 223-34.

[188] B. Cunderlikova, O. Kaalhus, R. Cunderlik, A. Mateasik, J. Moan, and M. Kongshaug. *pH-dependent modification of lipophilicity of porphyrin-type photosensitizers. Photochemistry and photobiology*, 2004, 79(3), 242-7.

[189] R. Bonnett and G. Martínez. *Photobleaching of sensitisers used in photodynamic therapy. Tetrahedron*, 2001, 57(47), 9513-9547.

[190] T.J. Dougherty, C.J. Gomer, B.W. Henderson, G. Jori, D. Kessel, M. Korbelik, J. Moan, and Q. Peng. *Photodynamic therapy. Journal of the National Cancer Institute*, 1998, 90(12), 889-905.

[191] R.W. Boyle and D. Dolphin. *Structure and biodistribution relationships of photodynamic sensitizers. Photochemistry and photobiology*, 1996, 64(3), 469-85.

[192] H.P. Lassalle, D. Dumas, S. Grafe, M.A. D'Hallewin, F. Guillemin, and L. Bezdetnaya. *Correlation between in vivo pharmacokinetics, intratumoral distribution and photodynamic efficiency of liposomal mTHPC. Journal of controlled release : official journal of the Controlled Release Society*, 2009, 134(2), 118-24.

[193] M. Garcia-Diaz, M. Kawakubo, P. Mroz, M.L. Sagrista, M. Mora, S. Nonell, and M.R. Hamblin. *Cellular and vascular effects of the photodynamic agent temocene are modulated by the delivery vehicle. Journal of controlled release : official journal of the Controlled Release Society*, 2012, 162(2), 355-63.

[194] M. Eckhauser, J. Persky, A. Bonaminio, J. Crespin, A. Imbembo, and S. Holt. *Biodistribution of the photosensitizer dihaematoporphyrin ether. Lasers in medical science*, 1987, 2(2), 101-105.

[195] Q. Peng, J. Moan, M. Kongshaug, J.F. Evensen, H. Anholt, and C. Rimington. *Sensitizer for photodynamic therapy of cancer: a comparison of the tissue distribution of Photofrin II and aluminum phthalocyanine tetrasulfonate in nude mice bearing a human malignant tumor. International journal of cancer Journal international du cancer*, 1991, 48(2), 258-64.

[196] M. Tronconi, A. Colombo, M. De Cesare, R. Marchesini, K.W. Woodburn, J.A. Reiss, D.R. Phillips, and F. Zunino. *Biodistribution of haematoporphyrin analogues in a lung carcinoma model. Cancer letters*, 1995, 88(1), 41-8.

[197] A. Hajri, S. Wack, C. Meyer, M.K. Smith, C. Leberquier, M. Kedinger, and M. Aprahamian. *In vitro and in vivo efficacy of photofrin and pheophorbide a, a bacteriochlorin, in photodynamic therapy of colonic cancer cells. Photochemistry and photobiology*, 2002, 75(2), 140-8.

[198] J.M. Dabrowski, M. Krzykawska, L.G. Arnaut, M.M. Pereira, C.J. Monteiro, S. Simoes, K. Urbanska, and G. Stochel. *Tissue uptake study and photodynamic therapy of melanoma-bearing mice with a nontoxic, effective chlorin. ChemMedChem*, 2011, 6(9), 1715-26.

[199] J.M. Dabrowski, K. Urbanska, L.G. Arnaut, M.M. Pereira, A.R. Abreu, S. Simoes, and G. Stochel. *Biodistribution and photodynamic efficacy of a water-soluble, stable, halogenated bacteriochlorin against melanoma. ChemMedChem*, 2011, 6(3), 465-75.

[200] E. Ben-Hur, M.M. Zuk, S. Chin, D. Banerjee, M.E. Kenney, and B. Horowitz. *Biodistribution and virus inactivation efficacy of a silicon phthalocyanine in red blood cell concentrates as a function of delivery vehicle. Photochemistry and photobiology*, 1995, 62(3), 575-9.

[201] K. Woodburn, C.K. Chang, S. Lee, B. Henderson, and D. Kessel. *Biodistribution and PDT efficacy of a ketochlorin photosensitizer as a function of the delivery vehicle. Photochemistry and photobiology*, 1994, 60(2), 154-9.

[202] A.M. Richter, S. Cerruti-Sola, E.D. Sternberg, D. Dolphin, and J.G. Levy. *Biodistribution of tritiated benzoporphyrin derivative (3H-BPD-MA), a new potent photosensitizer, in normal and tumor-bearing mice. Journal of photochemistry and photobiology B, Biology*, 1990, 5(2), 231-44.

[203] A.M. Richter, E. Waterfield, A.K. Jain, B. Allison, E.D. Sternberg, D. Dolphin, and J.G. Levy. *Photosensitising potency of structural analogues of benzoporphyrin derivative (BPD) in a mouse tumour model. British journal of cancer*, 1991, 63(1), 87-93.

[204] A.M. Richter, E. Waterfield, A.K. Jain, A.J. Canaan, B.A. Allison, and J.G. Levy. *Liposomal delivery of a photosensitizer, benzoporphyrin derivative monoacid ring A (BPD), to tumor tissue in a mouse tumor model. Photochemistry and photobiology*, 1993, 57(6), 1000-6.

[205] W. Alian, S. Andersson-Engels, K. Svanberg, and S. Svanberg. *Laser-induced fluorescence studies of meso-tetra(hydroxyphenyl)chlorin in malignant and normal tissues in rats. British journal of cancer*, 1994, 70(5), 880-5.

[206] R. Whelpton, A.T. Michael-Titus, S.S. Basra, and M. Grahn. *Distribution of temoporfin, a new photosensitizer for the photodynamic therapy of cancer, in a murine tumor model. Photochemistry and photobiology*, 1995, 61(4), 397-401.

[207] H.J. Hopkinson, D.I. Vernon, and S.B. Brown. *Identification and partial characterization of an unusual distribution of the photosensitizer meta-tetrahydroxyphenyl chlorin (temoporfin) in human plasma. Photochemistry and photobiology*, 1999, 69(4), 482-8.

[208] S.A. Blant, T.M. Glanzmann, J.P. Ballini, G. Wagnieres, H. van den Bergh, and P. Monnier. *Uptake and localisation of mTHPC (Foscan) and its 14C-labelled form in normal and tumour tissues of the hamster squamous cell carcinoma model: a comparative study. British journal of cancer*, 2002, 87(12), 1470-8.

[209] P. Cramers, M. Ruevekamp, H. Oppelaar, O. Dalesio, P. Baas, and F.A. Stewart. *Foscan uptake and tissue distribution in relation to photodynamic efficacy. British journal of cancer*, 2003, 88(2), 283-90.

[210] H.J. Jones, D.I. Vernon, and S.B. Brown. *Photodynamic therapy effect of m-THPC (Foscan) in vivo: correlation with pharmacokinetics. British journal of cancer*, 2003, 89(2), 398-404.

[211] E. Maugain, S. Sasnouski, V. Zorin, J.L. Merlin, F. Guillemin, and L. Bezdetnaya. *Foscan-based photodynamic treatment in vivo: correlation between efficacy and Foscan accumulation in tumor, plasma and leukocytes. Oncology reports*, 2004, 12(3), 639-45.

[212] A.J. ten Tije, J. Verweij, W.J. Loos, and A. Sparreboom. *Pharmacological effects of formulation vehicles : implications for cancer chemotherapy. Clinical pharmacokinetics*, 2003, 42(7), 665-85.

[213] Y.Y. Huang, T. Balasubramanian, E. Yang, D. Luo, J.R. Diers, D.F. Bocian, J.S. Lindsey, D. Holten, and M.R. Hamblin. *Stable synthetic bacteriochlorins for photodynamic therapy: role of dicyano peripheral groups, central metal substitution (2H, Zn, Pd), and Cremophor EL delivery. ChemMedChem*, 2012, 7(12), 2155-67.

[214] J. Szebeni, F.M. Muggia, and C.R. Alving. *Complement activation by Cremophor EL as a possible contributor to hypersensitivity to paclitaxel: an in vitro study. Journal of the National Cancer Institute*, 1998, 90(4), 300-6.

[215] H. Gelderblom, J. Verweij, K. Nooter, and A. Sparreboom. *Cremophor EL: the drawbacks and advantages of vehicle selection for drug formulation. Eur J Cancer*, 2001, 37(13), 1590-8.

[216] W.G. Roberts, K.M. Smith, J.L. McCuliough, and M.W. Berns. *Skin photosensitivity and photodestruction of several potential photodynamic sensitizers. Photochemistry and photobiology*, 1989, 49(4), 431-438.

[217] J.C. Maziere, R. Santus, P. Morliere, J.P. Reyftmann, C. Candide, L. Mora, S. Salmon, C. Maziere, S. Gatt, and L. Dubertret. *Cellular uptake and photosensitizing properties of anticancer porphyrins in cell membranes and low and high density lipoproteins. Journal of photochemistry and photobiology B, Biology*, 1990, 6(1-2), 61-8.

[218] B.A. Allison, P.H. Pritchard, and J.G. Levy. *Evidence for low-density lipoprotein receptor-mediated uptake of benzoporphyrin derivative. British journal of cancer*, 1994, 69(5), 833-9.

[219] K.W. Woodburn, Q. Fan, D. Kessel, Y. Luo, and S.W. Young. *Photodynamic therapy of B16F10 murine melanoma with lutetium texaphyrin. J Invest Dermatol*, 1998, 110(5), 746-51.

[220] S. Andrejevic-Blant, C. Hadjur, J.P. Ballini, G. Wagnieres, C. Fontolliet, H. van den Bergh, and P. Monnier. *Photodynamic therapy of early squamous cell carcinoma with tetra(m-hydroxyphenyl)chlorin: optimal drug-light interval. British journal of cancer*, 1997, 76(8), 1021-8.

[221] M. Torres-Gonzalez, S. Shrestha, M. Sharman, H.C. Freake, J.S. Volek, and M.L. Fernandez. *Carbohydrate restriction alters hepatic cholesterol metabolism in guinea pigs fed a hypercholesterolemic diet. The Journal of nutrition*, 2007, 137(10), 2219-23.

[222] H.P. Wijnand. *Pharmacokinetic model equations for the one- and two-compartment models with first-order processes in which the absorption and exponential elimination or distribution rate constants are equal. Journal of pharmacokinetics and biopharmaceutics*, 1988, 16(1), 109-28.

[223] A.M. Richter, S. Yip, E. Waterfield, P.M. Logan, C.E. Slonecker, and J.G. Levy. *Mouse skin photosensitization with benzoporphyrin derivatives and Photofrin: macroscopic and microscopic evaluation. Photochemistry and photobiology*, 1991, 53(2), 281-6.

[224] *International Conference on Harmonisation, Guidance on Nonclinical Safety Studies for the Conduct of Human Clinical Trials and Marketing Authorization for Pharmaceuticals*. 2009 01-07-2015]; Available from: http://www.ich.org/fileadmin/Public_Web_Site/ICH_Products/Guidelines/Multidisciplinary/M3_R2/Step4/M3_R2__Guideline.pdf.

[225] N. Lin, C. Li, Z. Wang, J. Zhang, X. Ye, W. Gao, A. Wang, H. Jin, and J. Wei. *A safety study of a novel photosensitizer, sinoporphyrin sodium, for photodynamic therapy in Beagle dogs. Photochemical & Photobiological Sciences*, 2015, 14(4), 815-832.

[226] S. Chevalier, F.L. Cury, E. Scarlata, E. El-Zayat, L. Hamel, J. Rocha, F.Z. Zouanat, S. Moussa, A. Scherz, M. Elhilali, and M. Anidjar. *Endoscopic Vascular Targeted Photodynamic Therapy with the Photosensitizer*

WST11 for Benign Prostatic Hyperplasia in the Preclinical Dog Model. The Journal of Urology, 190(5), 1946-1953.

[227] P. Li and L. Zhao. *Developing early formulations: Practice and perspective. International Journal of Pharmaceutics*, 2007, 341(1–2), 1-19.

[228] M. Schreckenberger, R. Amberg, A. Scheurich, M. Lochmann, W. Tichy, A. Klega, T. Siessmeier, G. Grunder, H.-G. Buchholz, C. Landvogt, J. Stauss, K. Mann, P. Bartenstein, and R. Urban. *Acute Alcohol Effects on Neuronal and Attentional Processing: Striatal Reward System and Inhibitory Sensory Interactions under Acute Ethanol Challenge. Neuropsychopharmacology*, 2004, 29(8), 1527-1537.

[229] Z. Zhang, H. Jin, J. Bao, F. Fang, J. Wei, and A. Wang. *Intravenous repeated-dose toxicity study of ZnPcS2P2-based-photodynamic therapy in Wistar rats. Photochemical & photobiological sciences : Official journal of the European Photochemistry Association and the European Society for Photobiology*, 2006, 5(11), 1006-17.

[230] Y.M. Cho, H. Onodera, M. Ueda, T. Imai, and M. Hirose. *A 13-week subchronic toxicity study of dietary administered morin in F344 rats. Food and chemical toxicology : an international journal published for the British Industrial Biological Research Association*, 2006, 44(6), 891-7.

[231] T. Green, J. Dow, and J. Foster. *Increased formic acid excretion and the development of kidney toxicity in rats following chronic dosing with trichloroethanol, a major metabolite of trichloroethylene. Toxicology*, 2003, 191(2-3), 109-19.

[232] CharlesRiverLaboratories. *Baseline Hematology and Clinical Chemistry Values for Charles River Wistar Rats*. 1998; Available from: http://www.criver.com/files/pdfs/rms/wistar-rats/rm_rm_r_hematology_crl_wi_br_sex_age.aspx.

[233] P. Brancaccio, G. Lippi, and N. Maffulli. *Biochemical markers of muscular damage. Clinical chemistry and laboratory medicine : CCLM / FESCC*, 2010, 48(6), 757-67.

[234] European Medicines Agency (EMA). *European public assessment report (EPAR) for Foscan - Scientific Discussion*. 2005 [cited 2015 13/07/2015]; Available from: http://www.ema.europa.eu/docs/en_GB/document_library/EPAR_-_Scientific_Discussion/human/000318/WC500024394.pdf.

[235] E.F. Silva, F.A. Schaberle, C.J. Monteiro, J.M. Dabrowski, and L.G. Arnaut. *The challenging combination of intense fluorescence and high singlet oxygen quantum yield in photostable chlorins--a contribution to theranostics. Photochemical & photobiological sciences : Official journal of the European Photochemistry Association and the European Society for Photobiology*, 2013, 12(7), 1187-92.

[236] D. Preise, A. Scherz, and Y. Salomon. *Antitumor immunity promoted by vascular occluding therapy: lessons from vascular-targeted photodynamic therapy (VTP). Photochemical & Photobiological Sciences*, 2011, 10(5), 681-688.

[237] H. Zhao, D. Xing, and Q. Chen. *New insights of mitochondria reactive oxygen species generation and cell apoptosis induced by low dose photodynamic therapy. Eur J Cancer*, 2011, 47(18), 2750-61.

[238] Q. Peng, J. Moan, L.W. Ma, and J.M. Nesland. *Uptake, localization, and photodynamic effect of meso-tetra(hydroxyphenyl)porphine and its corresponding chlorin in normal and tumor tissues of mice bearing mammary carcinoma. Cancer research*, 1995, 55(12), 2620-6.

[239] J.M. Houle and A. Strong. *Clinical pharmacokinetics of verteporfin. Journal of clinical pharmacology*, 2002, 42(5), 547-57.

[240] M.T. Huggett, M. Jermyn, A. Gillams, R. Illing, S. Mosse, M. Novelli, E. Kent, S.G. Bown, T. Hasan, B.W. Pogue, and S.P. Pereira. *Phase I/II study of verteporfin photodynamic therapy in locally advanced pancreatic cancer. British journal of cancer*, 2014, 110(7), 1698-704.

[241] P.C. Kousis, B.W. Henderson, P.G. Maier, and S.O. Gollnick. *Photodynamic therapy enhancement of antitumor immunity is regulated by neutrophils. Cancer research*, 2007, 67(21), 10501-10.

[242] M. Krzykawska, J.M. Dabrowski, M. Szczygiel, G. Stochel, L.G. Arnaut, M.M. Pereira, K. Urbanska, and M. Elas. *808 Non-invasive Prognostic Tools for Phototherapeutic Response in Murine Tumors. European Journal of Cancer*, 48(S193.

[243] N. Agrawal, C. Bettegowda, I. Cheong, J.F. Geschwind, C.G. Drake, E.L. Hipkiss, M. Tatsumi, L.H. Dang, L.A. Diaz, Jr., M. Pomper, M. Abusedera, R.L. Wahl, K.W. Kinzler, S. Zhou, D.L. Huso, and B. Vogelstein. *Bacteriolytic therapy can generate a potent immune response against experimental tumors. Proceedings of the National Academy of Sciences of the United States of America*, 2004, 101(42), 15172-7.

[244] V.H. Fingar and B.W. Henderson. *Drug and light dose dependence of photodynamic therapy: a study of tumor and normal tissue response. Photochemistry and photobiology*, 1987, 46(5), 837-41.

[245] M.J. Gooden, G.H. de Bock, N. Leffers, T. Daemen, and H.W. Nijman. *The prognostic influence of tumour-infiltrating lymphocytes in cancer: a systematic review with meta-analysis. British journal of cancer*, 2011, 105(1), 93-103.

[246] D. Preise, R. Oren, I. Glinert, V. Kalchenko, S. Jung, A. Scherz, and Y. Salomon. *Systemic antitumor protection by vascular-targeted photodynamic therapy involves cellular and humoral immunity. Cancer immunology, immunotherapy : CII*, 2009, 58(1), 71-84.

[247] M. Wachowska, M. Gabrysiak, A. Muchowicz, W. Bednarek, J. Barankiewicz, T. Rygiel, L. Boon, P. Mroz, M.R. Hamblin, and J. Golab. *5-Aza-2'-deoxycytidine potentiates antitumour immune response induced by photodynamic therapy. Eur J Cancer*, 2014, 50(7), 1370-81.

[248] M. Korbelik, I. Cecic, S. Merchant, and J. Sun. *Acute phase response induction by cancer treatment with photodynamic therapy. International journal of cancer Journal international du cancer*, 2008, 122(6), 1411-7.

[249] S. Schreiber, S. Gross, A. Brandis, A. Harmelin, V. Rosenbach-Belkin, A. Scherz, and Y. Salomon. *Local photodynamic therapy (PDT) of rat C6 glioma xenografts with Pd-bacteriopheophorbide leads to decreased metastases and increase of animal cure compared with surgery. International journal of cancer Journal international du cancer*, 2002, 99(2), 279-85.

[250] M.J. Niedre, A.J. Secord, M.S. Patterson, and B.C. Wilson. *In vitro tests of the validity of singlet oxygen luminescence measurements as a dose metric in photodynamic therapy. Cancer research*, 2003, 63(22), 7986-94.

[251] C.J. Gomer, A. Ferrario, and A.L. Murphree. *The effect of localized porphyrin photodynamic therapy on the induction of tumour metastasis. British journal of cancer*, 1987, 56(1), 27-32.

[252] P. Mroz, F. Vatansever, A. Muchowicz, and M.R. Hamblin. *Photodynamic therapy of murine mastocytoma induces specific immune responses against the cancer/testis antigen P1A. Cancer research*, 2013, 73(21), 6462-70.

[253] S. Coutier, L.N. Bezdetnaya, T.H. Foster, R.M. Parache, and F. Guillemin. *Effect of irradiation fluence rate on the efficacy of photodynamic therapy and tumor oxygenation in meta-tetra (hydroxyphenyl) chlorin (mTHPC)-sensitized HT29 xenografts in nude mice. Radiat Res*, 2002, 158(3), 339-45.

[254] S.L. Gibson, K.R. VanDerMeid, R.S. Murant, R.F. Raubertas, and R. Hilf. *Effects of various photoradiation regimens on the antitumor efficacy of photodynamic therapy for R3230AC mammary carcinomas. Cancer research*, 1990, 50(22), 7236-41.

[255] T.M. Busch, X. Xing, G. Yu, A. Yodh, E.P. Wileyto, H.W. Wang, T. Durduran, T.C. Zhu, and K.K. Wang. *Fluence rate-dependent intratumor heterogeneity in physiologic and cytotoxic responses to Photofrin photodynamic therapy. Photochemical & photobiological sciences : Official journal of the European Photochemistry Association and the European Society for Photobiology*, 2009, 8(12), 1683-93.

[256] H.W. Wang, E. Rickter, M. Yuan, E.P. Wileyto, E. Glatstein, A. Yodh, and T.M. Busch. *Effect of photosensitizer dose on fluence rate responses to photodynamic therapy. Photochemistry and photobiology*, 2007, 83(5), 1040-8.

[257] T.M. Busch, H.W. Wang, E.P. Wileyto, G. Yu, and R.M. Bunte. *Increasing damage to tumor blood vessels during motexafin lutetium-PDT through use of low fluence rate. Radiat Res*, 2010, 174(3), 331-40.